

Friedrich-Schiller-Universität Jena
Fakultät für Biowissenschaften
Max-Planck-Institut für chemische Ökologie
Abteilung Biochemie



**FRIEDRICH-SCHILLER-
UNIVERSITÄT
JENA**

**Engineering of the benzoxazinoid pathway in *Nicotiana
benthamiana***

Masterarbeit
zur Erlangung des Grades eines
Master of Science (M.Sc.)

vorgelegt von
Paul Anton Himmighofen
aus Bornich
Jena, **12.2019**

Gutachter:

1. Prof. Dr. Dirk Hoffmeister
2. Dr. Tobias G. Köllner

Content

Content	3
I. List of tables	6
II. List of Figures	7
III. List of abbreviations	9
IV. Zusammenfassung	12
V. Abstract	13
1. Introduction	14
1.1 The role of secondary plant metabolism in ecological interactions	14
1.2 Benzoxazinoids – A group of specialized metabolites in grasses	15
1.4 Connection of BXDs to primary metabolism	18
1.4 The Reactivity and mechanisms of action of BXDs	20
1.5 BXD Lactams – Unsolved origins	20
1.6 Elucidating the origin of lactams – Choice of methods	21
1.7 Objective	22
2. Material and methods	23
2.1 Cultivation of plants	23
2.2 Microbiological methods	23
2.2.1 Cultivation of <i>Escherichia coli</i>	23
2.2.2 Cultivation of <i>Agrobacterium tumefaciens</i>	24
2.2.3 Preparation of competent <i>A. tumefaciens</i> stocks	24
2.2.4 Glycerol stocks	24
2.3 Subcloning	25
2.3.1 RNA Extraction	25
2.3.2 cDNA Synthesis	25
2.3.3 Amplification of DNA	25
2.3.4 Gene synthesis	26
2.3.5 Gelelectrophoresis	26
2.3.6 Purification of PCR-products	27
2.3.7 Transformation of <i>E. coli</i>	27

2.3.8 Colony PCR	27
2.3.9 Plasmid Purification	28
2.3.10 Sequencing	28
2.4 Uracil-specific excision reagent (USER)-cloning	29
2.4.1 USER-based DNA amplification	30
2.4.2 <i>DpnI</i> -Digestion	31
2.4.3 Linearization of pCambia2300U	31
2.4.4 USER-Reaction	31
2.4.5 Transformation of <i>E. coli</i> with pCambia2300U vectors	31
2.4.6 Transformation of <i>A. tumefaciens</i> with pCambia2300U vectors	32
2.5 Heterologous expression of Bx genes in <i>N. benthamiana</i>	32
2.5.1 Agroinfiltration of <i>N. benthamiana</i>	32
2.5.2 Anthranilate assay	34
2.5.3 qPCR	34
2.6. Fluorescence microscopy	35
2.7 Analytics	35
2.7.1 Methanol extraction	35
2.7.2 Targeted LC-MS Analysis	36
2.7.3 Nontargeted LC-MS Analysis	37
2.7.4 Statistical analysis and graphic design	37
3. Results	38
3.1 Cloning of BXD biosynthesis genes	38
3.2 Measurement of eGFP-fluorescence in transgenic tobacco – Confirming the functionality of agroinfiltration	38
3.3 Introducing the BXD biosynthetic pathway in tobacco – Production of the lactam HBOA	39
3.3.1 Detection and characterization of putative HBOA analyte	39
3.3.2 Influence of downstream BXD enzyme genes on the accumulation of HBOA-Glc	43

3.4. Negative effect of dehydration in pre-transformed plants on transformation effectiveness	45
3.5 Introducing the BXD biosynthetic pathway in tobacco – Production of the first hydroxamic acid DIBOA	46
3.6 Supply of the BXD biosynthetic pathway in transgenic plants – Effect of providing additional substrate on the accumulation of BXDs	51
3.7 Quantification of Bx gene expression in transgenic tobacco	56
4. Discussion	57
4.1 Detecting BXDs in transgenic plants – Achievements and obstacles	57
4.2 Optimization of the transformation process	59
4.3 Experimental parameters of the transformation process can be tuned to improve results	60
4.4 Interference with endogenous enzymes in transgenic tobacco leads to production of conjugates	62
4.5 Supplementation of the BXD biosynthesis in transgenic plants by increasing the substrate availability	65
4.6 The drawbacks of cloning a complex pathway – and how to tackle them	66
5. Conclusion	69
A. Literature	70
B. Supplementary	78
C. Danksagung	84
D. Selbständigkeitserklärung	85

I. List of tables

Table 1:	Phusion- and Q5-PCR Protocol.	26
Table 2:	Colony-PCR protocol.	28
Table 3:	Sequencing PCR protocol.	29
Table 4:	Phusion U and PfuTurbo Cx Hotstart USER-PCR protocol.	30
Table 5:	qPCR programme for <i>N. benthamiana</i> cDNA samples.	34
Table 6:	Multiple reaction monitoring parameters for selected BXDs.	36
Table 7:	Cloning procedures for <i>Bx</i> genes.	38
Table I:	List of used chemicals and their vendors.	78
Table II:	List of primers for amplification of <i>Bx</i> genes from <i>Zea mays</i> cDNA.	79
Table III:	List of USER-PCR primers for amplification of <i>Bx</i> genes.	80
Table IV:	List of primers for outward sequencing of <i>Bx</i> genes in reverse direction.	80
Table V:	List of qPCR primers for <i>Bx</i> genes and <i>GAPDH</i> gene.	81
Table VI:	Average Cq values for <i>Bx</i> genes and <i>GAPDH</i> gene from qPCR.	82
Table VII:	DIBOA mono- and di-glucoside content of transgenic <i>Nicotiana benthamiana</i> plants in different treatments.	83

II. List of Figures

Figure 1:	Benzoxazinoid biosynthetic pathway in maize.	16
Figure 2:	Benzoxazinoid derivatives and their degradation products benzoxazolinones.	17
Figure 3:	Tryptophan biosynthesis in plants.	19
Figure 4:	Setup of the vacuum chamber for agroinfiltration of <i>Nicotiana benthamiana</i> .	33
Figure 5:	Fluorescence microscopy pictures from leaves of <i>Nicotiana benthamiana</i> plants.	39
Figure 6:	Extracted ion chromatograms of HBOA-Glc.	41
Figure 7:	Quantification of hypothesized HBOA-Glc analyte.	42
Figure 8:	MS/MS-Spectrum of hypothesized HBOA-Glc analyte.	43
Figure 9:	Extracted ion chromatograms of HBOA-Glc in different transformants of <i>Nicotiana benthamiana</i> .	44
Figure 10:	Quantification of hypothesized HBOA-Glc analyte in extracts of transgenic <i>Nicotiana benthamiana</i> plants.	45
Figure 11:	Dependence of HBOA-Glc accumulation on plant watering state.	46
Figure 12:	Extracted ion chromatograms of DIBOA-Glc for transgenic <i>Nicotiana benthamiana</i> lines.	48
Figure 13:	Extracted ion chromatograms of DIBOA glucosides.	49
Figure 14:	Quantification of DIBOA glucosides in transgenic <i>Nicotiana benthamiana</i> plants.	50
Figure 15:	Supplementation of transgenic <i>Nicotiana benthamiana</i> leaves with anthranilate.	51
Figure 16:	Tryptophan content of transgenic <i>Nicotiana benthamiana</i> leaves supplemented with anthranilate.	53
Figure 17:	HBOA-Glc content of transgenic <i>Nicotiana benthamiana</i> leaves supplemented with anthranilate.	54
Figure 18:	DIBOA glucoside content of transgenic <i>Nicotiana benthamiana</i> leaves supplemented with anthranilate.	55
Figure 19:	qPCR analysis of <i>Bx</i> genes in <i>Nicotiana benthamiana</i> plants transiently co-transformed with <i>Bx1</i> to <i>Bx7</i> .	56
Figure 20:	Reaction mechanism proposed for DIMBOA with thiols.	64
Figure I:	Tryptophan content of transgenic <i>Nicotiana benthamiana</i> plants.	82

Figure II:	HBOA-Glc content of transgenic <i>Nicotiana benthamiana</i> leaves in different treatments.	82
Figure III:	HBOA-Glc content of <i>Nicotiana benthamiana</i> plants transformed with <i>Bx</i> genes up to <i>Bx3</i>.	83

III. List of abbreviations

%	Percent
°C	Degree Celsius
µg	Microgram
µl	Microliter
µM	Micromol
AA	Anthranilate
ANOVA	Analysis of variance
approx.	approximately
AS	Anthranilate synthase
bp	Base pair
BP	Bandpass
Bx	Benzoxazinless
BXD	Benzoxazinoids
cDNA	Coding desoxyribonucleic acid
CE	Collision energy
CPMV-HAT	Cow pea mosaic virus-hypertranslatable
cps	counts per second
Cq	Cycle quantification
	Clustered Regularly Interspaced Short Palindromic
CRISPR/Cas9	Repeats/CRISPR associated protein 9
CXP	Collision cell exit potential
Da	Dalton
ddH ₂ O	Double-distilled water, sterilized by millipore and autoclave
DHBOA	2,7-Dihydroxy-(2H)-1,4-benzoxazin-3(4H)-one
DIBOA	2,4-Dihydroxy-(2H)-1,4-benzoxazin-3(4H)-one
DIMBOA	2,4-Dihydroxy-7-methoxy-(2H)-1,4-benzoxazin-3(4H)-one
DMSO	Dimethyl sulfoxide
DNA	Desoxyribonucleic acid
dNTP	Desoxynucleosid triphosphate
DTT	Dithiothreitol
EDTA	Ethylenediaminetetraacetic acid
eGFP	Enhanced green fluorescent protein
EP	Entrance potential
EPI	Enhanced product ion
ESI	Electrospray ionisation

EtOH	Ethanol
eV	electronic Volt
GAPDH	Glyceraldehyd-3-phosphate dehydrogenase
GC-MS	Gas chromatography - Mass spectrometry
Glc	Glucose
GOI	Gene of interest
GST	Glutathione-S-Transferase
h	Hour
HBOA	2-Hydroxy-(2H)-1,4-benzoxazin-3(4H)-one
HE	High Efficiency
HKG	Housekeeping gene
HMBOA	2-Hydroxy-7-methoxy-(2H)-1,4-benzoxazin-3(4H)-one
HPLC	High pressure liquid chromatography
HSP	Heat shock protein
IGL	Indole glycerolphosphate lyase
IGP	Indole-3-glycerolphosphate
IGPS	Indole glycerolphosphate synthase
kb	kilo base pair
l	liter
LB	Lysogeny broth
LC-MS	Liquid chromatography - Mass spectrometry
m/z	mass/charge
mbar	millibar
MES	2-(N-morpholino)ethanesulfonic acid
MgCl ₂	Magnesium chloride
min	Minute
ml	Milliliter
mM	Millimol
MRM	Multiple reaction monitoring
msec	Milliseconds
NaCl	Natrium chloride
nm	Nanometer
OD	Optical density
PCR	Polymerase chain reaction
ppm	parts per million
PRAI	Phosphoribosylanthranilate Isomerase
PRAS	Phosphoribosylanthranilate Synthase

PTGS	Posttranscriptional gene silencing
qPCR	quantitative polymerase chain reaction
rcf	Relative centrifugal force
RDR6	RNA-dependent RNA Polymerase 6
RNA	Ribonucleic acid
rpm	Rounds per minute
sec	Second
T _m	Melting temperature
TRIBOA	2,4,7-Trihydroxy-(2H)-1,4-benzoxazin-3(4H)-one
TRIS	Tris(hydroxymethyl)aminomethane
Trp	Tryptophan
TS	Tryptophan synthase
U	Unit
UDP	Uracil diphosphate
UDP-GT	UDP-Glykosyltransferase
USER	Uracil specific excision reagent
UV	Ultraviolet
UV/VIS	Ultraviolet-visible
V	Volt
WT	Wild type

IV. Zusammenfassung

Benzoxazinoide (BXDs) sind spezialisierte Metabolite, welche primär bei Vertretern der Süßgräser (Poaceae) wie Mais, Weizen oder Gerste vorkommen. Die Biosynthese von BXDs ist in Mais völlig aufgeklärt worden. Als Ausgangssubstrat des Stoffwechselweges dient Indol-3-glycerolphosphat, welches zu der zyklischen, glykosylierten Hydroxamsäure 2,4-Dihydroxy-7-methoxy-1,4-benzoxazin-3-on (DIMBOA-Glc) konvertiert wird. Dies ist das häufigste BXD in unbeschädigtem Maisgewebe. Es besitzt eine verteidigende Funktion gegen Herbivoren und mikrobielle Pathogene. Bei Fraß von Herbivoren kann es in weitere toxische Produkte umgewandelt werden. Insgesamt werden acht Enzyme benötigt, um DIMBOA-Glc herzustellen. Dazu gehören BX1 bis BX7 sowie eine der beiden UDP-Glycosyltransferasen BX8 oder BX9. Neben Hydroxamsäuren werden in den Extrakten von produzierenden Pflanzen Lactamderivate gefunden, welche nicht am Stickstoff des heterozyklischen Ringes hydroxyliert sind. Das strukturell einfachste dieser dieser Derivate ist 2-Hydroxy-2-1,4-benzoxazin-3-on (HBOA), welches vom Enzym BX4 gebildet wird. Im Gegensatz zu Hydroxamsäuren akkumulieren Lactame nur in geringen Mengen in der Pflanze. Weder ist ihre biologische Funktion, noch der enzymatische Ursprung bekannt. Es besteht die Annahme, dass keine neuen Enzyme an ihrer Synthese beteiligt sind, sondern sie durch die Enzyme BX6 und BX7 produziert werden. Dabei wird HBOA nicht am Stickstoff durch BX5 hydroxyliert, sondern direkt von BX6 und BX7 als Substrat verwendet. Um diese Hypothese zu testen, wurden die Gene der BXD Biosynthese heterolog in Individuen der Tabakspezies *Nicotiana benthamiana* durch Agroinfiltration exprimiert. Das Enzym BX5, welches HBOA zur ersten Hydroxamsäure 2,4-Dihydroxy-1,4-benzoxazin-3-on (DIBOA) konvertiert, wurde dabei nicht in die Pflanzen eingebracht, um die Synthese von Hydroxamsäuren zu unterbinden. Die Expression der *Bx* Gene wurde mittels qPCR bestätigt. Extrakte der transformierten Pflanzen wurden mit gezielter LC-MS/MS, welche ein hochsensitives Triple-Quadrupol-System einsetzt, sowie mit ungezielten qTOF-Untersuchungen analysiert. HBOA-Glc wurde in Pflanzen detektiert, welche *Bx1* bis *Bx4* exprimieren. HBOA wurde auch ohne Co-Transformation von *Bx8* oder *Bx9* glykosyliert, was auf die Aktivität endogener Enzyme hindeutet. Zusätzliche Transformation mit *Bx6* und *Bx7* führte nicht zu einer nachweislichen Bildung von Lactamen und veränderte nicht den Gehalt von HBOA-Glc. Transformation mit *Bx5* dagegen führte zu Akkumulation von DIBOA-Glc. Bei heterologer Expression aller beteiligten Gene konnten keine BXDs nachgewiesen werden. Dies deutet darauf hin, dass die Enzyme aktiv sind, aber Endprodukte in nicht nachweisbare Konjugate umgewandelt werden. Daher konnte nicht gezeigt werden, dass BX6 und BX7 in der Lage sind, Lactame zu bilden.

V. Abstract

Benzoxazinoids (BXDs) are specialized metabolites primarily produced by members of the grass family (*Poaceae*) such as maize, wheat and barley. The BXD biosynthetic pathway is fully elucidated in maize. The core pathway starts with indole-3-glycerol phosphate and leads to the cyclic hydroxamic acid 2,4-dihydroxy-7-methoxy-1,4-benzoxazin-3-one glucoside (DIMBOA-Glc), which is the most abundant BXD in undamaged maize. It serves as defence compound against herbivores and microbial pathogens but can be further modified after herbivore attack into more toxic products. A total of eight enzymes are needed to synthesize DIMBOA-Glc, BX1 to BX7 as well as the UDP-glucosyltransferases BX8/9. Besides hydroxamic acids, corresponding lactam derivatives lacking hydroxylation at the nitrogen atom are always observed in minor amounts in maize, the first lactam 2-hydroxy-2-1,4-benzoxazin-3-one (HBOA) being an intermediate produced by BX4. However, neither the biological function nor the enzymes producing these lactams are known so far. It was postulated that they are not synthesized by novel enzymes but instead by BX6 and BX7 using HBOA as substrate. To test this hypothesis, in this study the BXD biosynthetic pathway was introduced and transiently expressed in *Nicotiana benthamiana* by agroinfiltration. BX5, which converts HBOA to 2,4-dihydroxy-1,4-benzoxazin-3-one (DIBOA), the first hydroxamic acid in the pathway, was not co-transformed in order to suppress formation of hydroxamic acids. The expression of *Bx* genes was confirmed and quantified by qPCR. Extracts of transformed plants were analysed in a targeted LC-MS/MS approach employing a triple-quadrupole system for high sensitivity as well as untargeted qTOF-scans for broad analysis. HBOA-Glc was detected in plants expressing *Bx1* to *Bx4*, while additional co-transformation of *Bx6* and *Bx7* yielded no other lactams and did not affect HBOA-Glc content. Occurrence of BXD glucoside without co-transforming *Bx8* or *Bx9* indicates activity of endogenous enzymes. Co-transformation of *Bx5* led to the production of DIBOA-Glc. No accumulation of DIMBOA-Glc or any other BXD was observed after expression of the complete pathway. This has led to the assumption, that enzymes are active, but downstream products are conjugated in an unknown manner. Thus, the ability of BX6 and BX7 to utilize lactams could not be confirmed.

1. Introduction

1.1 The role of secondary plant metabolism in ecological interactions

As sessile organisms, plants are subjected to the environment in which they grow. To survive, they must hold up against abiotic and biotic stress conferred by their surroundings (Mukherjee et al., 2016). Plants are constantly threatened by pathogen infections and herbivores feeding. They are competing with neighbouring plants for resources such as water, light, space and nutrients. In order to assert themselves, they have evolved mechanical and biochemical defences. Mechanical defences include structural changes like thorns, spines, hardened leaves, and granular minerals in leaf tissue (Hanley et al., 2007). These modifications either impede or prevent herbivore feeding. Plant trichomes protect against sunlight, drought, and can sense insect herbivores on the plant surface (Johnson, 1975). Biochemical defence is mediated by so-called specialized metabolites (Wisecaver et al., 2017), sometimes also referred to as secondary metabolites (Grotewold, 2005). Secondary, in contrary to primary, describes any compound that is not strictly essential for growth or survival of plants. At first, no function could be assigned for such metabolites although plants produce a wide range of them (Hartmann, 2007). In the last few decades, researchers have come to know that they play an important part in the interaction of plants with their environment. They can support structural defence by production of resins or waxes to hinder herbivores. Compounds such as anthocyanins (Feild et al., 2001) protect against UV-light or excessive sun exposure. Colourful pigments and volatiles attract pollinators to promote sexual reproduction (Glover, 2011). A wide variety of metabolites confer toxic effects on both herbivores and non-related plants growing in the surrounding environment (Matsuura and Fett-Neto, 2017). They can be produced directly upon pathogen infection or herbivore attack by plants sensing the tissue damage. In case of low molecular weight and induction by microbial infections, these compounds are referred to as phytoalexins (VanEtten et al., 1994). However, often defence chemicals are constitutively produced and stored in the plant tissue as inert derivatives or precursors. Whenever cells are ruptured or sense pathogenic elicitors, compounds are immediately released and are converted to their active form. The term of phytoanticipins has been chosen for such preformed metabolites released upon microbial attack. In special cases volatiles serve as a defence by attracting predators of attacking herbivores (McCormick et al., 2014). Today, over 200,000 specialized metabolites are known, and the list is continuously expanding. Interestingly, these secondary metabolites are often

specific in their taxonomic distribution, meaning that the corresponding pathways are restricted to a certain taxon.

1.2 Benzoxazinoids – A group of specialized metabolites in grasses

Benzoxazinoids (BXD) are a group of taxon-specific compounds, which can be mostly found in two subfamilies of the Poaceae, including important agricultural plants like maize, wheat or rye (Frey et al., 2009). The first BXD was discovered in the 1950s in rye (Willard and Penner, 1976). However, they have been described in some dicotylous species as well. These include a single species each in plant families Ranunculaceae, Lamiaceae and Plantaginaceae (Sicker et al., 2000; Alipieva et al., 2003) as well as several species in the Acanthaceae (Baumeler et al., 2000). BXDs and their derivatives have been found to exert protection against herbivores, bacteria and fungi (Niemeyer, 2009). They are active against a wide range of herbivores such as specialists like the European corn borer or generalists like nematodes and aphids. By deterring feeding insects like aphids, they can increase virus resistance (Ahmad et al., 2011). Moreover, BXDs confer allelopathic function against plants growing in near proximity. Concerning maize, the highest concentration of BXDs is found in seedlings from which they are actively secreted into the ground. Here, they are degraded spontaneously but also by microbial communities (Macias et al., 2005). Degradation products are taken up by surrounding plants and cause inhibition of growth, especially in the roots. Some studies suggest BXDs may play a role as phytosiderophores by chelating iron and mediating its uptake in plants producing them (Petho, 2002), exceeding the function as a protective chemical.

The most prominent BXDs in maize are the hydroxamic acids 2,4-dihydroxy-(2H)-1,4-benzoxazin-3(4H)-one (DIBOA) and its C-7-methoxy derivative 2,4-dihydroxy-7-methoxy-(2H)-1,4-benzoxazin-3(4H)-one (DIMBOA), which are usually stored as glucosides in the vacuole to reduce their toxicity and prevent damage to the plant itself. Upon tissue disruption by chewing herbivores or pathogens, the glucose moiety is cleaved off by β -glucosidases and the aglucones are released. Thus, these compounds could be referred to as phytoanticipins, although they do not solely work on microbes. The pathway responsible for synthesizing BXDs up to DIMBOA-Glc is well characterized and fully elucidated in maize (Frey et al., 1997; von Rad et al., 2001; Jonczyk et al., 2008).

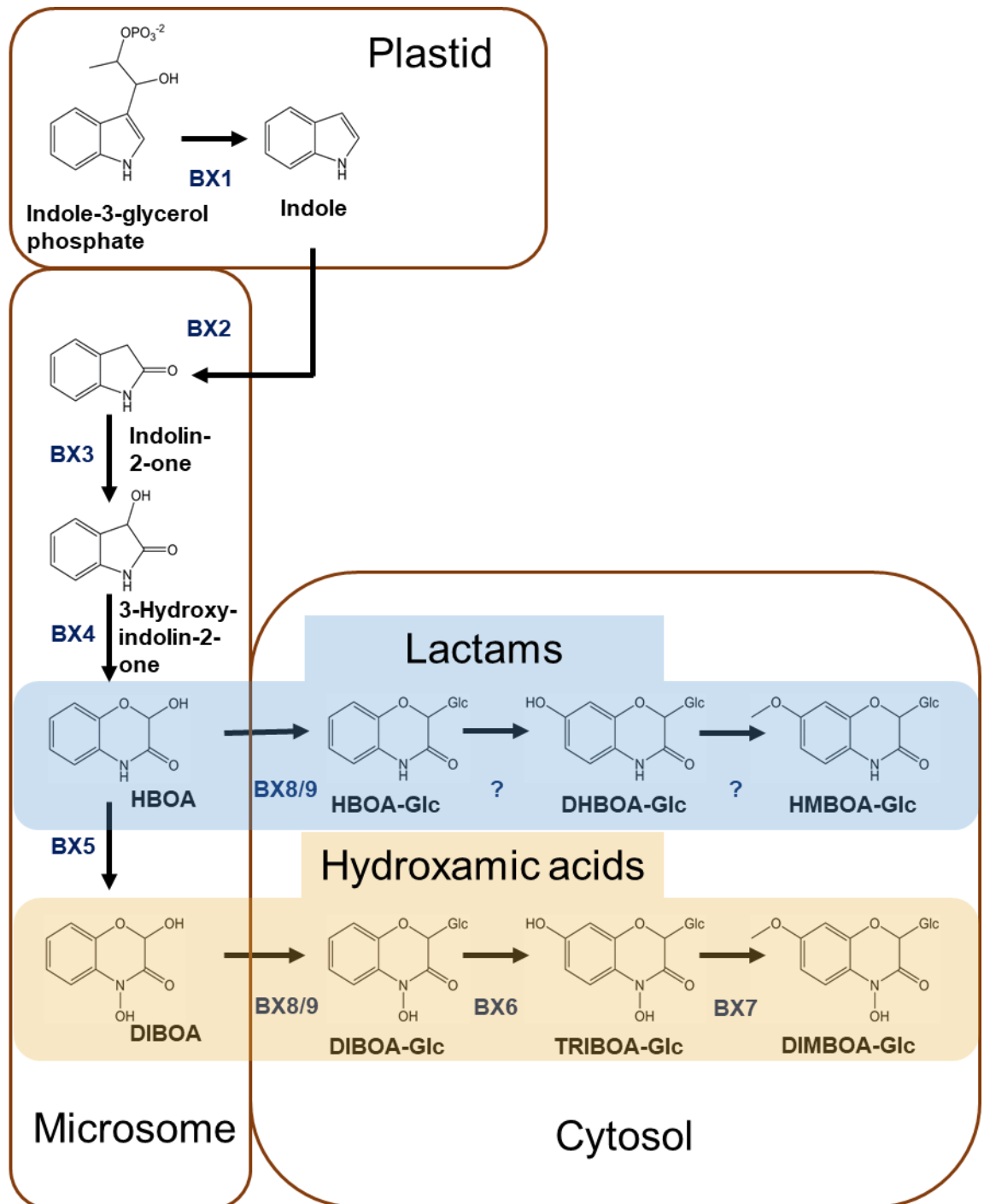


Figure 1: Benzoxazinoid biosynthetic pathway in maize. The localization of involved enzymes and groups of lactams and hydroxamic acids are highlighted. Glucosides can be further stored in the vacuole. Modified after Frey et al, 2009.

DIBOA is produced from indole-3-glycerol phosphate by the sequential catalysis of several enzymes (Figure 1). The indole-3-glycerol phosphate lyase (IGL) BX1 converts indole-3-glycerol phosphate (IGP) to indole by cleaving off glycerol phosphate. In this regard BX1 fulfils the same function as the α -subunit of tryptophan synthase (TS). Additionally, maize possesses another IGL, but in *Bx1*-knockout plants, BXDs are not produced (Wisecaver et al., 2017). This means, that indole from other sources cannot be used, probably due to direct substrate channelling. In case of the TS, free indole does

not accumulate in the tissue but is directly converted by the β -subunit to tryptophan (Trp). Free indole from BX1 can be subsequently oxidized to DIBOA by four different cytochrome P450 dependent monooxygenases (P450s), BX2-5. These P450s most likely work in close proximity as a complex at the endoplasmic reticulum. This hypothesis is supported by the fact that the genes for BXD biosynthesis up to DIBOA-Glc are clustered on the short arm of chromosome 4 in maize (Nutzmann et al., 2016). Remarkable is the ring expansion catalysed by BX4 leading to production of 2-hydroxy-(2H)-1,4-benzoxazin-3(4H)-one (HBOA), for which the mechanism is so far unknown. DIBOA, being the first toxic compound of the pathway, is glycosylated specifically by an UDP-glucosyltransferase (UDP-GT), which is either BX8 or BX9. Afterwards, DIBOA-Glc can be converted to DIMBOA-Glc by hydroxylation through the 2-oxoglutarate dependent dioxygenase BX6, converting it to TRIBOA-Glc, which is subsequently methylated by the O-methyltransferase BX7.

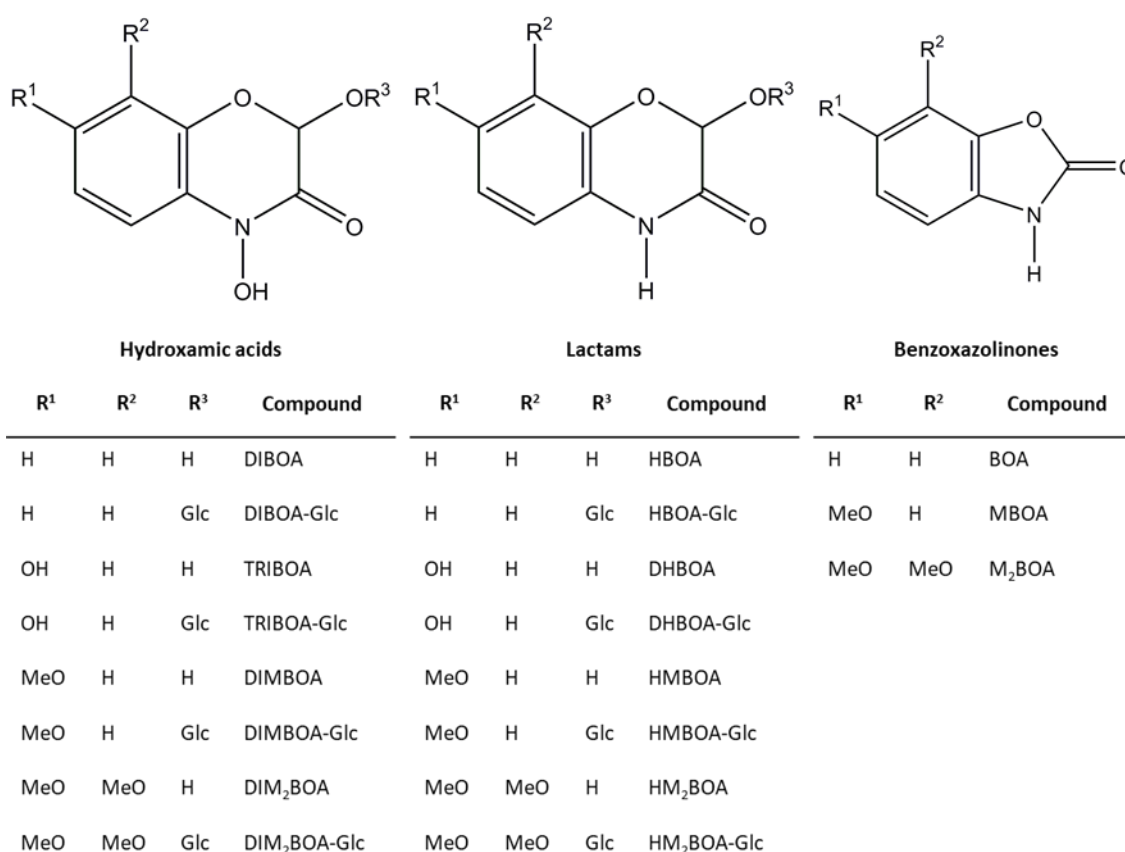


Figure 2: Benzoxazinoid derivatives and their degradation products benzoxazolinones. Methyl derivatives with methoxylated nitrogen are not depicted. Adapted after Niemeyer, 1988.

DIMBOA-Glc can then be even further converted by a set of additional enzymes, including O-methyltransferases BX10-BX12 and BX14 as well as the dioxygenase BX13 (Meihls et al., 2013; Handrick et al., 2016), which are not further described here. Apart from the hydroxamic acids, some lactam derivatives lacking the hydroxy group at the

nitrogen atom can also occur in the plants. Other than that, they are structurally homologous to the hydroxamic acids. They are accumulated in minor amounts and so far, no major activity has been ascribed to them. Enzymes responsible for the production of downstream lactams 2,7-dihydroxy-(2H)-1,4-benzoxazin-3(4H)-one (DHBOA) and 2-hydroxy-7-methoxy-(2H)-1,4-benzoxazin-3(4H)-one (HMBOA) have not been identified. Besides lactams and hydroxamic acids, so-called benzoxazolinones (Figure 2) were found in the early days of BXD research due to extraction in water. Non-glycosylated hydroxamic acids are not stable and convert quickly to benzoxazolinones in aqueous media. Therefore, they are not synthesized by enzymes but formed from hydroxamic acids by spontaneous degradation (Niemeyer, 1988). This process contributes to the biological activity of BXDs.

1.4 Connection of BXDs to primary metabolism

BX1, the first enzyme in the BXD biosynthetic pathway, uses IGP as substrate. This compound is an intermediate of the Trp biosynthetic pathway responsible for production of this essential amino acid in plants (Figure 3). The pathway has already been fully investigated in the mid-90s (Radwanski and Last, 1995). The starting compound is chorismate, which is converted to anthranilate (AA) by the anthranilate synthase (AS). AA is the first specific metabolite in Trp biosynthesis. Moreover, this step is the most important in the regulation of the pathway. Trp can bind to the AS as an allosteric inhibitor and suppress formation of AA. Therefore, its production is controlled by a negative feedback loop. If AA is made by the AS, it is subsequently converted to IGP by three enzymes. The phosphoribosylanthranilate synthase (PRAS) adds a phosphoribose-unit to the amino group. This compound is isomerized by the phosphoribosylanthranilate isomerase (PRAI), which opens the ribose ring. The indole-glycerolphosphate synthase (IGPS) closes the heterocyclic ring including the nitrogen from the amino group, thus converting the *o*-carboxyphenylamino intermediate to IGP. The TS, a tetramer comprised of two different subunits α and β , first cleaves off the glycerolphosphate, producing indole. This step performed by the α subunit is homologous to the reaction conferred by BX1. However, indole is not released but instead tunnelled directly to the β subunit, which ultimately converts it to Trp.

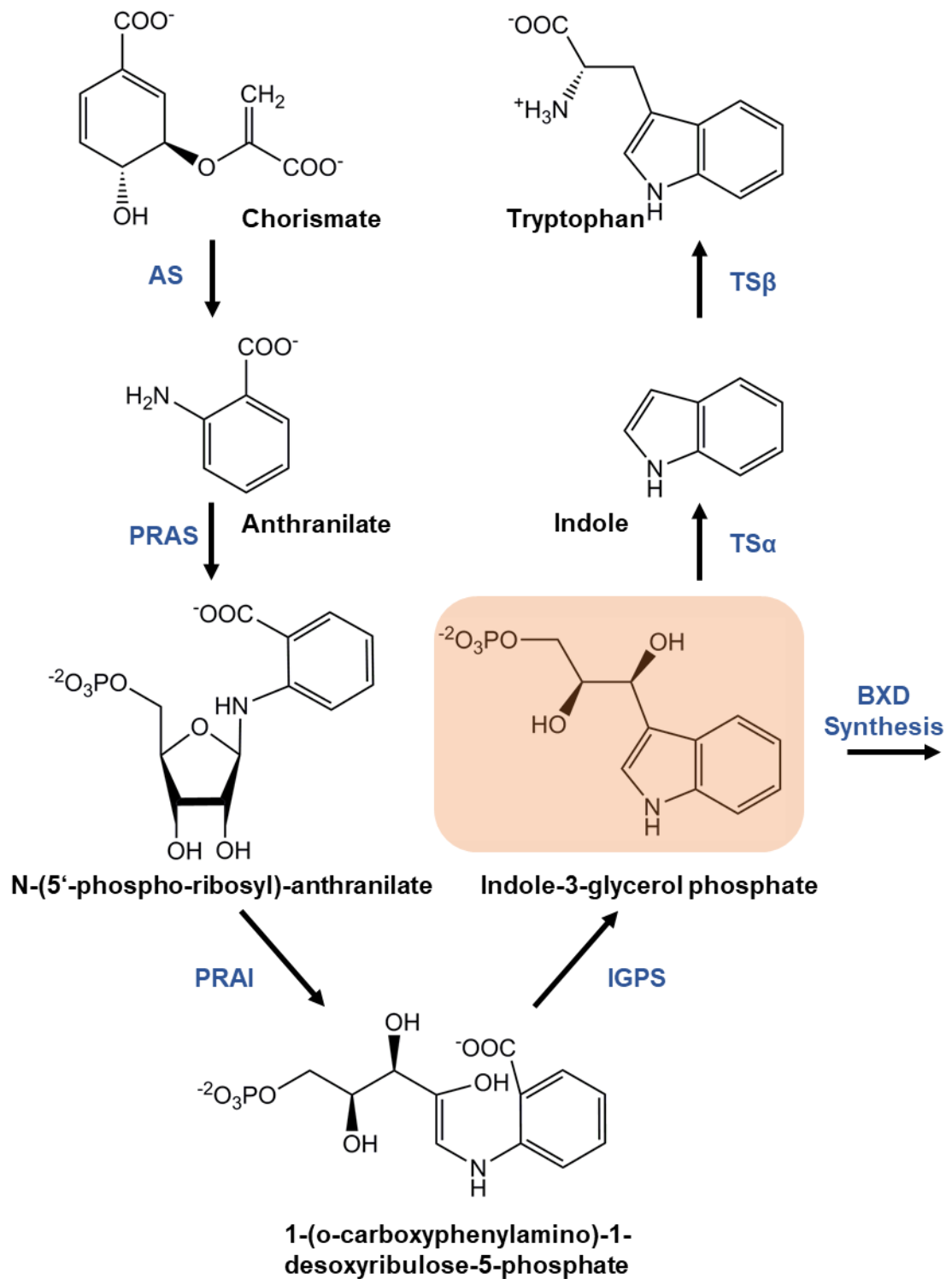


Figure 3: Tryptophan biosynthesis in plants. The pathway is controlled via negative feedback regulation of tryptophan inhibiting anthranilate synthase. Indole-3-glycerol phosphate, marked in red, is the compound used by BX1 in BXD biosynthesis as a substrate. AS = Anthranilate synthase, PRAS = Phosphoribosylanthranilate synthase, PRAI = Phosphoribosylanthranilate isomerase, IGPS = Indole-Glycerol Phosphate synthase, TS α / β = Tryptophan synthase A/B. Modified after Radwanski and Last, 1995.

1.4 The Reactivity and mechanisms of action of BXDs

Reaction mechanisms conferring the biological activity of BXDs have been extensively reviewed. Reactivity of hydroxamic acids is dependent on the instability caused by the nitrogen atom in the heterocyclic ring as well as hydroxylation at the nitrogen and the C2-atom (Wouters et al., 2016). Reversible ring opening by oxo-cyclo tautomerism seems to play a role, leading to degradation of BXDs to reactive benzoxazolinones. The exact mechanism is not clear yet, but generally formic acid is released. Lactams lacking the hydroxylation at the nitrogen are less likely to undergo ring opening and are thus overall less reactive. BXDs glycosylated at the C2-hydroxyl functionality are chemically inert as well, probably also due to higher hydrophilicity. By ring opening, hydroxamic acids can react with thiol groups in cysteine and impair enzyme function. It has been hypothesized this mechanism leads to glutathione depletion in the cytosol (Dixon et al., 2012) by which hydroxamic acids act as pro-oxidants. Benzoxazolinones are structurally similar to growth-inducing auxins and compete with them for auxin receptors, effectively reducing growth of plants (Hoshisakoda et al., 1994). They have further been identified to activate hormonal receptors in animals since they resemble signalling molecules like melatonin, serotonin and Trp (Zhou et al., 2018). In this regard, they were observed to stimulate reproductive systems. Lactams, although tested on biological activity towards a wide range of organisms, do not exhibit notable impact on any of them. Some antimicrobial properties were detected, but both hydroxamic acids and benzoxazolinones show lower minimal inhibitory concentrations. Since neither the enzymatic origin nor their biological function has been revealed so far, lactams were designated as degradation products (Macias et al., 2004).

1.5 BXD Lactams – Unsolved origins

It is remarkable, that BXD lactam derivatives accumulate in amounts much lower than other BXDs. Even when biological activity was observed, required concentrations are unlikely to occur *in planta*. This raises the question why the plant produces these compounds – and how. It was observed in *in vitro* assays, that DIMBOA can be reduced to the corresponding lactam HMBOA by thiols (Wouters et al., 2016), but the mechanism for this has not been fully characterized yet. When looking for BXDs in soil treated with rye residues, lactams were the predominant group of compounds detected (Teasdale et al., 2012). These findings have led to the hypothesis, that lactams are simply leftovers from hydroxamic acids by degradation processes or after having exerted their influence on a target organism. On the other hand, lactams such as DHBOA and HMBOA are also

proposed as precursors of hydroxamic acids since they only differ in hydroxylation at the nitrogen. Structural similarity of both groups provides an alternative hypothesis for the origin of lactams. The conversion of HBOA to HMBOA-Glc requires the same modifications as from DIBOA to DIMBOA-Glc. Although both pathways can be the result of two different sets of enzymes, it might as well be the same. Independent of the hydroxylation at the nitrogen, BX6 and BX7 could be able to use both HBOA- and DHBOA-Glc as substrate (Figure 1).

1.6 Elucidating the origin of lactams – Choice of methods

To test whether BX6 and BX7 can convert HBOA to HMBOA, enzyme activity can be monitored in e.g. knockout lines or *in vitro* assays. However, these approaches require tedious preparations of isolating specific mutants, enzymes and substrate. Moreover, it is questionable whether *in vitro* assays depict the situation given in plants. An easy way to test the activity of BX6 and BX7 towards lactams is by transient expression *in planta* (Gelvin, 2003). This is achieved by introducing the BXD biosynthetic genes into a novel plant host by agroinfiltration. For this, genes need to be inserted into a compatible vector and subsequently, the vector is transferred into *Agrobacterium tumefaciens*. Agrobacteria naturally enter wounded plants and integrate genes into the plant genome, causing massive cell replication leading to callus formation in plant organs. This is referred to as crown gall disease (Zupan et al., 2000). Agrobacteria introduce genes encoding the biosynthetic pathway of small molecules such as octopines and nopalines, which can be efficiently metabolized by the bacteria. Researchers have identified these pathogenic genes on the so-called T-plasmid and replaced them with genes of interest to utilize Agrobacteria for plant transformation. By now, advances in binary vector systems and cloning techniques have made this technology of genetic engineering widely applicable (Norkunas et al., 2018). *Nicotiana benthamiana*, a close relative of the well-known tobacco plant *Nicotiana tabacum*, has emerged as the model organism for agroinfiltration (Bally et al., 2018). Their short life cycle and susceptibility to the transformation process is suitable for both transient and stable transformation applications. The overall efficiency measured by heterologous protein expression levels is comparably high and requires no additional treatments such as sonication. The BXD biosynthetic pathway can be reconstructed bit by bit. Since BXDs have not been described in *Nicotiana*, endogenous enzymes are not expected to interfere specifically with the expressed pathway, although conjugation reactions cannot be ruled out.

1.7 Objective

The following approach attempts to elucidate the BXD lactam origin. The BXD pathway of maize (*Zea mays*) up to DIMBOA-Glc is reconstructed in *N. benthamiana* by a transient transformation approach. *Bx* genes are isolated from genomic maize DNA and cloned with a suitable vector system using the highly efficient USER-cloning technique. The constructed plasmids are introduced into a compatible *A. tumefaciens* strain via a binary vector system. Subsequently, plants are inoculated with bacteria carrying these vectors via vacuum infiltration for introduction of *Bx* genes. Transiently expressed plants are tested on BXD production by targeted and untargeted liquid chromatography-mass spectrometry (LC-MS) analysis. *Bx* gene expression is analysed by quantitative polymerase chain reaction (qPCR) to verify the integration of heterologous genes. Additionally, to achieve the production of the lactam HMBOA-Glc, BX5 is excluded from the reconstructed pathway to suppress conversion of HBOA to hydroxamic acids and instead test the ability of BX6 and BX7 to utilize HBOA as a substrate for production of downstream lactam derivatives. Here, plants are tested for the accumulation of HMBOA-Glc, the corresponding lactam to the hydroxamic acid DIMBOA-Glc. Furthermore, substrate feeding experiments with transformed plants are carried out to increase the overall production of BXDs.

2. Material and methods

2.1 Cultivation of plants

Seeds of tobacco (*Nicotiana benthamiana*) were sown in TEKU JP 3050 104 pots (Pöppelmann GmbH & Co. KG, Lohne, Germany) using Klasmann plug soil (Klasmann-Deilmann GmbH, Geesten, Germany). TEKU pots were placed in plastic trays under a lid and transferred to the greenhouse set to 23-25 °C at day and 19-23 °C at night under 16 h of supplemental light (Intensity: ~200 $\mu\text{mol}/\text{m}^2$). The lids remained closed until seedlings developed cotyledons, after which it was opened gradually until complete removal three days after. After 15-20 days, seedlings were transferred to larger pots (7 cm x 7 cm) in Fruhstorfer Nullerde (Hawita GmbH, Vechta, Germany) supplemented with 0.9 g Superphosphate, 0.5 g Multimix 14:16.18 (Yara, Vlaardingen B.V., Netherlands), 0.35g $\text{MgSO}_4 \cdot 7\text{H}_2\text{O}$ (Merck KGaA, Darmstadt, Germany) and 0.05 g Micromax (Scotts Deutschland GmbH, Nordhorn, Germany) per 1 l soil. The plants were fertilized once per week with 0.1 % Peters Professional Allrounder (ICL, Nordhorn, Germany).

2.2 Microbiological methods

2.2.1 Cultivation of *Escherichia coli*

E. coli were plated out after transformation (see chapters 2.3.7, 2.4.5, and 2.5.3) on prewarmed LB plates (100 mm x 15 mm) with the following composition: 10 g Tryptone, 5 g yeast extract, 5 g NaCl and 20 g agarose. Plates were additionally supplemented with the antibiotic kanamycin (50 $\mu\text{g}/\text{ml}$) for selection of bacteria with the introduced vectors. After plating out transformed *E. coli* cells, plates were incubated overnight at 37 °C and 220 rpm. The following day, positive colonies containing the target construct, which was determined by colony PCR (see chapter 2.3.8), were picked with a toothpick for inoculation of liquid LB medium without agarose. Liquid cultures were again incubated overnight at 37 °C and 220 rpm. From these cultures, plasmids are purified according to instructions in chapter 2.3.9.

2.2.2 Cultivation of *Agrobacterium tumefaciens*

Stocks of GV3101 *A. tumefaciens* cells transformed with pCambia-vectors (see chapter 2.4.6) were plated out on prewarmed LB agar plates. To select for successfully transformed bacteria, plates include antibiotics rifampicin (25 µg/ml) and gentamycin (25 µg/ml) due to the internal resistance genes of the GV3101 strain as well as kanamycin (50 µg/ml) for selection of pCambia-transformed cells. Plates were incubated for 2 days at 28 °C and 220 rpm. Afterwards, colonies were checked by colony PCR and positive clones picked for inoculation of liquid LB medium to prepare cultures for agroinfiltration or glycerol stocks (see chapters 2.5.1 and 2.2.4). For the production of chemically competent GV3101 stocks, LB medium containing only rifampicin and gentamycin was inoculated with non-transformed cells. Liquid cultures were incubated at 28 °C and 220 rpm for 1-2 d.

2.2.3 Preparation of competent *A. tumefaciens* stocks

10 ml of LB medium were inoculated with 20 µl of GV3101 *A. tumefaciens* stock and incubated according to instructions in chapter 2.2.2. The following day, 2 ml of preculture were added to 50 ml of fresh LB medium and incubated at 28°C and 220 rpm until an OD⁶⁰⁰ of approx. 0.6 had been reached. OD was measured on an Ultrospec 2100 Pro photometer (Amersham Biosciences, Little Chalfont, UK). The culture was put on ice and centrifuged for 5 min at 4200 rcf and 4°C in an Avanti J-20 XP centrifuge (Beckman Coulter GmbH, Krefeld, Germany). Supernatant LB medium was removed, the cell pellet resuspended in 4 ml of 20 mM CaCl₂ and left on ice for 15 min. Resuspended cells were split into aliquots of 100 µl each, flash frozen in liquid nitrogen and stored at -80°C.

2.2.4 Glycerol stocks

10 ml of LB medium (+ 50 µg/ml Kanamycin, 25 µg/ml Gentamycin, 25 µg/ml Rifampicin) were inoculated with an *A. tumefaciens* colony transformed with pCambia2300U carrying p19, *eGFP* or a *Bx* gene. Cultures were grown overnight (28°C, 220 rpm). 750 µl of overnight culture were mixed with 750 µl of sterile 50% glycerol solution in 1.7 ml Safe-Twist[®] tubes (Eppendorf AG, Hamburg, Germany) and flash frozen in liquid nitrogen. Stocks were immediately stored at -80°C.

2.3 Subcloning

To simplify the process of cloning *Bx* genes into the vectors compatible for agroinfiltration, target genes were first introduced into a subcloning vector. In the following cloning procedure, this was meant to reduce disrupting influences by the maize genome which may possibly lead to unspecific primer annealing due to the more complicated process of the applied cloning technique.

2.3.1 RNA Extraction

RNA was extracted from 60-70 mg non-induced B73 or fungus-induced W22 maize (*Zea mays*) leaf material, which was ground to a homogenous powder. RNA-Extraction was done using the Invitrap® Spin Plant RNA Mini Kit (STRATEC Molecular GmbH, Berlin, Deutschland) according to manufacturer's instructions. To remove residual genomic DNA, 1 µl DNase I (Fisher Scientific GmbH, Schwerte, Germany) was added to 1 µg of extracted RNA with 1 µl DNase I buffer in a total volume of 10 µl. This reaction mix was incubated for 30 min at 37 °C. Afterwards, 1 µl of EDTA (Fisher Scientific GmbH) was added and the incubation continued for 10 min at 65 °C.

2.3.2 cDNA Synthesis

For cDNA synthesis the First strand cDNA Synthesis Kit (Fisher Scientific GmbH) was used. 1 µl of oligo-dT primer and 1 µl dNTPs was added to the total DNase-treated RNA and incubated for 5 min at 65 °C. Then, 4 µl of 5X first strand buffer, 1 µl of DTT, 1 µl of RNase Out and 1 µl of SuperScript™ III reverse transcriptase was added to give a total volume of 20 µl. This preparation was incubated for 5 min at 25 °C, 1 h at 50 °C and finally 15 min at 70 °C.

2.3.3 Amplification of DNA

Bx-genes were amplified from *Z. mays* cDNA via polymerase chain reaction (PCR) in the peqSTAR 2X Gradient Thermocycler (VWR International GmbH, Darmstadt, Germany) using the Phusion High-Fidelity DNA Polymerase (Fisher Scientific GmbH) or Q5 High-Fidelity DNA Polymerase (New England Biolabs, Ipswich, USA). Components are listed in table 1 for Phusion and Q5 PCR. Gene specific primers are listed in the supplementary table I.

Table 1: Phusion- and Q5-PCR Protocol. Reaction composition and thermocycler conditions.

PCR Reaction		
Reagent	Amount (µl)	
5X High GC / 5X Q5 Buffer	10	
10 mM dNTPs	1	
10 µM Primer forward	2.5	
10 µM Primer reverse	2.5	
DMSO (Phusion)	1.5	
5X Q5 High GC Enhancer (Q5)	10	
Phusion/Q5 HF DNA Polymerase	0.5	
cDNA	2-4	
ddH ₂ O	ad 50	

Thermocycler conditions		
Step	Temperature	Duration
Initial Denaturation	98 °C	2 min
Denaturation	98 °C	10 sec
Annealing	58-65 °C	30 sec
Elongation	72 °C	45 sec
Final Elongation	72 °C	5 min

} x35

2.3.4 Gene synthesis

Bx8 could not be amplified from *Z. mays* cDNA and was therefore synthesized by GeneArt Gene synthesis (Fisher Scientific GmbH) and subsequently cloned into the standard pMK expression vector with kanamycin resistance gene.

2.3.5 Gelelectrophoresis

To visualize the amplification of target genes, PCR-products were analysed on 1.5 % agarose gels (Agarose-broad range, Carl Roth GmbH & Co. KG, Karlsruhe, Germany) made with 0.5X TAE buffer (20 mM TRIS, 10 mM acetic acid, 0.5 mM EDTA) containing 2.5 µl of Midori^{Green} (Nippon Genetics Europe, Düren, Deutschland) per 100 ml for DNA staining. Gels were run using the Mupid®-One Electrophoresis System (Biozym Scientific GmbH, Hessisch Oldendorf, Deutschland) in 0.5X TAE buffer for 20 min at a voltage of 135V. For comparison of fragment length, 5 µl of Gene Ruler™ 1kb DNA ladder (Fisher Scientific GmbH) was loaded onto each gel.

Fragments amplified by qPCR (see chapter 2.5.3) were run on 2 % agarose gels for 15 min at 135 V since target sequences were below 100 bp. Invitrogen™ Low mass DNA ladder (Fisher Scientific GmbH) was used for determining fragment length.

2.3.6 Purification of PCR-products

PCR-products were purified using either the QIAquick® PCR-purification or Gel Extraction kit (QIAGEN, Venlo, Niederlanden) according to the manufacturer's instructions. For gel extraction, the total volume of PCR reactions was loaded onto an agarose gel for separation of the target gene. The bands were made visible under blue light with the DarkReader® (Clare Chemical Research, Dolores, USA) and excised from the gel using a scalpel. DNA concentration of purified samples was measured with a Nanodrop 2000c UV/VIS spectral photometer (Fisher Scientific GmbH).

2.3.7 Transformation of *E. coli*

6-8 ng of purified DNA was mixed with 0.5 µl salt solution and 0.5 µl pCR®-Blunt II-TOPO® vector (Fisher Scientific GmbH) for subcloning *Bx* genes in a total volume of 3 µl. This reaction mixture was incubated for 30 min at room temperature. Afterwards it was added to 50 µl of chemically competent 10-beta *E. coli* cells (New England Biolabs). Cells were incubated on ice for 30 min, heat shocked for 45 sec in a 42 °C water bath type 1002 (GFL mbH, Burgwedel, Germany) and immediately transferred back to ice. 150 µl of SOC medium (New England Biolabs) was added and the cells were incubated for 1 h at 37 °C and shaking with 220 rpm. Then they were plated on pre-warmed selective LB medium plates and incubated overnight.

2.3.8 Colony PCR

For each plate, colonies were analysed via colony PCR (Table 2) using the GoTaq® G2 DNA Polymerase (Promega GmbH, Walldorf, Germany). The insertion site was amplified by using flanking primers specific for the vector. This process served the purpose of investigating whether a gene with the expected size was introduced into the vector. Colonies were suspended in the PCR reaction and run in the peqSTAR 2X Gradient Thermocycler. PCR products were analysed on 1.5 % agarose gels (see chapter 2.3.5). Afterwards, positive clones were picked to prepare overnight cultures in 5 ml LB medium (see chapter 2.2.1).

Table 2: Colony-PCR protocol. Reaction composition and thermocycler conditions.

PCR Mix		
Reagent	Amount (µl)	
5X Green GoTaq Buffer	5	
10 mM dNTPs	0.5	
10 µM Primer forward	1	
10 µM Primer reverse	1	
5X GoTaq DNA Pol.	0.125	
H ₂ O	ad 25	

Thermocycler conditions		
Step	Temperature	Duration
Initial Denaturation	95 °C	10 min
Denaturation	95 °C	30 sec
Annealing	55 °C	30 sec
Elongation	72 °C	1.5 min
Final Elongation	72 °C	5 min

} x25

2.3.9 Plasmid Purification

Positive *E. coli* clones determined by colony PCR were picked to inoculate 5 ml LB medium for overnight incubation. The following day, plasmids were purified from the cultures using the low copy protocol of the NucleoSpin® Plasmid Kit (Macherey-Nagel, Düren, Deutschland). Cultures and samples were centrifuged with a 5424 R centrifuge (Eppendorf AG) at 11363 rcf. DNA from columns was eluted at 70 °C with a volume of 30 µl provided elution buffer.

2.3.10 Sequencing

Before using the subcloning vectors for subsequent cloning, inserted fragments were amplified using the BigDye® Terminator v1.1 Cycle Sequencing Kit (Fisher Scientific GmbH) to confirm sequences of *Bx* genes. Components and PCR conditions are listed in table 3. To remove the terminator dyes from the fragments, PCR samples were purified with the Agencourt CleanSEQ Dye-Terminator Removal Protocol (Beckman Coulter GmbH). Sequencing was done using the ABI Prism® - Gen- Analysator 3130xl (Fisher Scientific GmbH).

Table 3: Sequencing PCR protocol. PCR mix is prepared with either forward or reverse primer for each sample.

PCR Mix		
Reagent	Amount (μl)	
5X BD Seq Buffer	2	
10 μ M Primer forward/reverse	1	
BD	2	
DNA 70-75 ng/ μ l	2	
H ₂ O	ad 10	

Thermocycler conditions		
Step	Temperature	Duration
Initial Denaturation	96°C	10 min
Denaturation	96°C	30 sec
Annealing	55°C	30 sec
Elongation	60°C	1.5 min

} x35

2.4 Uracil-specific excision reagent (USER)-cloning

For cloning *Bx* genes into a suitable vector for plant transformation by agroinfiltration, subcloning vectors containing the corresponding genes were subjected to a USER-based cloning technique (Nour-Eldin et al., 2006). USER-compatible primers were designed by adding eight nucleotides to the 5'-end of gene specific forward and reverse primer (Supplementary table II). To ensure directional insertion, overhangs for forward and reverse primers differed in one nucleotide. Overhangs were complementary to the linearized USER cassette in the destination vector, pCambia2300U (Cambia, Cranberra, Australia). This specific vector was derived by the pCambia2300 construct by implementing a *PacI* USER cassette for USER-cloning compatibility. Cambia constructs are commonly used plasmids for binary vector systems employed in transformation of plant hosts by agroinfiltration. The pCambia2300U vectors containing genes for Enhanced green fluorescent protein (eGFP) and viral suppressor p19, which were used in agroinfiltration besides *Bx* genes, were provided by members of the research group.

2.4.1 USER-based DNA amplification

Bx genes were amplified from subcloning vectors using the Phusion U Hotstart Polymerase (Fisher Scientific GmbH) or PfuTurbo® Cx Hotstart DNA Polymerase (Agilent Technologies, Santa Clara, USA), described in table 4. PCR reactions were analysed on agarose gel to confirm the correct fragment size (see chapter 2.3.5).

Table 4: Phusion U and PfuTurbo Cx Hotstart USER-PCR protocol. Thermocycler conditions include two different cycles, the first one annealing at a temperature for the gene specific part of the primer, the second at a temperature suitable for the complete USER primer with 8 bp overhangs. The amounts used in the PCR-Reaction are mentioned for Phusion U and PfuTurbo Cx polymerase, respectively.

PCR-Reaction		
Reagent	Amount (µl)	
Plasmid DNA template	1 (≈30 ng)	
5X Phusion GC Buffer/10X PfuTurbo Reaction Buffer	10/5	
10 mM dNTPs	1	
10 µM USER-Primer forward	2.5/1	
10 µM USER-Primer reverse	2.5/1	
DMSO (Phusion)	1.5-3	
Phusion U/ PfuTurbo Cx Hotstart Pol.	0.5/1	
ddH ₂ O	ad 50	

Thermocycler conditions		
Step	Temperature	Duration
Initial Denaturation	95 °C	2 min
Denaturation	95 °C	30 s
Annealing	T _m -5 (see Table II)	30 s
Elongation	72 °C	1 min 30 s
} x10		
Denaturation	95 °C	30 s
Annealing	T _m -5 (see Table III)	30 s
Elongation	72 °C	30 s
} x25		
Final Elongation	72 °C	10 min

2.4.2 *DpnI*-Digestion

Subcloning and pCambia2300U-vectors both contained kanamycin resistance genes for selection, therefore all subcloning vector template needed to be removed to prevent false positives in the following transformation. To digest remaining pCR®-Blunt II-TOPO® vector, 40 µl of USER-PCR mix were incubated with 1 µl of *DpnI* enzyme (New England Biolabs) for 1 h at 37 °C. The enzyme was deactivated at 80 °C for 20 min. The digestion reaction was purified, and DNA content measured according to instructions in chapter 2.3.6.

2.4.3 Linearization of pCambia2300U

10 µl of circular plasmid DNA (≈5 ng) were mixed with 10 µl 10X CutSmart Buffer (New England Biolabs) and 4 µl (40 U) PaeI (New England Biolabs) in a total volume of 100 µl and incubated for 1 h and 15 min at 37°C. Afterwards, 2 µl (20 U) of Nt.BbvCI (New England Biolabs) were added and the mix incubated for 1 h and 30 min at 37°C. Enzymes were deactivated at 80°C for 20 min.

2.4.4 USER-Reaction

DpnI-digested and purified PCR-product was mixed with linearized pCambia2300U vector in relation of 10:1 and 1 µl USER® Enzyme (New England Biolabs) in a total volume of 10 µl. The ligation mix was incubated for 20 min at 37 °C, followed by 20 min at 25 °C.

2.4.5 Transformation of *E. coli* with pCambia2300U vectors

The ligation reaction mix prepared in the USER-reaction was used to transform chemically competent 10-beta *E. coli* cells (New England Biolabs). The same protocol was applied as described in chapter 2.3.7. Incorporation of the *Bx* gene with the correct fragment size in pCambia2300U-vector was tested by colony PCR (see chapter 2.3.8). Positive transformants were picked for inoculation of 5 ml LB cultures left overnight to grow (see chapter 2.2.1). Plasmids were purified from overnight cultures and inserts sequenced as described in chapter 2.3.9 and 2.3.10, respectively.

2.4.6 Transformation of *A. tumefaciens* with pCambia2300U vectors

1 µg of pCambia2300U plasmid DNA was added to one vial of 100 µl chemically competent GV3101 *A. tumefaciens* cells. Cells were thawed for a few minutes in a water bath at 37 °C. Afterwards, cells were flash frozen in liquid nitrogen and again put into a 37 °C water bath. After thawing, they were incubated on ice for 30 min with mixing from time to time. 1 ml of LB medium was added, and the vials were incubated for 2 h at 28°C and 220 rpm. The cells were pelleted for 30 sec at 11363 rcf in a table top centrifuge, resuspended in 100 µl LB medium and plated on prewarmed LB plates prepared according to the instructions in chapter 2.2.2.

2.5 Heterologous expression of Bx genes in *N. benthamiana*

2.5.1 Agroinfiltration of *N. benthamiana*

20 ml of LB medium prepared as described in chapter 2.2.2 were inoculated with a small amount of glycerol stocks containing *A. tumefaciens* transformed with pCambia2300U carrying either genes p19, eGFP or one of *Bx* genes *Bx1* to *Bx9* and incubated overnight at 28°C and 220 rpm for a preculture. For the main culture, 5 ml of preculture were added to 100 ml LB medium containing the corresponding antibiotics for selection. The amount of main culture was adjusted to the number of transformed plants. Main cultures were incubated overnight at 28°C and 220 rpm. The following day, cultures were centrifuged for 5 min at 3752 rcf in an Avanti J-25 centrifuge (Beckman Coulter GmbH). LB medium was removed, and cell pellets were resuspended in infection medium (10 mM MES 5.7 pH, 10 mM MgCl₂, 100 µM Acetosyringone). Acetosyringone was added to the medium shortly before use. Absorption of resuspended cultures was measured at 600 nm and cultures were diluted with infection medium to an OD of 0.4-0.6. Cell dilutions were incubated for 2 h at room temperature and 110 rpm.

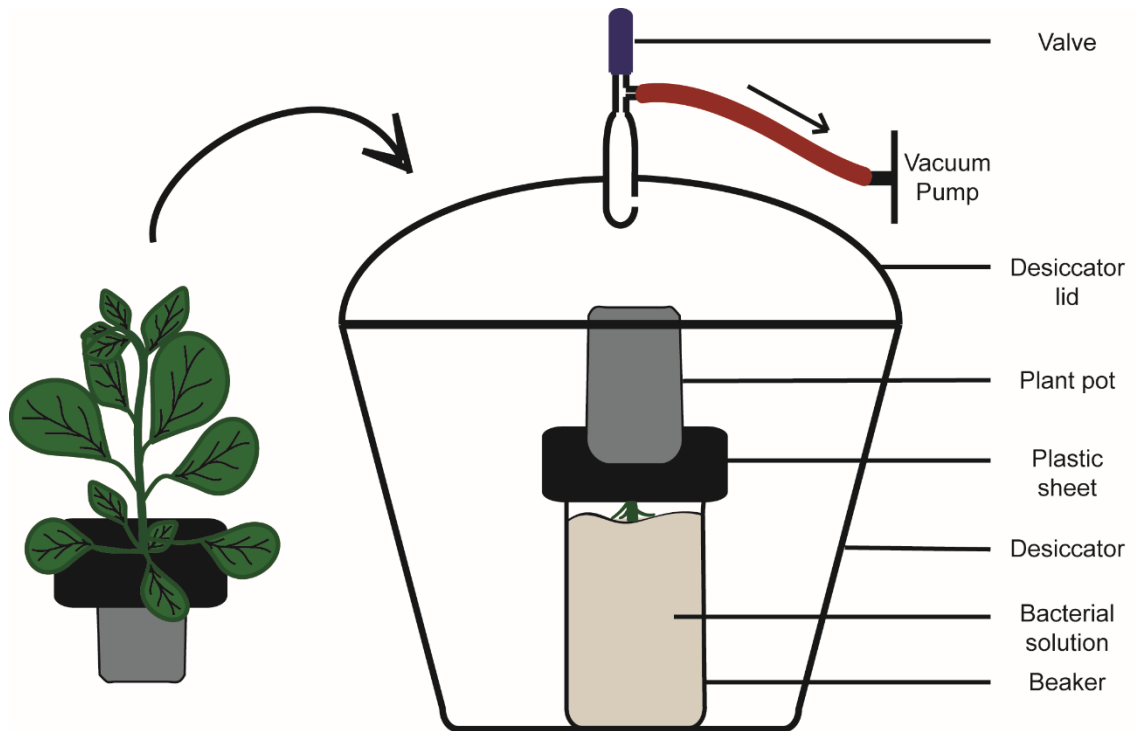


Figure 4: Setup of the vacuum chamber for agroinfiltration of *Nicotiana benthamiana*. Plants were dipped upside down into a beaker with Agrobacteria solution, after which the lid was sealed, and vacuum was applied by a connected pump.

3-4-week-old *N. benthamiana* plants were watered a few hours before transformation and again at the beginning of the experiment. In case of stress caused by dehydration, stomata through which bacteria enter the plant are closed, thus frequent watering facilitated a more effective infiltration. For each treatment, solutions of Agrobacteria transformed with the genes chosen to be transferred were mixed evenly in a 1 l beaker. Bacteria containing the *p19* construct were always added for suppression of post-transcriptional gene silencing (PTGS) to ensure higher expression levels of *Bx* genes (Voinnet et al., 2003). The beaker was positioned in a vacuum chamber and plants were dipped upside down into the beaker (Figure 4). The soil in the plant pots was covered by plastic sheets to prevent it from dropping into the solution. After closing the chamber lid, vacuum was applied for a total amount of 2 min for each plant, reaching a minimum pressure of 25 mbar. Plants were left in a dimmed room for 2-3 days and afterwards moved under a Valoya® R300 NS1 light source (Valoya Oy, Helsinki, Finland) emitting at 75 % intensity leading to a total measured light efficacy of 145 $\mu\text{mol}/\text{m}^2$ on the leaf surface. 1-2 days later, leaves were harvested from each plant and flash frozen in liquid nitrogen.

Frozen leaves were subsequently ground to a homogenous powder with mortar and pestle in liquid nitrogen.

2.5.2 Anthranilate assay

Directly after moving transformed plants under a light source, leaves were cut off from each plant and placed into 15 ml falcon tubes containing 1 mM or 10 mM anthranilate (Merck KGaA) solution. Anthranilate was solved in ethanol before adding it due to poor solubility in water, leading to a 1 % EtOH concentration in the solution. dH₂O with 1 % EtOH was used as control. Leaves were left for 2 days in the solution under the light source described in 2.5.1, after which they were flash frozen in liquid nitrogen and ground in liquid nitrogen with mortar and pestle to a homogenous powder.

2.5.3 qPCR

For expression analysis of transformed genes, RNA was extracted from ground leaf material of *N. benthamiana* plants. 50-75 mg were used from each sample for purification of RNA and synthesis of cDNA according to chapters 2.31 and 2.3.3, respectively. For qPCR, cDNA was diluted with ddH₂O at a ratio of 1:10.

For each sample, 1 µl of cDNA was mixed with 1 µl of forward and reverse primer, 10 µl of 2X Brilliant III SYBR® Green QPCR (Agilent Technologies) and added up to final volume of 20 µl with ddH₂O on a 96-well plate (Bio-Rad Laboratories GmbH, Feldkirchen, Germany). Conditions for PCR and determination of melting curve are described in Table 5. The plates were analysed on a CFXConnect™ Optics Module (Bio-Rad Laboratories GmbH).

Table 5: qPCR programme for *N. benthamiana* cDNA samples.

Step	Temperature	Time	
Initial Denaturation	95°C	3 min	
Denaturation	95°C	10 sec	} x40
Annealing/Elongation	60°C	10 sec	
Plate read after every cycle			
Denaturation	95°C	10 sec	
Calculation of melting curve (with constant plate read)	65°C to 95°C	0.5°C per 5 sec (5 min)	

For relative quantification, the expression of target genes was normalized to the expression of the housekeeping gene (HKG) GAPDH from *N. benthamiana* as internal reference. cDNA from plants transformed with *eGFP* was used as control. Each cDNA

sample was measured in triplicates. Normalized expression was calculated by the “ $\Delta\Delta Cq$ ” method with the following algorithm in the CFX Manager 3.1 software (Bio-Rad Laboratories GmbH):

$$\begin{aligned}\Delta Cq &= Cq_{Target} - Cq_{GAPDH} \\ \Delta\Delta Cq &= \Delta Cq_{Treatment} - \Delta Cq_{Control} \\ Normalized\ Expression &= 2^{-\Delta\Delta Cq}\end{aligned}$$

To verify the amplification of the chosen fragments, qPCR samples were purified by PCR purification as described in chapter 2.3.6. Afterwards they were ligated into the pCR™4-TOPO™ vector (Fisher Scientific GmbH) and used for transformation of competent *E. coli* cells (see chapter 2.3.7). Transformed clones were picked, tested for fragment length in colony PCR and incubated overnight in LB medium for plasmid amplification and following purification (see chapters 2.3.8 and 2.3.9, respectively). Plasmids were sequenced according to instructions in chapter 2.3.10.

2.6. Fluorescence microscopy

Leaves from *eGFP* transformed *N. benthamiana* plants were harvested and cut in cross sections with a razor blade. Sections were placed in water on a microscope slide and examined with a Zeiss Imager Z1 (Carl Zeiss AG, Oberkochen, Germany). Samples were illuminated with a X-Cite Series 120 fluorescence light source (EXFO Germany GmbH, Unterhaching, Germany), subsequently using a High efficiency (HE) *eGFP* shift free fluorescence filter with an excitation bandpass (BP) at 470 (+/-40 nm) and emission BP at 525 (+/-50) nm to select for *eGFP* fluorescence. Pictures were taken by an AxioCam HRc (Carl Zeiss AG) using ZEN 2012 Pro software.

2.7 Analytics

2.7.1 Methanol extraction

Approximately 100 mg of ground leaf powder was dissolved in five volumes of methanol and extracted for 5 min at 2000 rpm. Afterwards, samples were centrifuged for 20 min at 21130 rcf in a table top centrifuge. The supernatant was transferred to plastic vials for LC-MS analysis.

2.7.2 Targeted LC-MS Analysis

Analysis of methanol extracts was performed on an Agilent 1260 series HPLC system (Agilent Technologies) coupled with a tandem mass spectrometer QTRAP6500 (AB Sciex Germany GmbH, Darmstadt, Germany). Extracts were separated on a Zorbax Eclipse XDB-C18 column kept at 20 °C (50 x 4.6 mm, 1.8 µm; Agilent Technologies) using 0.05% formic acid in water (A) and acetonitrile (B) as mobile phases at a flow rate of 1.1 ml/min. Following solvent gradient was applied for elution: 0 to 0.5 min, 5 % B; 0.5 to 6.0 min, 5 % to 32.5 % B; 6.0 to 6.02 min, 32.5 % to 100 % B, maintaining to 7.0 min, 7.0 to 7.1 min, 95 % B and 7.1 to 9.5 min, 5 % B. For coupling of LC to MS, electrospray ionization (ESI) was used in negative mode. The parameters for the mass spectrometer were the following: ion spray voltage, -4500 V; turbo gas temperature, 650 °C, collision gas set to medium pressure; curtain gas: 40 psi; ion source gas 1: 70 psi; ion source gas 2: 70 psi. Parent ion to product ion was analysed by multiple reaction monitoring (MRM). Parameters for targeted analytes are listed in Table 6. Chromatograms were processed and analysed with the Analyst Software (AB Sciex Germany GmbH).

Table 6: Multiple reaction monitoring parameters for selected BXDs. Listed are parent ion mass (Q1), product ion mass (Q3), dwelling time, entrance potential (EP), collision energy (CE) and collision cell exit potential (CXP).

Analyte	Q1 mass (Da)	Q3 mass (Da)	Time (msec)	EP (volts)	CE (volts)	CXP (volts)
HBOA	164	108	10	-3	-23	-1.5
DIBOA	180	134	10	-2	-10	-3
DIMBOA	210	149	10	-8	-16	-4
HBOA-Glc	326	164	10	-4	-20	-5
DIBOA-Glc	342	134	10	-4	-24	-4
DIBOA-Glc ₂	504	134	10	-4	-24	-4
TRIBOA-Glc	358	196	10	-4	-20	-4
DIMBOA-Glc 1	418	372	10	-4	-18	-5
DIMBOA-Glc 2	372	210	10	-4	-15	-4
HMBOA-Glc 1	402	356	10	-4	-18	-5
HMBOA-Glc 2	356	194	10	-4	-15	-4
Tryptophan	203	116	10	-10	-22	-4

2.7.3 Nontargeted LC-MS Analysis

Methanol extracts were separated on a Zorbax Eclipse XDB-C18 column (100 x 2.1 mm; 1.8 μm ; Agilent Technologies) using a Dionex Ultimate 3000 RS pump system (Fisher Scientific GmbH). 0.1% formic acid in water (A) and acetonitrile (B) were used as mobile phases at a flow rate of 0.3 ml/min, the column temperature was maintained at 25°C. The elution gradient was as follows: 0-0.5 min, 5% B; 0.5-11 min, 5-60% B; 11.1-12 min, 100% B; 12.1-15 min, 5% B. The LC system was coupled to a timsTOF™ mass spectrometer (Bruker Daltonics, Billerica, USA) equipped with a turbospray ion source operating at a capillary voltage of 3500 V. Nitrogen was deployed as drying gas (10 l/min, 230°C) and nebulizer gas (1.8 bar). Samples were scanned in negative ionization mode with a range of m/z 50 to 1500. Sodium formate adducts were used for internal calibration.

2.7.4 Statistical analysis and graphic design

The data from targeted LC-MS/MS analysis on peak area of analytes was relatively quantified and statistically evaluated with SigmaPlot 12.0 (Systat Software GmbH, Erkrath, Germany). The graphs were designed in Microsoft Excel 2013 (Microsoft Corporation, Redmond, USA).

3. Results

3.1 Cloning of BXD biosynthesis genes

Bx genes from *Bx1* to *Bx9* were cloned into a standard expression vector from maize cDNA before integrating them into the pCambia2300U vector via USER-cloning (Table 7). An exception to this were *Bx6* and *Bx8*. *Bx6* was directly amplified by USER-PCR from cDNA without subcloning it, because PCR-results were satisfactory for attempting a direct cloning approach. *Bx8* was not amplified from cDNA, but instead newly synthesized by gene synthesis. This was due to the fact, that *Bx8* could not be amplified by any PCR-protocol from cDNA. All sequences were taken from the B73 maize genome except the *Bx2* sequence, which was easier amplified from W22 maize.

Table 7: Cloning procedures for *Bx* genes.

Bx gene	Maize line	Subcloning		USER-cloning	
		Synthesis	Source	Synthesis	Source
<i>Bx1</i>	B73	Q5-PCR	cDNA	PfuTurbo-PCR	Plasmid
<i>Bx2</i>	W22	Q5-PCR	cDNA	PfuTurbo-PCR	Plasmid
<i>Bx3</i>	B73	Phusion-PCR	cDNA	PfuTurbo-PCR	Plasmid
<i>Bx4</i>	B73	Phusion-PCR	cDNA	PfuTurbo-PCR	Plasmid
<i>Bx5</i>	B73	Q5-PCR	cDNA	PfuTurbo-PCR	Plasmid
<i>Bx6</i>	B73	-	-	PhusionU-PCR	cDNA
<i>Bx7</i>	B73	Q5-PCR	cDNA	PhusionU-PCR	Plasmid
<i>Bx8</i>	B73	Gene Synthesis	-	PhusionU-PCR	Plasmid
<i>Bx9</i>	B73	Phusion-PCR	cDNA	PfuTurbo-PCR	Plasmid

3.2 Measurement of eGFP-fluorescence in transgenic tobacco – Confirming the functionality of agroinfiltration

To confirm the functional capability of the applied plant transformation system using *A. tumefaciens*, *N. benthamiana* specimens were transformed with the eGFP (Enhanced Green Fluorescent Protein) gene. Afterwards, leaf samples were observed under the fluorescence microscope. eGFP-transformed plants were compared to plants treated with Agrobacteria carrying a *Bx* gene on the vector as a control. As shown in figure 5, leaves from eGFP-positive plants emitted fluorescence at the observed wavelength while control samples did not emit any fluorescence.

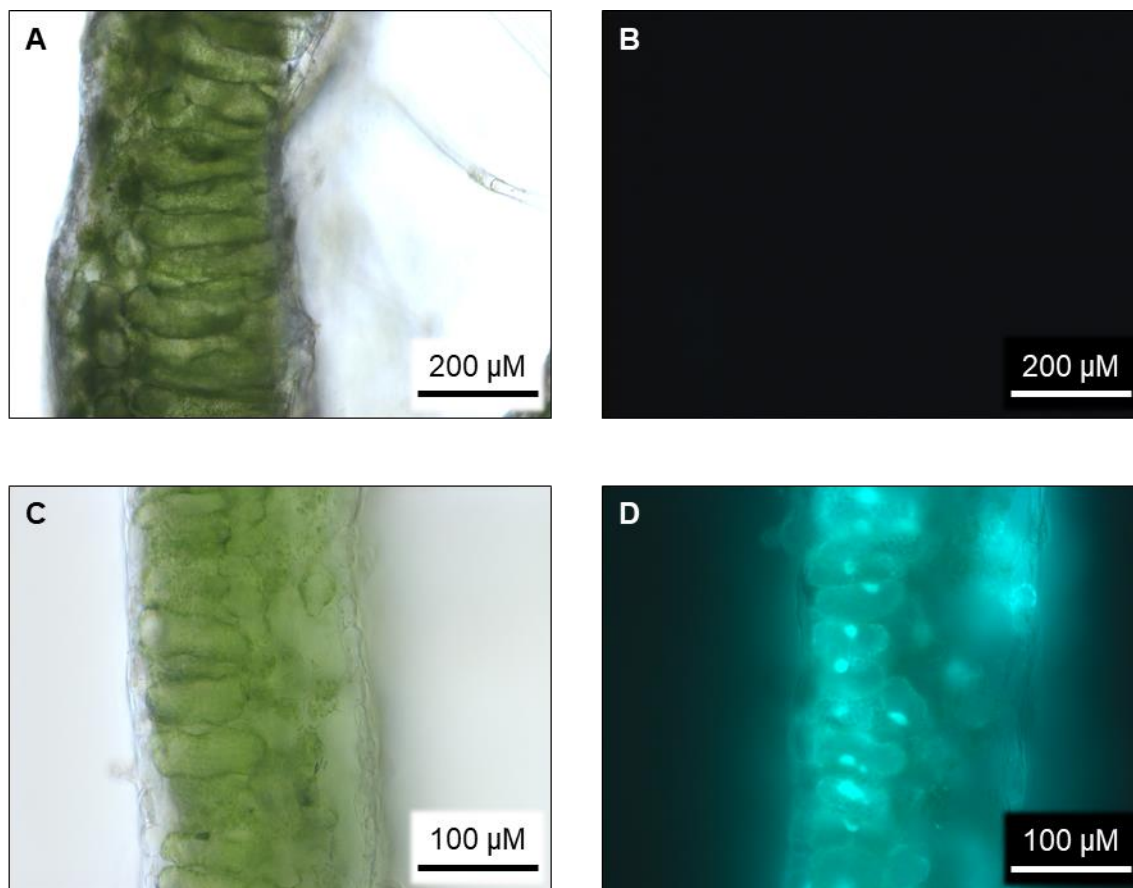


Figure 5: Fluorescence microscopy pictures from leaves of *Nicotiana benthamiana* plants. The plants were transiently transformed with *Bx* genes as control (**A, B**) or *eGFP* (**C, D**). Control samples are shown at a 100x magnification, *eGFP* transformed leaves with 200x. Samples were illuminated at approx. 470 nm wavelength. Pictures B and D show the emission of tissues at a wavelength of approx. 525 nm, including the emission optimum of *eGFP*.

3.3 Introducing the BXD biosynthetic pathway in tobacco – Production of the lactam HBOA

3.3.1 Detection and characterization of putative HBOA analyte

After co-transformation of tobacco plants with *Bx* genes *Bx1* to *Bx4*, extracts were analysed in a targeted LC-MS/MS approach, scanning the samples for the occurrence of BXDs. Extracts were specifically analysed for HBOA and HBOA glucoside (HBOA-Glc) content. Despite that UDP-GTs BX8 and BX9 responsible for glycosylating BXDs in maize were not co-transformed, glycosylation by endogenous GTs was assumed.

HBOA aglucone was not detected in any sample. Further analysis revealed a prominent peak in negative mode for the multiple reaction monitoring (MRM) of HBOA-Glc in extracts of transformed *N. benthamiana* at a retention time of 3.8 min. This peak, however, appeared in both *eGFP*- and *Bx1-4*-transformed plants as well as wild type (WT) plants (Figure 6). A comparison of the mean peak area of the analyte eluting at 3.8

min in samples from *Bx1-4*-transformed plants showed a significant increase compared to *eGFP*- or non-transformed WT-plants (Figure 7). *eGFP*- and WT-plants did not differ significantly. The change in intensity of this peak was the only observed difference after *Bx1-4* treatment and the corresponding compound was thus further analysed. Plants transformed with *Bx1*, *Bx1-2* or *Bx1-3* exhibited an intensity similar to *eGFP* and WT-plants (Supplementary figure III).

A standard of HBOA-Glc was not available, thus confirmation was not possible. To test whether the peak identified in *Bx1-4*-transformed samples could have been HBOA-Glc, extracts were analysed by an Enhanced Product Ion (EPI)-scan for the mass of HBOA-Glc at 326 *m/z* in negative mode. The fragments detected are shown in figure 8. Prominent masses were at 108, 118, 136, 164 and 326 *m/z* ratios. The latest two match with masses of HBOA and HBOA-Glc, respectively. As a control, *eGFP*-transformed samples were scanned for HBOA-Glc fragments but yielded no results due to the mass not present or in too low concentration in the sample. The same applied for WT extracts.

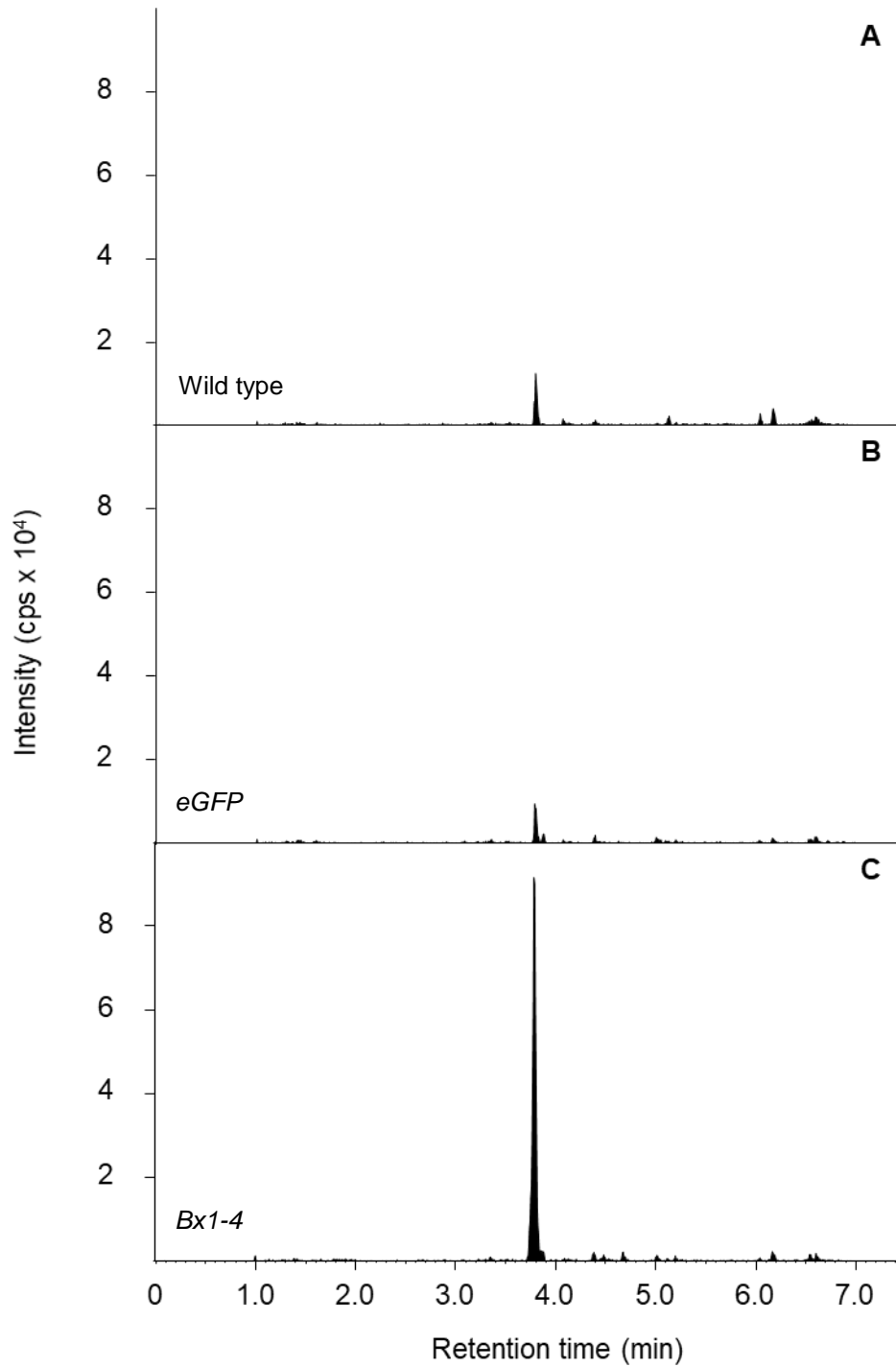


Figure 6: Extracted ion chromatograms of HBOA-Glc. Samples were scanned in a targeted approach using a LC-MS/MS setup in negative mode. Methanol extracts were analysed in the multiple reaction monitoring of HBOA-Glc from leaves of either WT *Nicotiana benthamiana* plants (A), transformed with *eGFP* (B) or *Bx1* to *Bx4* (C). cps = counts per second.

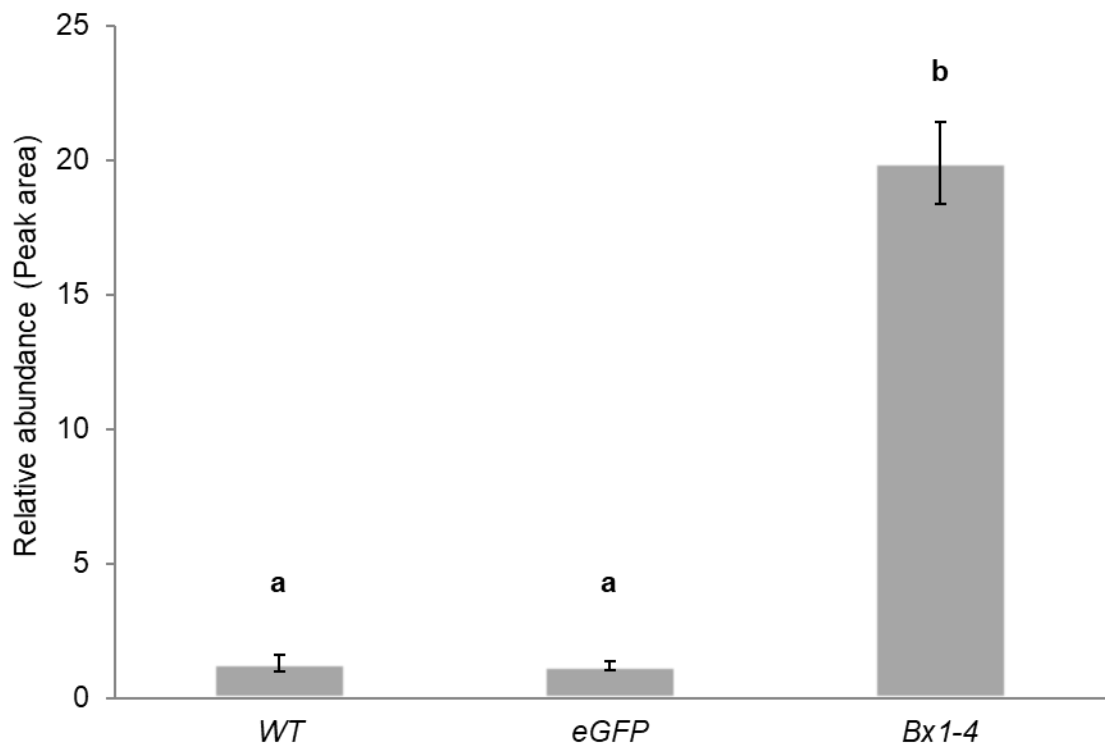


Figure 7: Quantification of hypothesized HBOA-Glc analyte. The area of the visible peak at 3.8 min was quantified for all plants. *eGFP*- and *Bx1-4*-transformed plants were compared to WT *Nicotiana benthamiana* specimen. *Bx1-4* treatment exhibits a significant increase in peak area, while plants transformed with *eGFP* were not different from WT plants. The letters indicate separation into statistically different groups. The bars show means \pm standard error (n=4, One-Way-ANOVA, followed by multiple comparison via Holm-Sidak, p-value < 0.001).

For further verification, samples were run on a timsTOF mass spectrometer in an untargeted analysis. The corresponding peak observed in targeted analysis was identified and analysed regarding the accurate mass. This revealed a mass of 326.0882 Da, matching the most with the accurate mass of HBOA-Glc [-H] at 326.08704 (Error [ppm] = -3.5, error [Da] = -1.2) tested by the SmartFormula 3D algorithm (Bruker Daltonics). This exact mass was not observed in either *eGFP* nor WT samples.

For further analysis, the analyte at 3.8 min retention time was assumed to be HBOA-Glc. In quantification, peak area of the analyte at the same retention time in control plants was used as background and compared to peak area in treated plants, although HBOA-Glc was not detected in WT or *eGFP*-transformed plants.

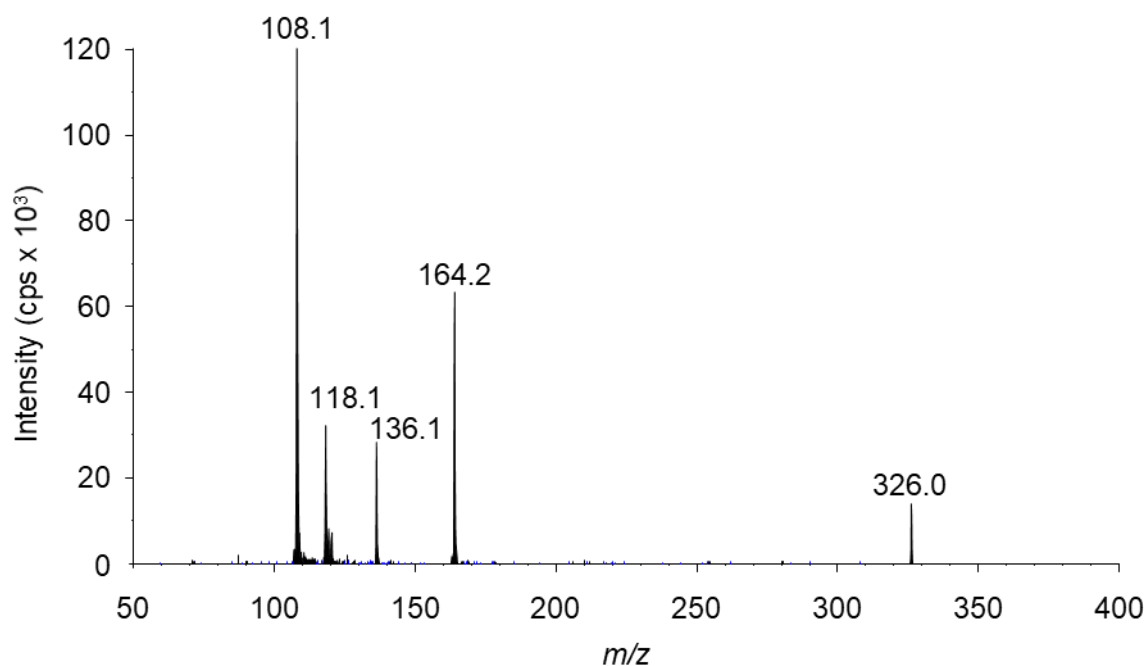


Figure 8: MS/MS-Spectrum of hypothesized HBOA-Glc analyte. The mass ratio of 326 m/z was selected for fragmentation in a LC-MS/MS setup. Shown are intensities of fragments with different m/z ratios. cps = counts per second.

3.3.2 Influence of downstream BXD enzyme genes on the accumulation of HBOA-Glc

N. benthamiana plants were transformed with further *Bx* genes downstream of enzyme genes *Bx1* to *Bx4* which mediate production of HBOA. Plants were either co-transformed with *Bx1-5* or *Bx1-7*. Additionally, a set of plants was also transformed with *Bx1-7* without *Bx5* to test whether the missing BX5 leads to accumulation of HBOA-Glc and other BXD lactams. All combinations were further co-expressed with UDP-GTs BX8 and BX9. Samples of these treatments were analysed for HBOA and HBOA-Glc content to see whether it was consumed by downstream enzymes (Figure 9).

HBOA was not detected in any sample, including treatments without UDP-GTs BX8 and BX9. The peak at 3.8 min., which has been proposed to be HBOA-Glc, showed the highest intensity in samples from *Bx1-4+8/9*-transformed plants. In treatments where *Bx5* to *Bx7* were additionally transformed, HBOA-Glc content was significantly lower (Figure 10). When *Bx5* was not co-transformed HBOA-Glc accumulated again but did not reach levels observed in *Bx1-4+8/9*-transformed plants.

The novel peak appearing at 1.8 min in treatments co-expressing *Bx5* was analysed in untargeted analysis to identify its mass, but amounts were too low to be detectable.

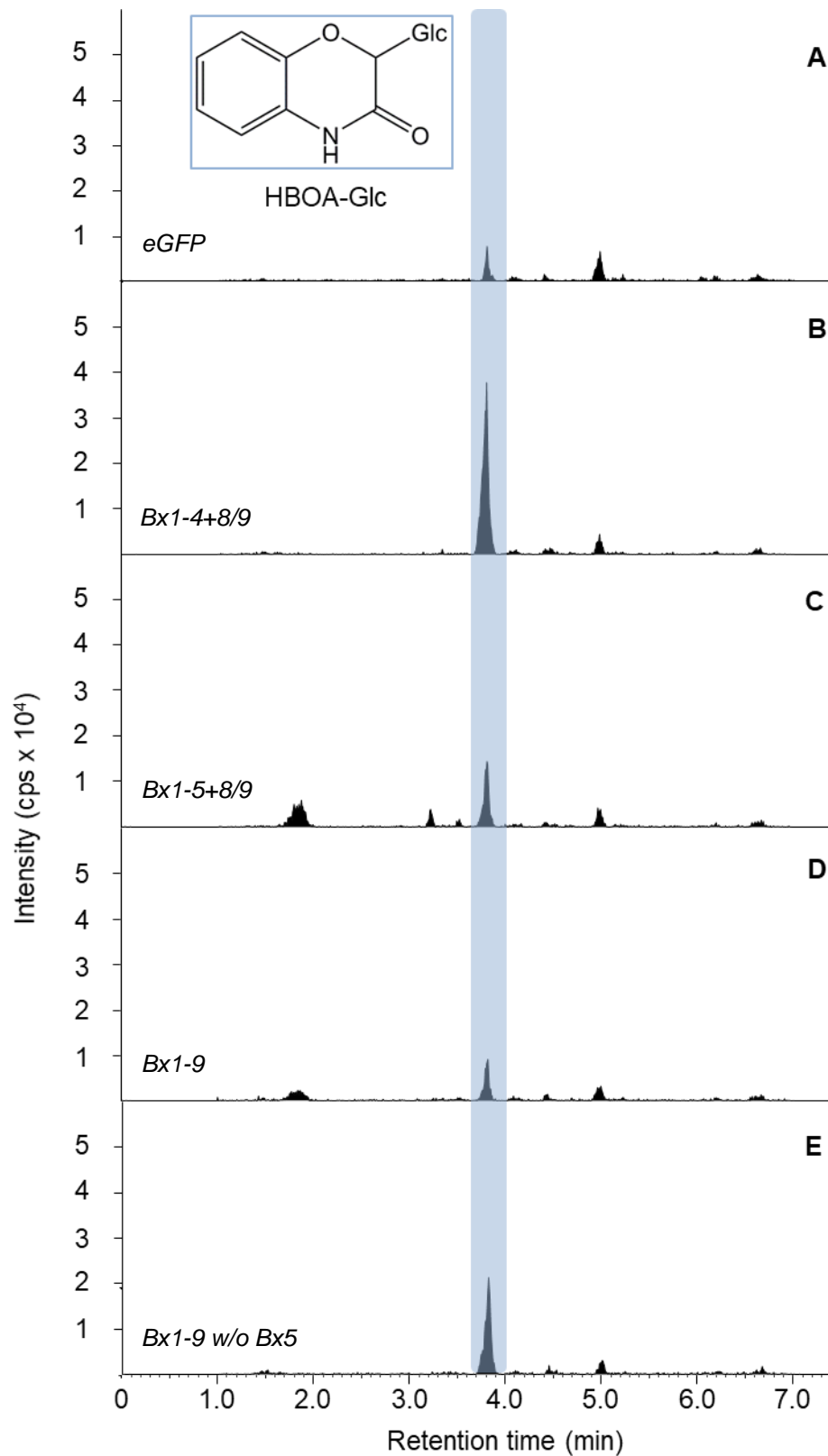


Figure 9: Extracted ion chromatograms of HBOA-Glc in different transformants of *Nicotiana benthamiana*. Methanol extracts from plants transformed with *eGFP* (A), *Bx1-4+8/9* (B), *Bx1-5+8/9* (C), *Bx1-9* (D) and *Bx1-9 w/o Bx5* (E) were scanned in negative mode of the multiple reaction monitoring of HBOA-Glc using a LC-MS/MS approach. cps = counts per second

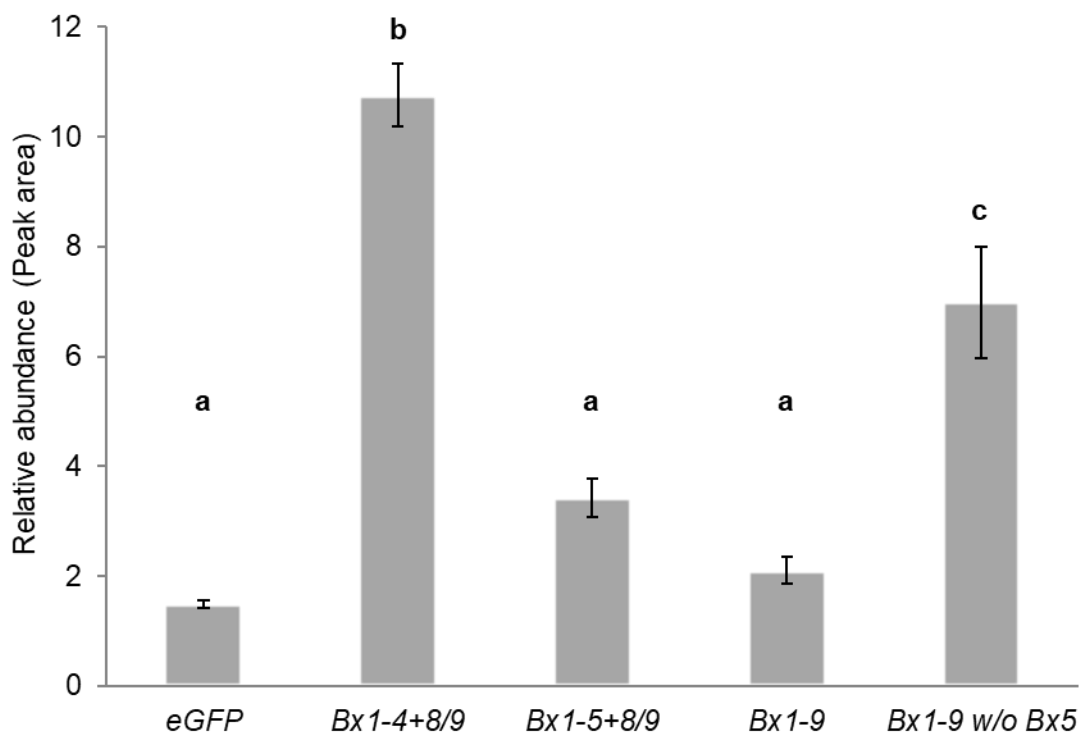


Figure 10: Quantification of hypothesized HBOA-Glc analyte in extracts of transgenic *Nicotiana benthamiana* plants. The combinations of co-transformed genes are shown on the x-axis. Plants were co-transformed with eGFP as control and several combinations of *Bx* genes encoding for the pathway up to BX4 and further downstream enzymes. One set of plants was transformed without *Bx5*. The letters indicate separation into statistically different groups. The bars show means +/- standard error (n=5, One-Way-ANOVA, followed by multiple comparison via Tukey, p-value < 0.01)

3.4. Negative effect of dehydration in pre-transformed plants on transformation effectiveness

It was observed that quantity and therefore detection of BXD analytes in transformed plants was dependent on the watering state of plants before the transformation. In several cases detection of HBOA-Glc was not possible when plants were not watered recently. For visualization of this effect, plants were kept in different conditions before the experiment, where the first group was not watered 36 h before transformation while the second was watered frequently up until 1 h before agroinfiltration. Results on the content of HBOA-Glc are depicted for both treatments in figure 11. In *Bx1-4*-transformed plants HBOA-Glc content was significantly increased in watered plants. *Bx1-4* plants which were not watered 36 h did not differ from eGFP-transformed plants in peak area, indicating no presence of HBOA-Glc.

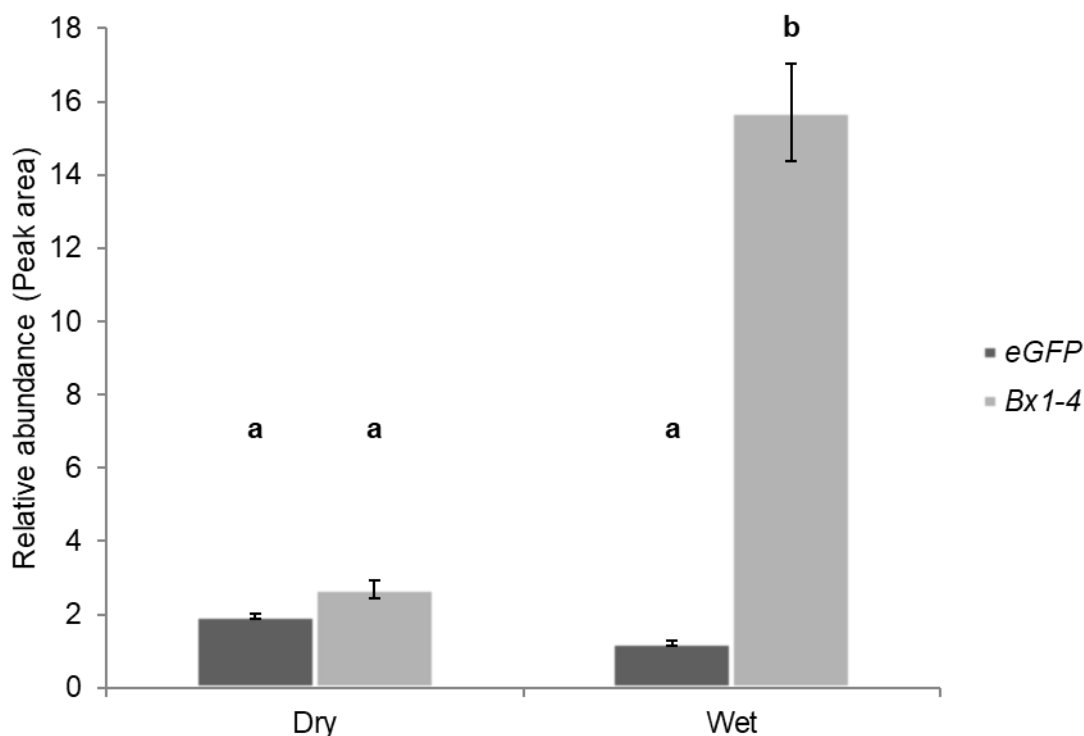


Figure 11: Dependence of HBOA-Glc accumulation on plant watering state. Depicted is the difference between plants put under water stress for 36 h (**Dry**) or watered before transformation (**Wet**). They were either transformed with *eGFP* or *Bx1-4*. In *eGFP*-transformed plants, area of the overlaying peak at the same retention time was taken as control. The letters indicate separation into statistically different groups. The bars show means +/- standard error (n=6, Two-Way-ANOVA, followed by multiple comparison via Holm-Sidak, p-value < 0.001).

3.5 Introducing the BXD biosynthetic pathway in tobacco – Production of the first hydroxamic acid DIBOA

In anticipation of DIBOA production, plants were transformed additionally with *Bx5*, encoding for the p450 enzyme BX5. Since in case of HBOA the aglucone could not be detected, plants were scanned for both DIBOA and DIBOA-Glc. Plants were additionally co-transformed with the UDP-GT genes *Bx8* and *Bx9* to increase yield of BXDs by glycosylating them. Since DIBOA is a toxic compound, its presence as aglucone might lead to lower accumulation in plant tissue, contrary to the non-toxic DIBOA-Glc. It was postulated that specific UDP-GTs can glycosylate BXDs more effectively (Jones and Vogt, 2001). Glycosylation is a usual process to detoxify and store compounds, thus promoting accumulation.

Bx1-5-transformed plants showed two peaks when scanning for DIBOA-Glc in negative mode at retention times 3.22 and 3.86 min, which did not appear in *eGFP* controls or any other treatment lacking BX5 as the latest enzyme from the pathway (Figure 12). DIBOA aglucone was not detected independent whether *Bx8* or *Bx9* were co-expressed. Since HBOA-Glc was identified at a retention time of 3.8 min, the peak at 3.86 rather than 3.22

min was assumed to be DIBOA-Glc due to both compounds differing in a single hydroxylation.

Hence two novel peaks were present in samples of plants transformed with *Bx1-5* either including or excluding *Bx8* and *Bx9*, extracts were analysed for multiple glycosylated DIBOA. MRMs for mono-, di- and tri-glucosides were included in the analysis. When scanning the sample for a hypothetical MRM of DIBOA-Glc₂, the peak at 3.86 minutes retention time was not visible anymore. However, the peak at 3.22 minutes was still present (Figure 13). In the MRM of DIBOA-Glc₃, both peaks disappeared (data not shown). It was therefore assumed that these compounds represented DIBOA mono- and di-glucoside.

As shown in figure 14, quantity of both compounds increased in plants transformed with *Bx1-5* and *Bx8/9* compared to plants without *Bx8/9*, yet in neither of these cases was the increase significantly higher. However, for both treatments, the statistics included an outlier with very low peak area value. For the compound at 3.86 min presumed to be DIBOA-Glc, the statistical value is close to significance. Low sampling size was possibly the reason for non-significant results. Therefore, genes of UDP-GTs were always co-transformed for higher BXD yield based on the original hypothesis.

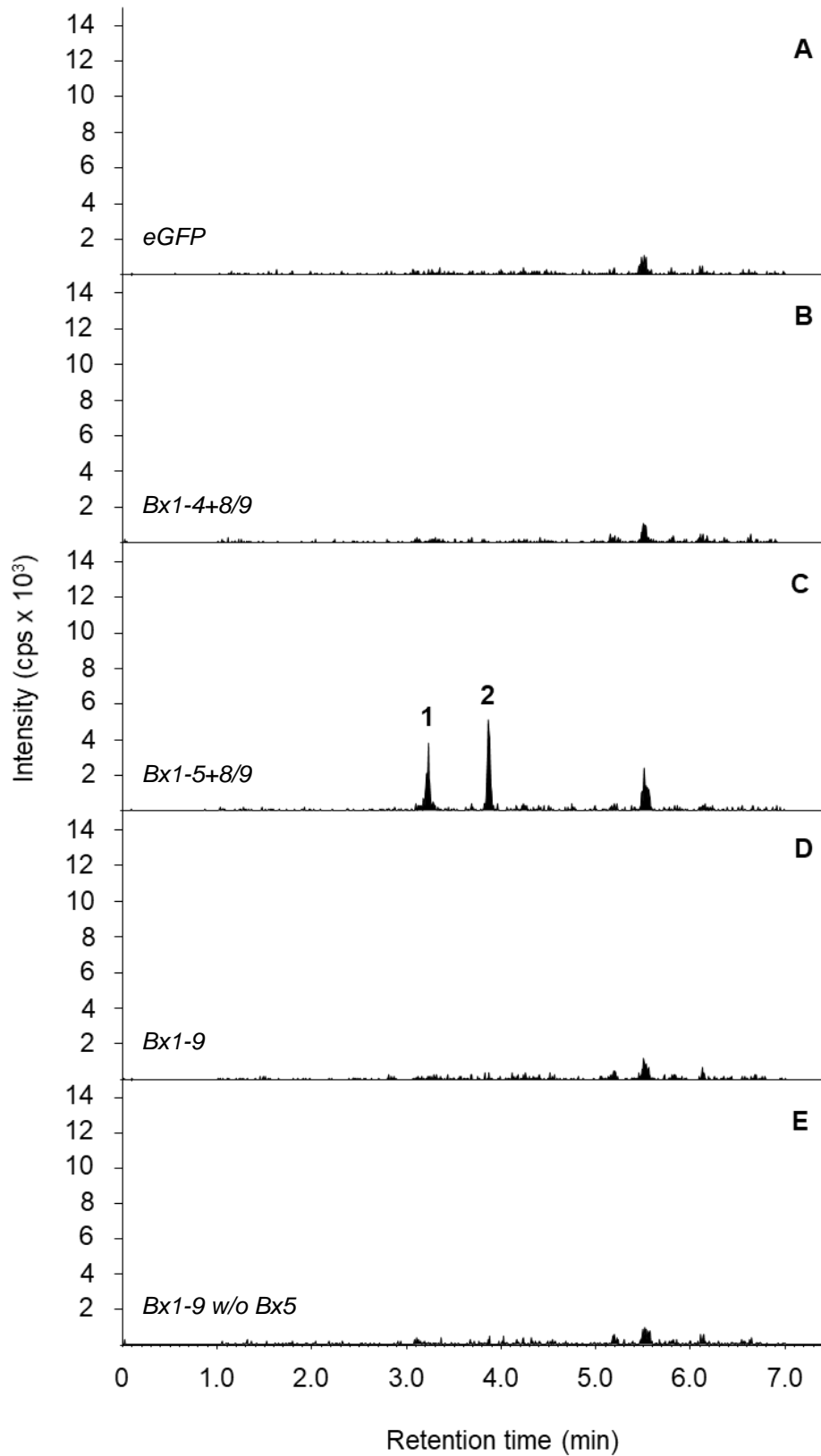


Figure 12: Extracted ion chromatograms of DIBOA-Glc for transgenic *Nicotiana benthamiana* lines. Plants were transformed with eGFP (A), Bx1-4+8/9 (B), Bx1-5+8/9 (C), Bx1-9 (D) or Bx1-9 w/o Bx5 (E) and scanned for DIBOA-Glc in negative mode, revealing novel analytes (1) at 3.22 and (2) at 3.86 minutes. cps = counts per second.

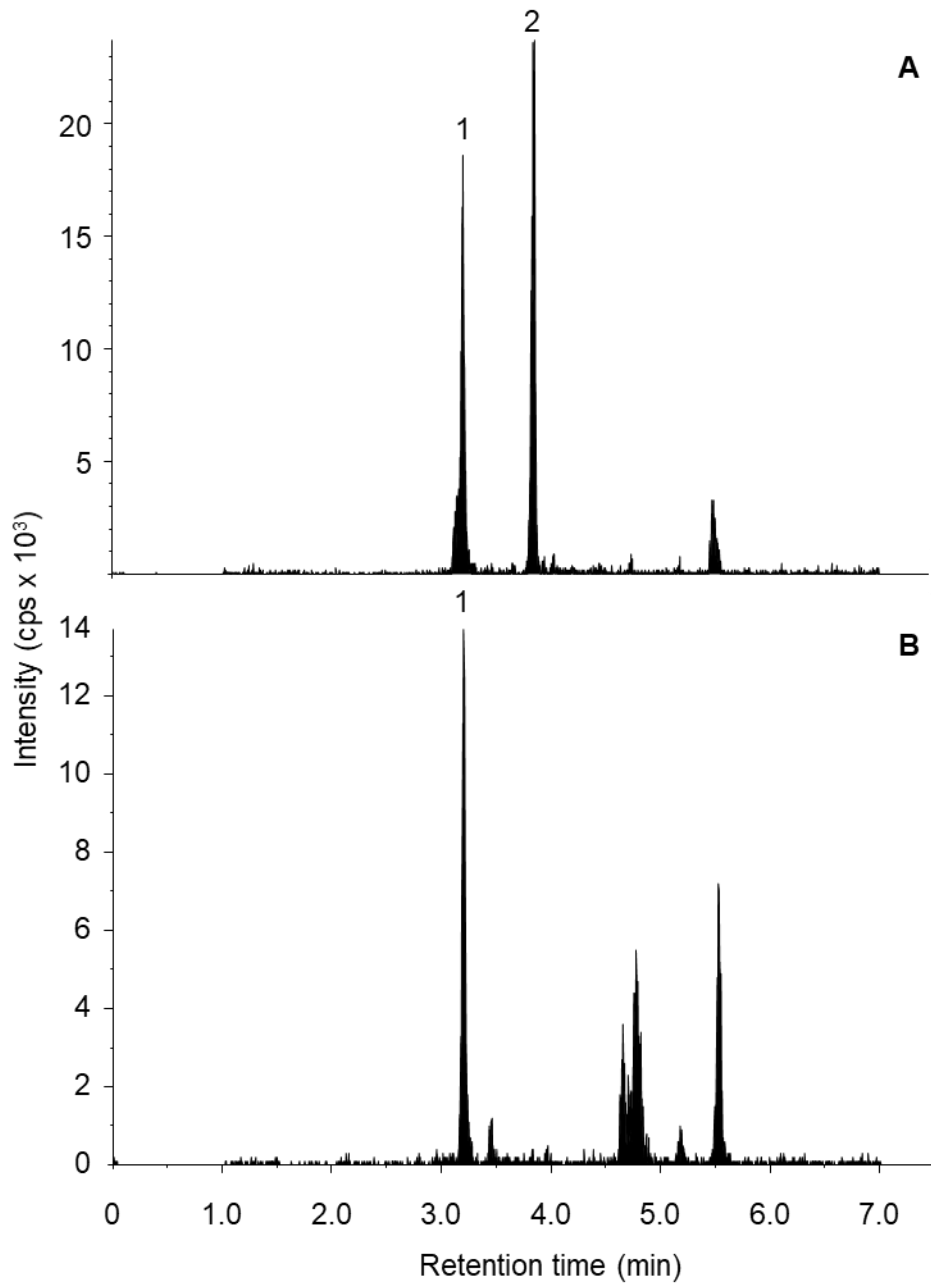


Figure 13: Extracted ion chromatograms of DIBOA glucosides. Shown are chromatograms for MRMs of DIBOA-Glc (**A**) and DIBOA-Glc₂ (**B**). Extracts of *Bx1-5+8/9*-transformed *Nicotiana benthamiana* plants were scanned in negative mode using a targeted LC-MS/MS approach. In (**A**) two peaks at 3.22 (**1**) and 3.86 min (**2**) are present, while in (**B**) only the first peak appears. cps = counts per second.

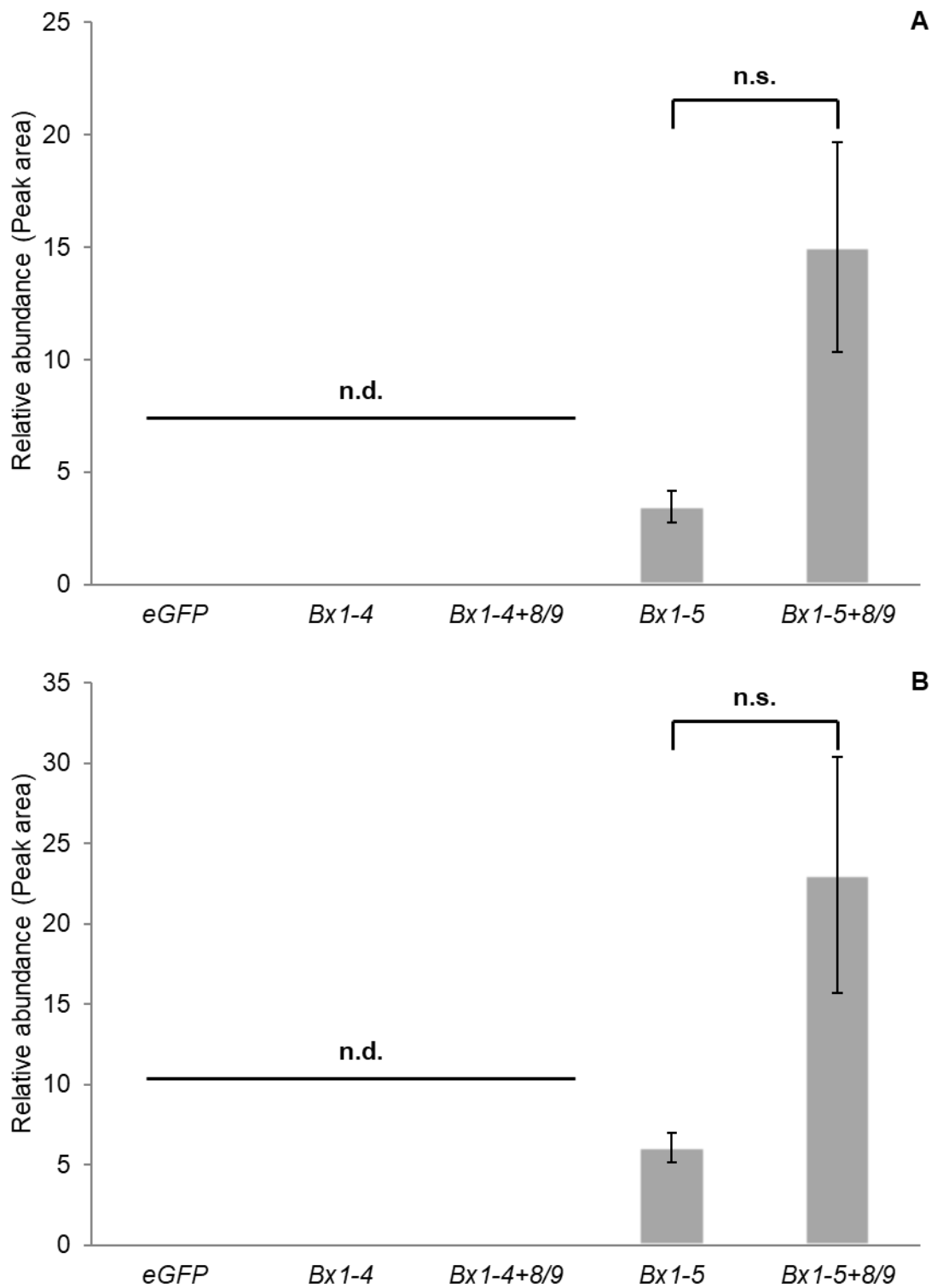


Figure 14 Quantification of DIBOA glucosides in transgenic *Nicotiana benthamiana* plants. Depicted is the amount of DIBOA-Glc (**A**) and DIBOA-Glc₂ (**B**) of plants carrying eGFP or different combinations of *Bx* genes described on the horizontal axis. The bars show means +/- standard error (n=5, [A]: t-test, p-value = 0.06; [B]: Wilcoxon-Mann-Whitney, p-value = 0.151). n.d. = not detected, n.s. = not significant.

3.6 Supply of the BXD biosynthetic pathway in transgenic plants – Effect of providing additional substrate on the accumulation of BXDs

The BXD pathway starts from indole-3-glycerol phosphate (IGP), which is an intermediate of Trp biosynthesis. BX1 produces free indole from IGP. In Trp synthesis, anthranilate (AA) is the first specific compound of the pathway, derived from chorismate. To increase yield of BXDs in transiently transformed plants, single leaves were supplemented with AA for boosting of the pathway by offering more substrate. Two concentrations of AA were tested, 1 mM and 10 mM, and compared to a water control.

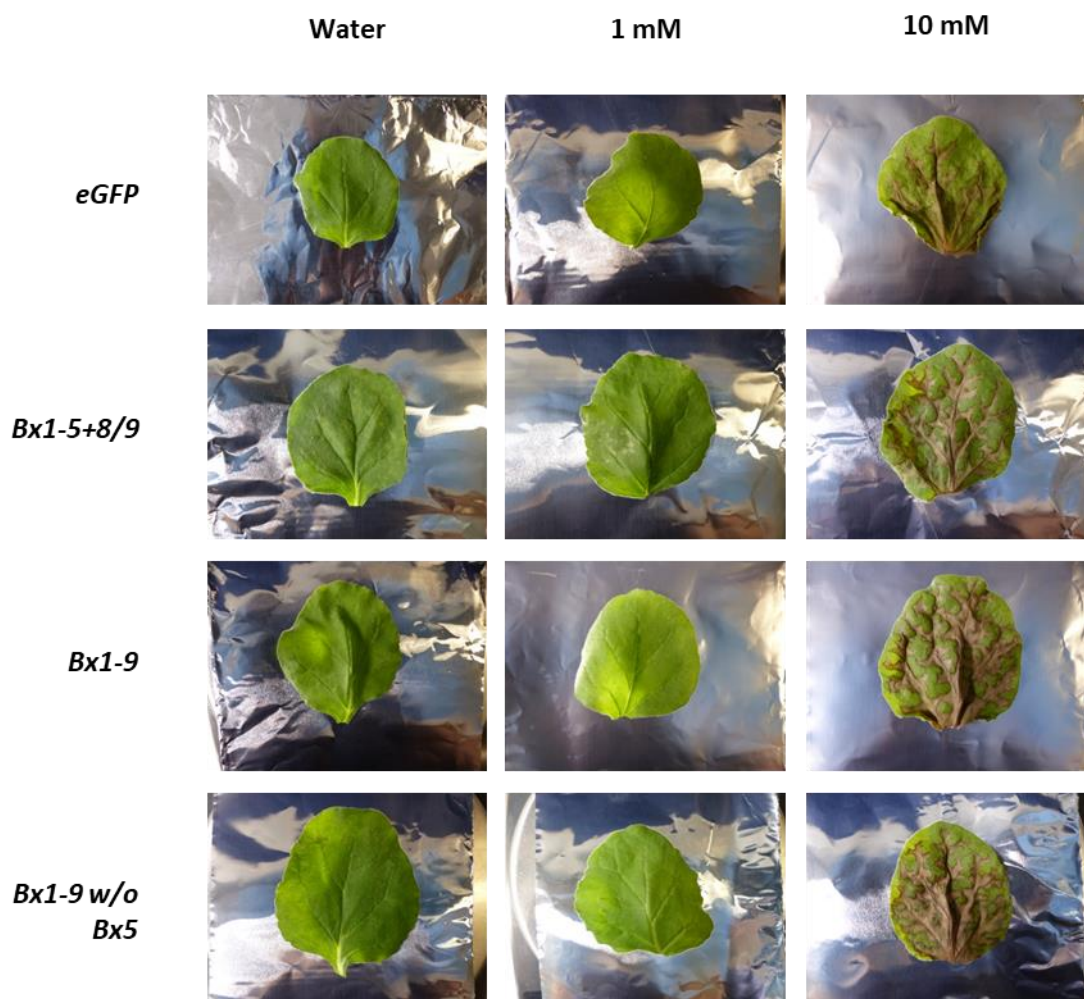


Figure 15: Supplementation of transgenic *Nicotiana benthamiana* leaves with anthranilate. Depicted are leaves from *N. benthamiana* plants transiently expressing *eGFP* or co-expressing *Bx* genes *Bx1-5+8/9*, *Bx1-9* as well as *Bx1-9* without *Bx5*. Leaves were placed in 1 mM anthranilate, 10 mM anthranilate solution or water three days after transformation. They were left for two days under light and harvested together with the transformed plants.

Leaves provided with water or 1 mM solution showed no morphological difference after two days, independent of the genes transferred in transformation (Figure 15). Leaves supplied with 10 mM solution turned partially brown and started to wilt after the first day. They were harvested together with other samples five days post-infiltration, but not included in the quantification of analysed compounds due to their lower water content and thus change in concentration of metabolites in the final extracts.

Methanol extracts of treated leaves were tested for changes in Trp content. Results are depicted in figure 16. Trp accumulation increased when 1 mM AA was added, compared to the water control. This trend was significant for *eGFP* and *Bx1-9 w/o Bx5* treatments, but not for *Bx1-5+8/9* and *Bx1-9* transformed plants. Trp accumulated the most in leaves provided with AA. The abundance of Trp was measured in plants not treated with AA as well (Supplementary figure I). Concerning the initial Trp content in the plants, it was not significantly lowered in *Bx* gene treatments compared to *eGFP* control.

After reviewing Trp content, samples were checked for HBOA-Glc levels. As was already shown in chapter 3.2, HBOA-Glc accumulated when *Bx5* was not expressed, visible in samples from *Bx1-9*-transformed plants without *Bx5* (Figure 17). Concerning other co-transformations, HBOA-Glc peak area was not significantly higher than the background from the *eGFP* control. Leaves incubated in 1 mM AA solution had a significantly higher HBOA-Glc content compared to leaves placed in water. Furthermore, HBOA-Glc levels of leaves incubated in water solution was not different from the *eGFP* background and thus significantly lower compared to samples directly taken from plants without supplementation with AA (Supplementary figure II).

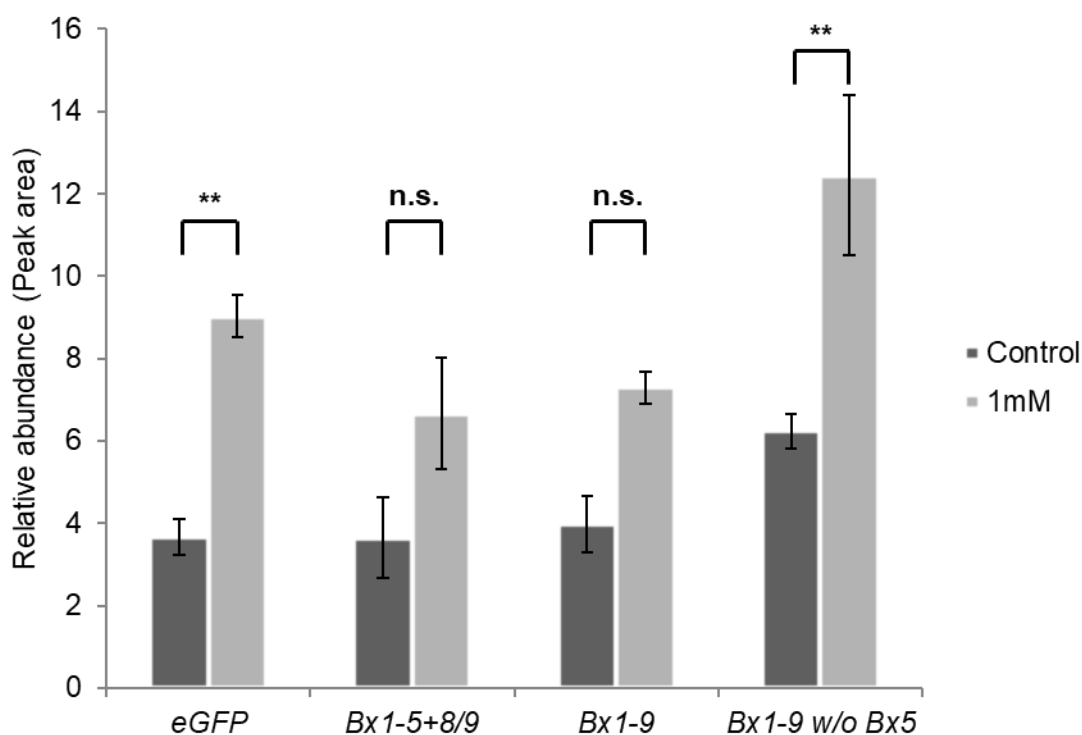


Figure 16: Tryptophan content of transgenic *Nicotiana benthamiana* leaves supplemented with anthranilate. Plants transformed with *Bx1-5+8/9*, *Bx1-9* as well as *Bx1-9* without *Bx5* were included in the analysis. The samples were harvested from leaves placed in water as a control or 1 mM anthranilate solutions and compared to each other. The leaves were supplemented for two days and all samples harvested five days after transformation. The bars show means +/- standard error (n=5, Two-Way-ANOVA, followed by multiple comparison via Holm-Sidak, ** = p-value < 0.01). n.s. = not significant.

Identical to observations from previous transformation experiments, DIBOA glucosides only accumulated when BX5 was present as the last downstream enzyme from the pathway. Therefore, DIBOA-Glc and DIBOA-Glc₂ content is only depicted for treatment *Bx1-5+8/9* in figure 18. A similar trend was observed compared to HBOA-Glc content. In samples from leaves placed in water DIBOA-Glc levels were low but increased in case 1 mM anthranilate was provided. However, for both compounds the amounts accumulated were not significantly higher compared to those in extracts from leaves directly harvested from transformed plants (Supplementary table VII).

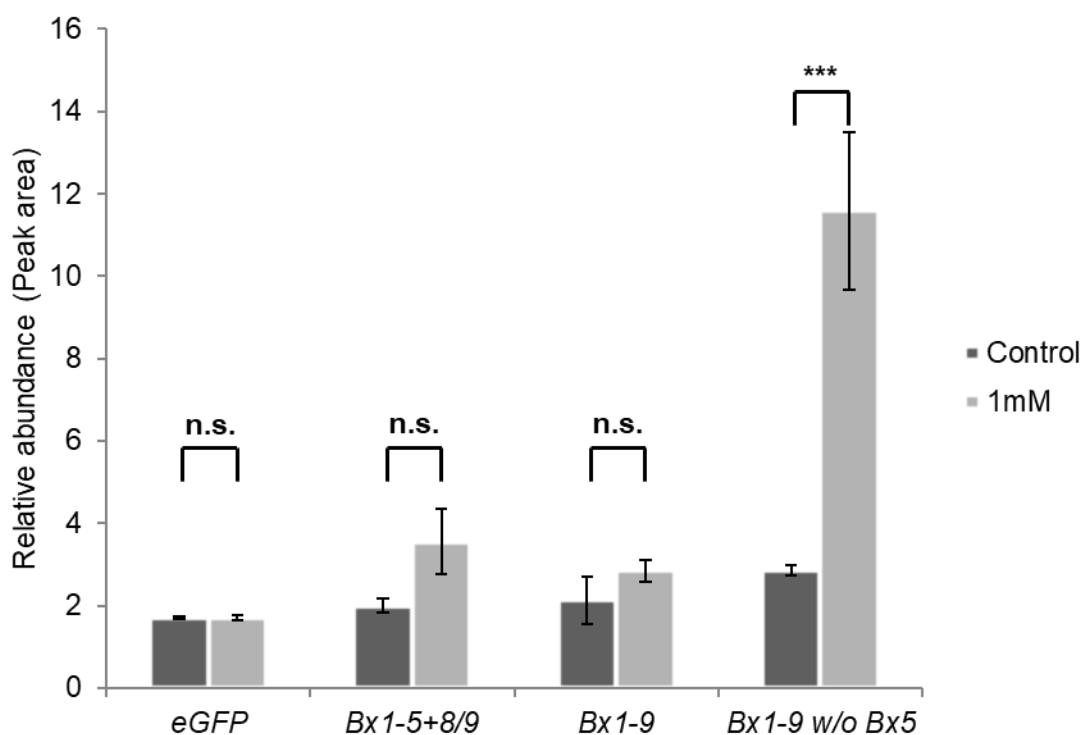


Figure 17: HBOA-Glc content of transgenic *Nicotiana benthamiana* leaves supplemented with anthranilate. Plants transformed with *eGFP*, *Bx1-5+8/9*, *Bx1-9* as well as *Bx1-9* without *Bx5* were included in the analysis. The samples were harvested from leaves placed in water as a control or 1 mM anthranilate solutions and compared to each other. The leaves were supplemented for two days and harvested five days after transformation. The bars show means \pm standard error ($n=5$, Two-Way-ANOVA, followed by multiple comparison via Holm-Sidak, *** = p -value < 0.001). n.s. = not significant.

Neither DIMBOA nor DIMBOA-Glc could be detected in any treatment with transgenic plants where *Bx1* to *Bx7* was co-transformed. DIMBOA-Glc had been identified in previous LC-MS measurements using partially purified DIMBOA-Glc as standard and applying the same method, in which it eluted at a retention time of 4.35 minutes (information provided by the supervisor). Samples were scanned for two MRMs. Boosting the pathway with anthranilate did not have any visible effect (data not shown). Plants co-expressing *Bx1-9* without *Bx5* were scanned for HMBOA-Glc production. Independent whether AA had been provided or not, no HMBOA-Glc was detected in any sample, same as the corresponding hydroxamic acid DIMBOA-Glc.

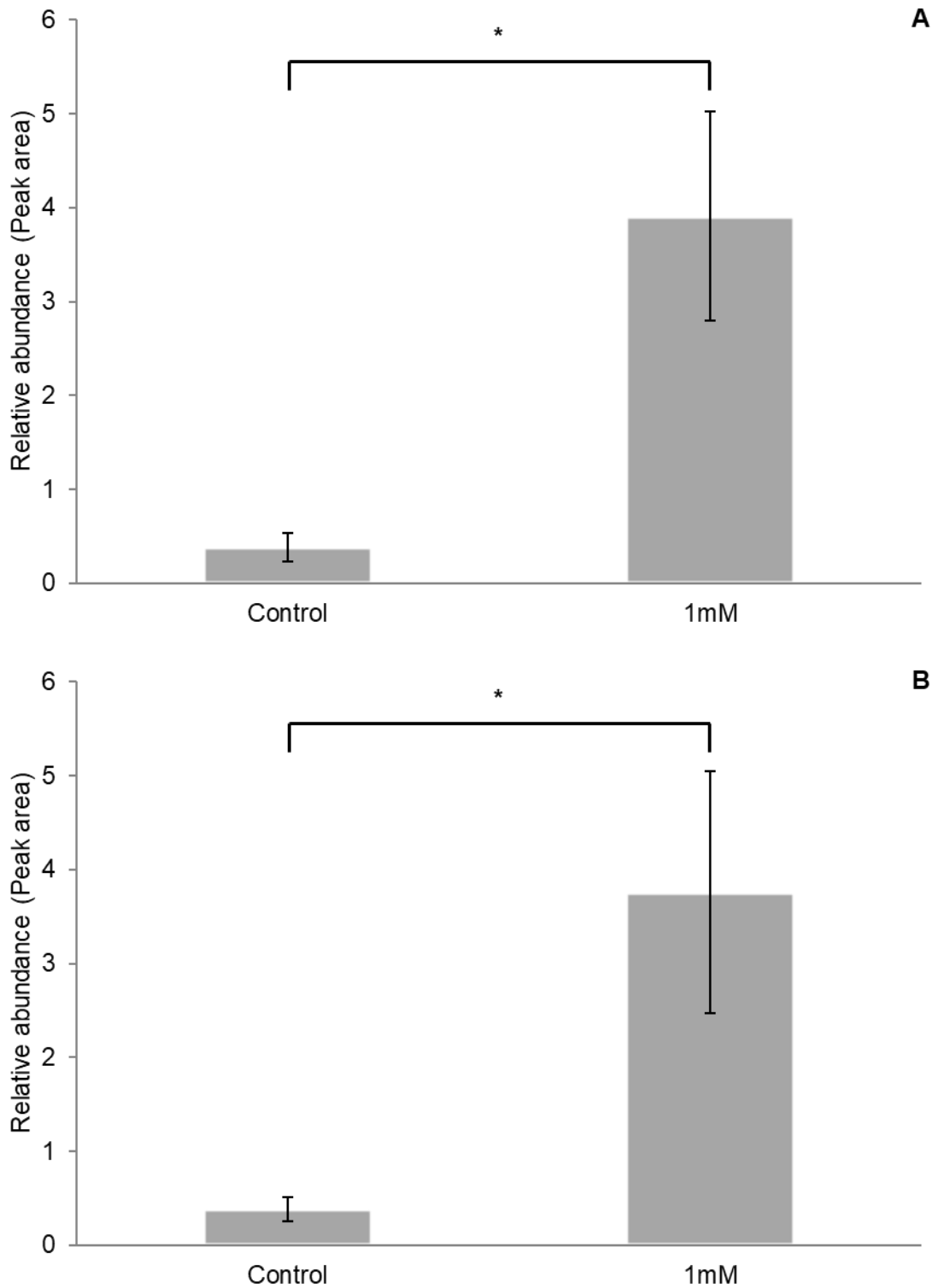


Figure 18: DIBOA glucoside content of transgenic *Nicotiana benthamiana* leaves supplemented with anthranilate. Solely the plants transformed with *Bx1-5+8/9* were evaluated, since DIBOA glucosides were not present in other treatments. The samples from leaves placed in water as a control or 1 mM anthranilate solutions and compared to each other. The leaves were supplemented for two days and harvested five days after transformation. The bars show means \pm standard error (n=5, Wilcoxon-Mann-Whitney, * = p-value < 0.05).

3.7 Quantification of *Bx* gene expression in transgenic tobacco

RNA was extracted from transgenic *N. benthamiana* plants and used to generate cDNA for qPCR analysis of BXD gene expression to see whether transferred genes have been introduced successfully in the plant genome. The expression was quantified relatively with the housekeeping gene (HKG) *GAPDH* from *N. benthamiana*, applying the $\Delta\Delta Cq$ -method. Since the main reason for this analysis was to see whether genes are expressed or not, primer efficiency was not determined and set at 100 % for each gene.

Normalized expression levels are depicted in figure 19. The expression in plants transformed with *Bx1* to *Bx7* was compared to expression in *eGFP* plants. In *eGFP* samples, no amplification was observed. In samples of plants transformed with *Bx1* to *Bx7*, amplification of chosen fragments was found for all *Bx* genes.

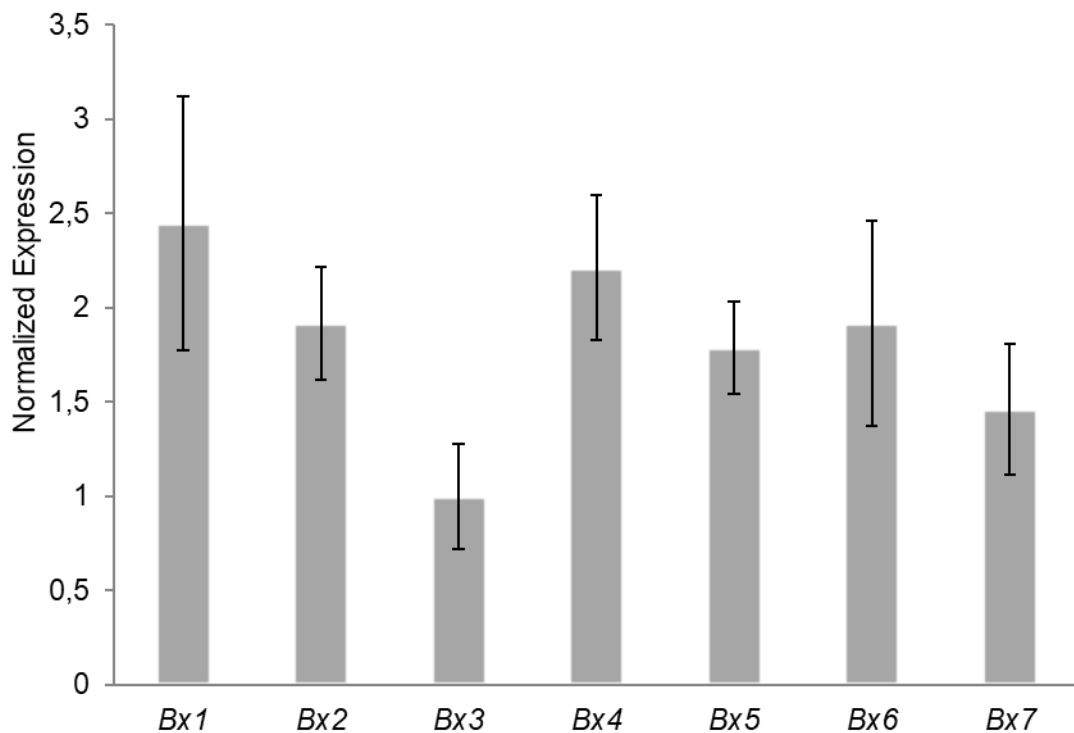


Figure 19: qPCR analysis of *Bx* genes in *Nicotiana benthamiana* plants transiently co-transformed with *Bx1* to *Bx7*. The expression was quantified using *GAPDH* as housekeeping gene and normalized according to the $\Delta\Delta Cq$ -method. The bars show means \pm standard error (n=5). Three technical replicates were measured from each biological replicate.

4. Discussion

4.1 Detecting BXDs in transgenic plants – Achievements and obstacles

Engineering of the BXD pathway from *Z. mays* in *N. benthamiana* has led to successful production of HBOA and DIBOA glucosides. Although no standards were available for both compounds, it was possible to detect HBOA-Glc and DIBOA-Glc by targeted MRM-based LC-MS/MS analysis. HBOA-Glc was additionally confirmed by investigation of MS/MS spectra and accurate mass measurements. Fragments detected in MS/MS analysis were specific for HBOA-Glc and consistent with fragmentation patterns of HBOA mono-glucoside found in rye bran extracts (Hanhineva et al., 2011). Together with accurate mass measurements performed in untargeted qTOF analysis, it can be concluded that co-transformation of *Bx1* to *Bx4* led to production of HBOA-Glc. UDP-GTs BX8/9 were not co-transformed but instead of HBOA only HBOA-Glc accumulated. Thus, it was assumed that HBOA was conjugated by the host plant to HBOA mono-glucoside. Strangely, a peak with the same retention time as HBOA-Glc also appeared in WT and *eGFP* transformed tobacco plants, but in smaller quantities. This has raised the question whether *N. benthamiana* is able to produce HBOA-Glc on itself. This hypothesis is not arbitrary, since there are a few dicotylous species which have independently developed the ability to produce BXDs (Schullehner et al., 2008). However, analysis of leaf extracts from WT or *eGFP* plants gave neither the expected fragmentation pattern for HBOA-Glc nor was the same accurate mass observed. Therefore, it can be concluded that HBOA-Glc was not present in WT or *eGFP* transformed tobacco but instead another analyte occurred for the same MRM transition and retention time.

Extracts from tobacco plants co-transformed with *Bx1* to *Bx5* revealed two novel peaks when scanning samples for the presence of DIBOA glucoside. Again, confirmation with a standard was not possible yet observed retention times are within expectations. The second compound eluting at 3.86 min is very close to HBOA-Glc at 3.8 min. Since both metabolites only differ by one hydroxyl group, elution time was assumed to be similar, also based on findings in the literature (Hanhineva et al., 2011). The first peak appeared at 3.22 min. Because glycosylation leads to a shorter retention time due to stronger interaction with the mobile phase and less with the stationary phase, it was postulated that this analyte is DIBOA to which multiple hexose units had been attached. The analysis revealed that the second peak disappears while scanning for DIBOA di-glucoside, but the first peak was still present. In case of the MRM designed for DIBOA tri-glucoside, both peaks did not appear. This indicates that the first peak represents the

di-glucoside while the latter represents the mono-glucoside. Therefore, it can be assumed that DIBOA with either one or two hexose units was generated, while modification with three units does not seem to occur.

Although the pathway was successfully reconstructed up to the production of DIBOA-Glc, DIMBOA-Glc or its aglucone could not be detected. Interestingly, a similar phenomenon comparable to the analysis on HBOA-Glc was observed. Scanning samples in a targeted approach for DIMBOA-Glc did yield a promising peak at 4.35 min, which is the expected retention time for DIMBOA-Glc that has been characterized via a semi-purified standard in an identical LC-MS/MS approach. Yet this peak appeared in WT *N. benthamiana* plants as well as specimen co-transformed with *Bx1* to *Bx7*. The peak intensity was low and just above the background threshold, which prohibits MS/MS analysis or accurate mass measurements. The samples were scanned with an alternative MRM transition for DIMBOA-Glc. No peak was observed at all. Based on these results it can be assumed, that neither DIMBOA glucoside or aglucone was present. However, BX5 was active and able to produce DIBOA-Glc. Upon additional co-transformation of *Bx6* and *Bx7* it was observed that plants did not accumulate DIBOA mono- or di-glucoside. The presence of BX6 and BX7 led to DIBOA glucosides being used up. Since DIMBOA-Glc was not present, it is possible that only BX7 was not active. Yet TRIBOA-Glc, the intermediate produced by BX6 was not detected either. TRIBOA or DIMBOA glucosides may have been converted to unknown conjugates by endogenous enzymes.

The project of reconstructing the BXD biosynthetic pathway was meant to elucidate how BXD lactams are synthesized. Lactams and hydroxamic acids only differ in the presence of a hydroxyl group introduced by BX5 at the nitrogen atom. Indolin-2-one is technically the first compound in the pathway holding a lactam functionality. HBOA, DHBOA and HMBOA are the lactam counterparts of DIBOA, TRIBOA and DIMBOA, respectively. Production of lactams up to HBOA is described, but the origin of DHBOA and HMBOA is not clear. It was assumed that BX6 and BX7 cannot only use DIBOA and TRIBOA as substrates, but HBOA and DHBOA as well. To test this hypothesis, plants were co-transformed with genes *Bx1* to *Bx9* but leaving out *Bx5* to suppress the conversion of lactams into hydroxamic acids. The production of HMBOA-Glc by BX7 was expected, yet this compound was not detected. Moreover, HBOA-Glc accumulated in amounts significantly higher than those measured in *Bx1-5+8/9-* or *Bx1-9*-transformed plants, indicating that BX6 is not able to use HBOA-Glc as a substrate. These results suggest that HMBOA-Glc is produced by an alternative route. However, there are other possibilities why HMBOA-Glc was not found in the samples. Again, BX7 may not be active, which would line up with the fact that DIMBOA-Glc did not occur either. Secondly,

lactams are not the main substrate of BX6 and BX7. HBOA-Glc content was decreased significantly in plants expressing *Bx1-9* without *Bx5* compared to those only co-expressing *Bx1-4+8/9*, which might indicate that BX6 cannot convert HBOA-Glc. However, these setups differ in the quantity of transformed genes and are thus not comparable. On the other hand, lactams may have been produced in too low amounts or converted to conjugates due to inefficient conversion of HBOA-Glc by BX6.

Effectivity is a major issue of the system. Formation of conjugates could have led to lower availability of intermediates. It is not clear if enzymes can use multiple glycosylated BXDs as substrate. DIBOA di-glucoside did not occur when co-transforming *Bx6* and *Bx7*. Whether this means that multiple glycosylated DIBOA is a suitable substrate or DIBOA mono-glucoside is simply converted fast enough to not be conjugated, also remains unclear.

Transient expression of heterologous genes in plants by agroinfiltration is an extensively studied method (Zupan et al., 2000; Gelvin, 2003; Gelvin, 2017). Researchers have faced several obstacles in obtaining metabolites produced by putatively expressed proteins. Many modifications have been developed to improve expression levels (Norkunas et al., 2018). I am going to discuss some of these options in the following chapters in order to evaluate how effective the applied system was and what could have been improved.

4.2 Optimization of the transformation process

It has been discussed in some publications that the number of constructs introduced simultaneously into a plant by agroinfiltration has a crucial effect on the overall transformation efficiency. Reports indicate a significant decrease in efficiency when co-transforming seven or more constructs (Wang et al., 2016). The benzoxazinoid pathway leading to DIMBOA-Glc is composed of nine enzymes, including UDP-GTs BX8 and BX9. When adding the viral suppressor p19 for RNA silencing, a complete introduction of the pathway by agroinfiltration would mean a total number of ten constructs. This can be expected to impact transformation efficiency.

Experimental results presented in chapter 3 show that implementing the pathway has been successful by detecting the occurrence of DIBOA-Glc in plants which have been transformed with *Bx1* to *Bx5* as well as *Bx8/Bx9*. Introduction of GTs led to an increase in DIBOA-Glc accumulation, probably due to more efficient glycosylation by the specific enzymes (von Rad et al., 2001). Although accumulation was not significantly higher, both DIBOA mono- and di-glucoside quantities reached a level almost near significance.

Overall, engineering of the BXD pathway from maize is technically possible in *N. benthamiana*.

A milestone in enhancing protein expression was achieved by co-transformation of viral suppressor genes tackling post-transcriptional gene silencing (PTGS). Usually, transient expression of genes only lasted for no more than 72 h due to RNA silencing (Voinnet et al., 2003). By employing proteins suppressing PTGS like p19, silencing of transient genes was successfully inhibited and allowed for much higher levels of heterologous protein expression. By now, more alternatives have been developed. A PTGS-deficient knock-out line of *N. benthamiana* was established by silencing RNA-dependent RNA Polymerase 6 (RDR6) with CRISPR/Cas9 technology (Matsuo and Atsumi, 2019). These plants can be used for agroinfiltration without the need for a viral suppressor protein. Unfortunately, RDR6-mutants are sterile which is not feasible for extensive applications and remains an obstacle in widespread applications.

For expression of the BXD pathway, p19 proved to be efficient in inhibiting PTGS. Plants were harvested after 4 days and analysed on the expression of transient proteins by qPCR. Results showed that all *Bx* genes which had been co-transformed are expressed at levels similar to the housekeeping gene *GAPDH* (Supplementary table VI).

4.3 Experimental parameters of the transformation process can be tuned to improve results

A successful agroinfiltration depends on a number of physical factors including temperature, pH, light, osmotic conditions, plant species, bacterial strain as well as their density and inoculation time (Norkunas et al., 2018). Temperature seems to have an overall influence. While *A. tumefaciens* grows most optimal at 28 °C, formation of the T-pilus required for T-plasmid transfer is most favourable at approx. 20 °C (Baron et al., 2001). Yet heat shocking plants at 37 °C 1-2 days after infiltration significantly increased transient protein expression (Norkunas et al., 2018). Interestingly, this was reported for sorghum embryos as well (Gurel et al., 2009), although heat shock treatment was applied minutes before the agroinfiltration in this case. Heat shock proteins (HSPs) were observed to be involved in the process of plant transformation by stabilizing components of the T-complex (Park et al., 2014). The increased expression of HSPs might contribute to the more effective transformation process. In terms of pH, an acidic environment is required for agroinfiltration. Therefore, pH in the infection medium was adjusted slightly acidic to 5.7. The infiltration is also feasible at higher pH up to 8.5 when overexpressing *virG*, a component of the transformation system responsible for initiating the setup of the secretion apparatus (Gelvin, 2003). Two constitutively expressed genes from the T-

plasmid are *virA* and *virG*, producing VirA and VirG. VirA is responsible for the perception of wounded plants by sensing elicitor molecules. Wounding most commonly induces production of phenolic compounds such as acetosyringone. To initiate the formation of the T-complex, acetosyringone has proven to be an effective additive to the infection medium in which *Agrobacteria* are incubated before infiltration. Concentrations of up to 500 μM can have a positive effect on transformation efficiency (Norkunas et al., 2018), although most laboratories use concentrations ranging from 100-150 μM .

As shown in chapter 3.3, osmotic conditions are crucial for agroinfiltration. Water stress of plants led to levels of HBOA-Glc in *Bx1-4*-transformed plants which were not significantly above the background. In terms of statistical analysis, no difference could be determined compared to plants expressing *eGFP*. A plausible explanation for this phenomenon is the lack of entry sites for the bacteria. Usually, *A. tumefaciens* infects plants by entering through wounds in the tissue. Plants are not wounded in this case, but their intercellular space is accessible by stomatal openings (Escudero and Hohn, 1997). *Agrobacteria* are pushed into the plant by the pressure difference from releasing the vacuum. However, stomata are closed when plants experience water stress, thus *Agrobacteria* have less or no openings through which they can enter.

There are several *A. tumefaciens* strains available for binary vector transformations. The strain GV3101 utilized in described experiments is a frequently employed strain and exhibits high plasmid copy numbers and transformation rates (Chetty et al., 2013). For vacuum infiltration, final bacterial density was set to an OD^{600} of 0.5 which is well within the optimal range. Densities below 0.1 lead to insufficient transformation rates while highly dense bacterial solutions >1.5 cause necrosis in the leaf tissue (Norkunas et al., 2018). Generally, there are three common methods for introducing *Agrobacteria* into plants, (i) floral bud dipping, (ii) Syringe infiltration and (iii) vacuum infiltration. All methods are in use in today's labs and have their advantages and disadvantages. As the name suggests, floral bud dipping is applied for creating stable transgenic lines by inoculating the reproductive structures (Zhang et al., 2006). During this process, plants are placed upside down into *Agrobacteria* solution. This solution contains a surfactant to decrease surface tension of the aqueous medium. Therefore, entering of the bacterial solution into the plant is promoted (Wiktorek-Smagur et al., 2009). For the second method, the bacterial solution is directly pushed into leaves with a needleless syringe in order to inoculate single leaves instead of the whole plant (Zhao et al., 2017). Vacuum infiltration works similar to floral bud dipping but instead of using a surfactant, *Agrobacteria* are sucked into the plant tissue by the physical force created from the applied vacuum. This method has the advantage of infiltrating the whole plant in a fast and efficient way. Tissues are not damaged if duration and strength of the vacuum is

chosen carefully. Inoculation time was set to 2 min for BXD gene transformation. Compared to inoculation times mentioned in literature for vacuum infiltration, this time frame is rather short. However, it has been proven to be sufficient in case pressures below 50 mbar were applied (Simmons et al., 2009). In the experiments carried out in this work pressures usually went down to 20 mbar. For plant species other than *N. benthamiana*, additional sonication has proven to increase expression of transient genes (Liu et al., 2005; de Oliveira et al., 2009; Bakshi et al., 2011). However, this is solely described for agroinfiltration of germinated seeds but not for *in planta* transformations. *N. benthamiana* is an excellent model organism for transient gene expression by *in planta* agroinfiltration since it is very amenable to agroinfiltration and thus commonly used for this purpose (Sheludko et al., 2007). Interestingly, yield of heterologous proteins strongly differs between plants, leaves and within leaves (Bashandy et al., 2015). Leaf position and plant age seems to play a role. While younger leaves are more susceptible to infiltration, young plantlets exhibit lower transient gene expression and the most suitable time for inoculation is shortly before the formation of flowers.

Besides the parameters of bacterial growth, the infiltration setup and choosing suitable plants for inoculation, some adjustments to the infection medium were evaluated in literature to increase vacuum infiltration efficiency. Although not required, adding surfactants usually used in floral bud dipping methods were reported to increase gene expression levels (Wiktorek-Smagur et al., 2009). Further additives like thiol compounds (Sivanandhan et al., 2015) or lipoic acid (Norkunas et al., 2018) led to a four to six fold higher change in reporter protein expression. Through their antioxidative capabilities they counteract the oxidative burst which is released by plant cells as an innate defence mechanism in case of pathogen infections.

Overall, the setup for the agroinfiltration was chosen in a way of promoting a successful transformation. However, some adjustments could have been tested to improve the system.

4.4 Interference with endogenous enzymes in transgenic tobacco leads to production of conjugates

N. benthamiana is a dicotylous plant with a specific metabolic profile, different from grasses producing BXDs. The pathway has not been described in tobacco or any other member of the *Solanaceae*. In this regard it is a suitable choice for heterologous *in planta* expression of the BXD pathway. Still, tobacco possesses a metabolism of its own and endogenous enzymes may interfere with the engineered pathway. This event has occurred in several cases described in literature with different pathways. A pathway

leading to the production of the sesquiterpene lactone costunolide was expressed, introducing three novel enzymes (Liu et al., 2011). They were able to detect the product of the first enzyme, germacrene A. Other intermediates, on the other hand, were not identified and the authors hypothesized that endogenous enzymes converted them to novel metabolites, possibly below the detection threshold. Moreover, the sought-after product costunolide did not accumulate, but was conjugated by glutathione S-transferases (GSTs), introducing glutathione or cysteine. Glutathione conjugates have also been observed when expressing the artemisinin pathway in *N. benthamiana*, along with hexose or malonylated hexose conjugates (Ting et al., 2013). Furthermore, activity of an endogenous reductase presumably led to the reversal of the production of artemisinin pathway intermediates, causing them to accumulate in higher amounts than the final product. In transient expression of saponin biosynthesis genes, additional glycosylation with up to five hexoses was discovered (Khakimov et al., 2015). In the case of engineering the complete indole glucosinolate pathway from *Arabidopsis thaliana*, new metabolites or conjugates were not described (Pfalz et al., 2011). Generally, modifications introduced by endogenous enzymes of *N. benthamiana* seem to aim for detoxification of foreign compounds. Many of the metabolites produced by transiently expressed enzymes in the above-mentioned examples have toxic properties. GSTs and GTs are common enzymes in detoxification processes of plants, so conjugates are likely the consequence of innate defences against autotoxicity (Edwards et al., 2000; Cummins et al., 2011).

Looking at compounds of the benzoxazinoid pathway, forming of conjugation products is a potential issue. It was observed, that HBOA and DIBOA are glycosylated without co-transforming specific GTs BX8 and BX9. Concerning the hypothesis that this is a detoxification reaction, it is surprising that HBOA was glycosylated since no toxic qualities have been ascribed to it so far (Wouters et al., 2016). Possibly, GTs in the cytosol generally transfer hexose units to any hydroxylated substrate. Glycosylation is conducted on the C2-atom, which is partly responsible for the biological activity of BXDs. The first toxic compound in the pathway is DIBOA. As mentioned above, in case of DIBOA, the glucoside was potentially accumulated in higher amounts when co-expressing BX8 and BX9, probably due to higher substrate specificity. This however indicates a higher production of DIBOA and raises the question, where DIBOA aglucone ends up in case specific GTs are not present. One compound was detected, which is assumed to be the di-glucoside of DIBOA. More glucoside conjugates may have been produced but could not be found due to amounts below the detection threshold or further unknown modifications. Samples were checked in untargeted analysis for carrying

multiple hexose units or malonylated hexose. Except DIBOA di-glucoside, no such conjugates were found for HBOA, DIBOA or DIMBOA.

Formation of DIMBOA or its glucoside were not observed in any experiment co-transforming *Bx1* to *Bx7*. The conversion to conjugates is a possible cause for this. As described above, a major conjugation reaction and defence against xenobiotics in *N. benthamiana* is the addition of glutathione or cysteine. These modifications occur mostly at electrophilic carbon atoms or activated double bonds (Dixon et al., 2010). Moreover, glutathione opens epoxide rings and heterocyclic compounds in general. The structure of both hydroxamic acid and lactam BXDs differ in their options for such conjugations. Electron density in the heterocyclic ring of hydroxamic acids favours ring opening which is crucial for their reactivity. Lactams, on the other hand, are more inert due to the missing hydroxylation at the nitrogen. Thiol adducts have been described for DIMBOA (Niemeyer et al., 1982) and were thoroughly investigated three decades later (Dixon et al., 2012). Thiols like glutathione or cysteine form complex spirocyclic adducts (Figure 20). This reaction is assumed to contribute to the toxicity of DIMBOA by depleting glutathione reservoirs in the cell and binding to cysteine residues in the active centre of enzymes. However, this reaction has been described solely for the DIMBOA aglucone. In maize, and accordingly transformed tobacco plants, DIMBOA is produced as glucoside in the cytosol and stored in the vacuole. Glucosides are generally less reactive than their aglucone counterparts (Jones and Vogt, 2001). The step of heterocyclic ring opening crucial to the conversion to thiol adducts is less likely in the glycosylated state.

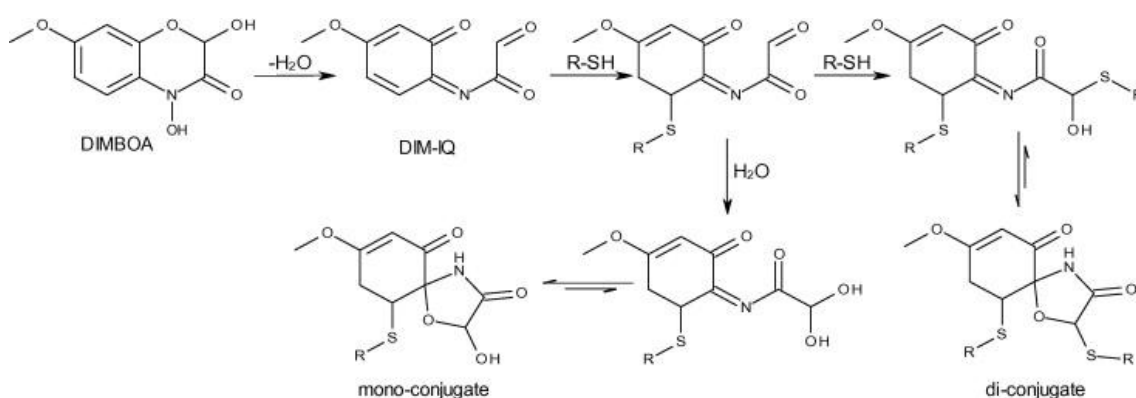


Figure 20: Reaction mechanism proposed for DIMBOA with thiols. DIMBOA can react with one or two thiols and form spirocyclic mono- or di-conjugates (Dixon et al., 2012).

It can be assumed that DIMBOA is not produced in high amounts because of low efficiency caused by co-transforming up to ten constructs. It would not be surprising if *N. benthamiana* converted all DIMBOA or DIMBOA-Glc available to possible conjugates. Plants could simply not accumulate enough. What exactly contributes to the absence of

DIMBOA-Glc is not clear. Several conjugation reactions paired with inefficient production may have collectively limited the quantity.

4.5 Supplementation of the BXD biosynthesis in transgenic plants by increasing the substrate availability

The first enzyme of the BXD pathway, BX1, is an IGL converting IGP to indole. Thus, the BXD biosynthetic pathway is branched from the Trp biosynthesis.

It was postulated that insufficient substrate concentrations may limit the output of BXD enzymes. In order to increase BXD content of transgenic plants, leaves were treated with AA to boost substrate availability. Leaves were cut off three days after infiltration and placed in AA solution for two days, right after plants were moved from the dimmed room under a light source.

At first, leaves were analysed on their Trp content to see whether the treatment influenced the accumulation of the amino acid. Looking at the initial Trp levels in non-treated leaves, co-transformation of *Bx* genes had no significant effect compared to the *eGFP* control, except for *Bx1-4+8/9* transformed plants. Yet, Trp accumulation seemed unstable dependent of the genes introduced by agroinfiltration. This may indicate that substrate availability was a limiting factor for the BXD biosynthesis. Adding 1 mM AA only led to a significant increase of Trp content in plants with *eGFP* or *Bx1-9* without *Bx5* compared to water controls. However, adding 1 mM AA seemed to increase Trp in other co-transformations as well.

Reviewing HBOA-Glc and DIBOA-Glc levels, an interesting correlation could be observed. In case of HBOA-Glc, accumulation was only expected in *Bx1-9 w/o Bx5* transformed plants based on previous experiments. This was the case. Yet, in leaves incubated in the water solution for control, HBOA-Glc apparently did not occur. Leaves placed in 1 mM solution, however, accumulated HBOA-Glc. The same trend was observed for DIBOA mono- and di-glucoside. Leaves accumulated the compound in *Bx1-5+8/9* transformed plants as usual, but not when placed in water for two days. In 1 mM solution, DIBOA glucoside content was again increased, independent whether it was mono- or di glucoside. There are two conclusions which can be drawn from these results. Leaves cut off and placed in water produced none or almost no BXDs but supplying them with AA somehow restored that capability. Theoretically, boosting the pathway with AA did increase BXD production in cut off leaves. The question arises how this treatment led to less or no accumulation of BXDs. Since AA restored the accumulation of BXDs, this might indicate a lack of substrate in cut-off leaves. However, Trp content would have been lowered as well, which was not the case. Furthermore, ethanol concentration in the

solutions may have had an inhibiting effect. Ethanol is reported to reduce growth as well as enzyme activity at concentrations lower than 10 mM (Perata et al., 1986). A 1% ethanol solution has a concentration of approx. 170 mM. Another reason could be due to the handling of the leaves itself. Plants were kept as usual in the dark after transformation and upon moving them under the light, leaves were immediately cut off. The metabolism in the leaves is generally lowered in the dark (Stitt et al., 1985) and as soon as the plants are under the light, it starts to be activated again. In the case of the treated leaves, this recovery may have never happened since they were separated from the main plant and put again under stress. The providing of additional substrate then compensated this effect.

To reveal the exact mechanisms behind this observed phenomenon, experiments would need to be repeated and leaves cut off after plants have been left under the light for at least a day. Clear is, that although AA had a significant effect, the desired impact on DIMBOA-Glc accumulation did not occur. To circumvent the drawbacks of the assay, an altogether different approach is available. Rather than supplying substrate for the biosynthesis, plants can be co-transformed with an enzyme boosting substrate biosynthesis. Introduction of an additional AS may be feasible for this task. Yet this approach is problematic since Trp biosynthesis is regulated at this step. Trp inhibits the AS at higher concentrations thus co-transforming this specific enzyme may not have a significant impact. However, there are enzyme varieties available which are feedback-insensitive, e.g. one derived from *Nicotiana tabacum* AS (Song et al., 1998). This gene would be a favourable choice for an alternative pathway boosting assay since it shares similar codon structures. Production of BXDs would not be biased by handling of the leaves. Nevertheless, this method has the disadvantage of cloning and introducing yet another gene into the tobacco plants. The complete BXD biosynthetic pathway up to DIMBOA-Glc already requires many gene transfers and increasing number of co-transformed constructs can lead to complications.

4.6 The drawbacks of cloning a complex pathway – and how to tackle them

Before genes of interest (GOI) can be introduced into plants by agroinfiltration, they must first be integrated into a vector suitable for *Agrobacteria* transformation. Choice of vector and *Agrobacteria* strain is essential for the success of transformation and should be considered carefully. Today, binary vector systems are the standard method for *Agrobacterium*-mediated plant transformation. Introducing GOIs into the Ti-Plasmid carrying *vir* genes for T-DNA transfer was a tedious process in the past (Gelvin, 2003). Instead, transforming a second replicon with the GOI between T-DNA borders has

proven to be a much cheaper and easier method for preparing an *Agrobacteria* strain. Oncogenic genes are simply removed from the Ti-plasmid and *vir* genes act *in trans* on the introduced vector (Hellens et al., 2000).

Deciding for a suitable vector depends on several variables like construct size, selection marker, copy number and availability. High copy numbers and a smaller vector size are desirable for a more efficient transformation, but price and technical effort is also an issue for most laboratories. The pCambia vector series developed by CambiaLabs comprises of a number of vectors which are small in size and exhibit fairly good copy numbers in *Agrobacteria* (Lee and Gelvin, 2008). The pCambia2300U vector chosen for introducing the BXD biosynthetic pathway is modified to be USER-cloning compatible. This simply requires the insertion of a USER-cassette into the ligation site (Nour-Eldin et al., 2006). Every *Bx* gene was ligated into a separate vector and thus separately transformed into different *Agrobacteria*. This approach bypasses the process of cloning multiple genes onto one vector which can be a tedious process. However, there is a severe disadvantage to this method. The more genes are supposed to be transferred simultaneously, the more decreases the efficiency of transient gene expression. To produce DIMBOA-Glc, *Bx1-7*, one of the UDP-GT genes *Bx8* or *Bx9* and viral suppressor *p19* is required. For a plant cell to produce DIMBOA-Glc, it needs to be infiltrated successfully by every *Agrobacteria* strain in the solution. It can be assumed, that the percentage of cells possessing all desired genes decreases with every additional gene. Thus, it has been hypothesized that this correlation is partly responsible for the low amounts of BXDs in transgenic plants.

Although pCambia vectors are easy-to-use for cloning and produce considerably good results, the market of cloning technology nowadays offers an immense portfolio of tools and techniques, especially when it comes to fusion of multiple genes on one construct. This approach has been developed for USER-cloning where up to three genes were reportedly fused at the same time (Geu-Flores et al., 2007). MultiSite Gateway® recombinational cloning allowed assembly of up to five fragments (Katzen, 2007). The strength of this cloning mechanism lies in its reversibility of fragment insertion and simple transfer of the GOI between different platforms. Furthermore, Golden Gate Cloning compatible vectors have been constructed for *A. tumefaciens*, which made it possible to combine five fragments on one vector in a single reaction (Emami et al., 2013). These cloning techniques are readily available and easy-to-use, removing the experimental bottleneck of assembling multiple GOIs on a single replicon. In recent years, viral deconstructed vectors have been on the rise, praised for their high efficiency in terms of transient protein production (Peyret and Lomonosoff, 2015). Especially the cow pea mosaic virus-hypertranslatable (CPMV-HT) system employed in the pEAQ vector series

has established as a user-friendly cloning tool. On the other hand, deconstructed vectors consist of several modules which need to be introduced for each GOI. The transfer of a whole biosynthetic pathway would still require numerous different *Agrobacteria* strains. In terms of BXD biosynthesis, construct number can be reduced significantly by fusing GOIs. Since *Bx1* to *Bx4* were always co-transformed, assembling them on one construct would simplify experimental procedures and ensure that these enzymes are completely present in transformed cells. The same applies for *Bx6* and *Bx7* as well as *Bx8* and *Bx9*. For the analysis of the production of BXD lactams, *Bx5* plays a major role. Keeping it isolated on one vector provides a more flexible setup for combination of *Bx* genes concerning the question about BXD lactam origin. Still, the number of co-transformed vectors can easily be reduced by half without fusing more than four genes in a single replicon or changing the experimental design.

5. Conclusion

Reconstructing a complex biosynthetic pathway by transient expression in another plant species is not a simple task. The task of transferring such a huge and complex group of enzymes will inevitably come across obstacles. Every part must be enabled to confer its task. Tobacco varies greatly in his morphology and biochemical profile compared to maize. Exogenous enzyme activity can be impaired by numerous reasons and components of the endogenous metabolism can interfere at any level of the pathway. It is impossible to predict all the obstacles of the heterologous expression system since it also depends on the genes co-transformed in the plants. In that regard, reconstruction of the BXD biosynthetic pathway in *N. benthamiana* has been a success. The presence of genes *Bx1* to *Bx7* was confirmed by qPCR and moreover, expression levels were in a reasonable range. It was possible to detect DIBOA-Glc, the first hydroxamic acid produced by the pathway. And although DIMBOA-Glc could not be found, co-transformation of *Bx6* and *Bx7* led to consumption of DIBOA-Glc, thus indicating the enzymatic activity.

The major setback of the setup was the low efficiency of BXD accumulation. The actual goal of confirming BX6 and BX7 as the enzymes converting HBOA-Glc to HMBOA-Glc was not reached. Since neither DIMBOA nor HMBOA glucosides were detected, no conclusion can be drawn regarding the ability of BX7 producing HMBOA-Glc. The fact that HBOA-Glc still accumulates after co-transformation of *Bx6* and *Bx7* suggests that HBOA-Glc is either converted by BX6 and BX7 at a very low rate or not at all. For further investigation, optimisation of the experimental system is crucial. Conjugation reactions conducted by endogenous enzymes of tobacco plants are difficult to control. The possibilities for conversion to novel metabolites are endless. Designing a highly efficient system with a sufficient output may compensate conjugation reactions enough to detect sought-after products. On the other hand, a completely different approach could be more feasible and easier to perform. Transient gene expression is an easy tool to use, but possibly not able to elucidate the origin of BXD lactams.

A. Literature

Ahmad S, Veyrat N, Gordon-Weeks R, Zhang YH, Martin J, Smart L, Glauser G, Erb M, Flors V, Frey M, Ton J (2011) Benzoxazinoid Metabolites Regulate Innate Immunity against Aphids and Fungi in Maize. *Plant Physiology* **157**(1): 317-327.

Alipieva KI, Taskova RM, Evstatieva LN, Handjieva NV, Popov SS (2003) Benzoxazinoids and iridoid glucosides from four *Lamium* species. *Phytochemistry* **64**(8): 1413-1417.

Bakshi S, Sadhukhan A, Mishra S, Sahoo L (2011) Improved *Agrobacterium*-mediated transformation of cowpea via sonication and vacuum infiltration. *Plant Cell Reports* **30**(12): 2281-2292.

Bally J, Jung H, Mortimer C, Naim F, Philips JG, Hellens R, Bombarely A, Goodin MM, Waterhouse PM (2018) The Rise and Rise of *Nicotiana benthamiana*: A Plant for All Reasons. *Annual Review of Phytopathology*, Vol 56 **56**: 405-426.

Baron C, Domke N, Beinhofer M, Hapfelmeier S (2001) Elevated temperature differentially affects virulence, VirB protein accumulation, and T-pilus formation in different *Agrobacterium tumefaciens* and *Agrobacterium vitis* strains. *Journal of Bacteriology* **183**(23): 6852-6861.

Bashandy H, Jalkanen S, Teeri TH (2015) Within leaf variation is the largest source of variation in agroinfiltration of *Nicotiana benthamiana*. *Plant Methods* **11**.

Baumeler A, Hesse M, Werner C (2000) Benzoxazinoids-cyclic hydroxamic acids, lactams and their corresponding glucosides in the genus *Aphelandra* (Acanthaceae). *Phytochemistry* **53**(2): 213-222.

Chetty VJ, Ceballos N, Garcia D, Narvaez-Vasquez J, Lopez W, Orozco-Cardenas ML (2013) Evaluation of four *Agrobacterium tumefaciens* strains for the genetic transformation of tomato (*Solanum lycopersicum* L.) cultivar Micro-Tom. *Plant Cell Reports* **32**(2): 239-247.

Cummins I, Dixon DP, Freitag-Pohl S, Skipsey M, Edwards R (2011) Multiple roles for plant glutathione transferases in xenobiotic detoxification. *Drug Metabolism Reviews* **43**(2): 266-280.

- de Oliveira MLP, Febres VJ, Costa MGC, Moore GA, Otoni WC** (2009) High-efficiency Agrobacterium-mediated transformation of citrus via sonication and vacuum infiltration. *Plant Cell Reports* **28**(3): 387-395.
- Dixon DP, Sellars JD, Kenwright AM, Steel PG** (2012) The maize benzoxazinone DIMBOA reacts with glutathione and other thiols to form spirocyclic adducts. *Phytochemistry* **77**: 171-178.
- Dixon DP, Skipsey M, Edwards R** (2010) Roles for glutathione transferases in plant secondary metabolism. *Phytochemistry* **71**(4): 338-350.
- Edwards R, Dixon DP, Walbot V** (2000) Plant glutathione S-transferases: enzymes with multiple functions in sickness and in health. *Trends in Plant Science* **5**(5): 193-198.
- Emami S, Yee MC, Dinneny JR** (2013) A robust family of Golden Gate Agrobacterium vectors for plant synthetic biology. *Frontiers in Plant Science* **4**.
- Escudero J, Hohn B** (1997) Transfer and integration of T-DNA without cell injury in the host plant. *Plant Cell* **9**(12): 2135-2142.
- Feild TS, Lee DW, Holbrook NM** (2001) Why leaves turn red in autumn. The role of anthocyanins in senescing leaves of red-osier dogwood. *Plant Physiology* **127**(2): 566-574.
- Frey M, Chomet P, Glawischnig E, Stettner C, Grun S, Winklmair A, Eisenreich W, Bacher A, Meeley RB, Briggs SP, Simcox K, Gierl A** (1997) Analysis of a chemical plant defense mechanism in grasses. *Science* **277**(5326): 696-699.
- Frey M, Schullehner K, Dick R, Fiesselmann A, Gierl A** (2009) Benzoxazinoid biosynthesis, a model for evolution of secondary metabolic pathways in plants. *Phytochemistry* **70**(15-16): 1645-1651.
- Gelvin SB** (2003) Agrobacterium-mediated plant transformation: The biology behind the "gene-Jockeying" tool. *Microbiology and Molecular Biology Reviews* **67**(1): 16-+.
- Gelvin SB** (2017) Integration of Agrobacterium T-DNA into the Plant Genome. *Annual Review of Genetics*, Vol 51 **51**: 195-217.
- Geu-Flores F, Nour-Eldin HH, Nielsen MT, Halkier BA** (2007) USER fusion: a rapid and efficient method for simultaneous fusion and cloning of multiple PCR products. *Nucleic acids research* **35**(7).

Glover BJ (2011) Pollinator Attraction: The Importance of Looking Good and Smelling Nice. *Current Biology* **21**(9): R307-R309.

Grotewold E (2005) Plant metabolic diversity: a regulatory perspective. *Trends in Plant Science* **10**(2): 57-62.

Gurel S, Gurel E, Kaur R, Wong J, Meng L, Tan HQ, Lemaux PG (2009) Efficient, reproducible Agrobacterium-mediated transformation of sorghum using heat treatment of immature embryos. *Plant Cell Reports* **28**(3): 429-444.

Handrick V, Robert CAM, Ahern KR, Zhou SQ, Machado RAR, Maag D, Glauser G, Fernandez-Penny FE, Chandran JN, Rodgers-Melnik E, Schneider B, Buckler ES, Boland W, Gershenzon J, Jander G, Erb M, Kollner TG (2016) Biosynthesis of 8-O-Methylated Benzoxazinoid Defense Compounds in Maize. *Plant Cell* **28**(7): 1682-1700.

Hanhineva K, Rogachev I, Aura AM, Aharoni A, Poutanen K, Mykkanen H (2011) Qualitative Characterization of Benzoxazinoid Derivatives in Whole Grain Rye and Wheat by LC-MS Metabolite Profiling. *Journal of Agricultural and Food Chemistry* **59**(3): 921-927.

Hanley ME, Lamont BB, Fairbanks MM, Rafferty CM (2007) Plant structural traits and their role in anti-herbivore defence. *Perspectives in Plant Ecology Evolution and Systematics* **8**(4): 157-178.

Hartmann T (2007) From waste products to ecochemicals: Fifty years research of plant secondary metabolism. *Phytochemistry* **68**(22-24): 2831-2846.

Hellens R, Mullineaux P, Klee H (2000) A guide to Agrobacterium binary Ti vectors. *Trends in Plant Science* **5**(10): 446-451.

Hoshisakoda M, Usui K, Ishizuka K, Kosemura S, Yamamura S, Hasegawa K (1994) Structure-Activity-Relationships of Benzoxazolinones with Respect to Auxin-Induced Growth and Auxin-Binding Protein. *Phytochemistry* **37**(2): 297-300.

Johnson HB (1975) Plant Pubescence - Ecological Perspective. *Botanical Review* **41**(3): 233-258.

Jonczyk R, Schmidt H, Osterrieder A, Fiesselmann A, Schullehner K, Haslbeck M, Sicker D, Hofmann D, Yalpani N, Simmons C, Frey M, Gierl A (2008) Elucidation of the final reactions of DIMBOA-glucoside biosynthesis in maize: Characterization of Bx6 and Bx7. *Plant Physiology* **146**(3): 1053-1063.

Jones P, Vogt T (2001) Glycosyltransferases in secondary plant metabolism: tranquilizers and stimulant controllers. *Planta* **213**(2): 164-174.

Katzen F (2007) Gateway (R) recombinational cloning: a biological operating system. *Expert Opinion on Drug Discovery* **2**(4): 571-589.

Khakimov B, Kuzina V, Erthmann PO, Fukushima EO, Augustin JM, Olsen CE, Scholtalbers J, Volpin H, Andersen SB, Hauser TP, Muranaka T, Bak S (2015) Identification and genome organization of saponin pathway genes from a wild crucifer, and their use for transient production of saponins in *Nicotiana benthamiana*. *Plant Journal* **84**(3): 478-490.

Lee LY, Gelvin SB (2008) T-DNA binary vectors and systems. *Plant Physiology* **146**(2): 325-332.

Liu Q, Majdi M, Cankar K, Goedbloed M, Charnikhova T, Verstappen FWA, de Vos RCH, Beekwilder J, van der Krol S, Bouwmeester HJ (2011) Reconstitution of the Costunolide Biosynthetic Pathway in Yeast and *Nicotiana benthamiana*. *Plos One* **6**(8).

Liu ZC, Park BJ, Kanno A, Kameya T (2005) The novel use of a combination of sonication and vacuum infiltration in *Agrobacterium*-mediated transformation of kidney bean (*Phaseolus vulgaris* L.) with *lea* gene. *Molecular Breeding* **16**(3): 189-197.

Macias FA, Oliveros-Bastidas A, Marin D, Castellano D, Simonet AM, Molinillo JMG (2004) Degradation studies on benzoxazinoids. Soil degradation dynamics of 2,4-dihydroxy-7-methoxy-(2H)-1,4-benzoxazin-3(4H)-one (DIMBOA) and its degradation products, phytotoxic allelochemicals from Gramineae. *Journal of Agricultural and Food Chemistry* **52**(21): 6402-6413.

Macias FA, Oliveros-Bastidas A, Marin D, Castellano D, Simonet AM, Molinillo JMG (2005) Degradation studies on benzoxazinoids. Soil degradation dynamics of (2R)-2-O-beta-D-glucopyranosyl-4-hydroxy-(2H)-1,4-benzoxazin-3(4H)-one (DIBOA-Glc) and its degradation products, phytotoxic allelochemicals from gramineae. *Journal of Agricultural and Food Chemistry* **53**(3): 554-561.

Matsuo K, Atsumi G (2019) CRISPR/Cas9-mediated knockout of the RDR6 gene in *Nicotiana benthamiana* for efficient transient expression of recombinant proteins. *Planta* **250**(2): 463-473.

Matsuura HN, Fett-Neto AG (2017) Plant Alkaloids: Main Features, Toxicity, and Mechanisms of Action. *Plant Toxins*: 243-261.

McCormick AC, Irmisch S, Reinecke A, Boeckler GA, Veit D, Reichelt M, Hansson BS, Gershenzon J, Kollner TG, Unsicker SB (2014) Herbivore-induced volatile emission in black poplar: regulation and role in attracting herbivore enemies. *Plant Cell and Environment* **37**(8): 1909-1923.

Meihls LN, Handrick V, Glauser G, Barbier H, Kaur H, Haribal MM, Lipka AE, Gershenzon J, Buckler ES, Erb M, Kollner TG, Jander G (2013) Natural Variation in Maize Aphid Resistance Is Associated with 2,4-Dihydroxy-7-Methoxy-1,4-Benzoxazin-3-One Glucoside Methyltransferase Activity. *Plant Cell* **25**(6): 2341-2355.

Mukherjee D, Mukherjee A, Ghosh TC (2016) Evolutionary Rate Heterogeneity of Primary and Secondary Metabolic Pathway Genes in *Arabidopsis thaliana*. *Genome Biology and Evolution* **8**(1): 17-28.

Niemeyer HM (1988) Hydroxamic Acids (4-Hydroxy-1,4-Benzoxazin-3-Ones), Defense Chemicals in the Gramineae. *Phytochemistry* **27**(11): 3349-3358.

Niemeyer HM (2009) Hydroxamic Acids Derived from 2-Hydroxy-2H-1,4-Benzoxazin-3(4H)-one: Key Defense Chemicals of Cereals. *Journal of Agricultural and Food Chemistry* **57**(5): 1677-1696.

Niemeyer HM, Corcuera LJ, Perez FJ (1982) Reaction of a Cyclic Hydroxamic Acid from Gramineae with Thiols. *Phytochemistry* **21**(9): 2287-2289.

Norkunas K, Harding R, Dale J, Dugdale B (2018) Improving agroinfiltration-based transient gene expression in *Nicotiana benthamiana*. *Plant Methods* **14**.

Nour-Eldin HH, Hansen BG, Norholm MHH, Jensen JK, Halkier BA (2006) Advancing uracil-excision based cloning towards an ideal technique for cloning PCR fragments. *Nucleic acids research* **34**(18).

Nutzmann HW, Huang AC, Osbourn A (2016) Plant metabolic clusters - from genetics to genomics. *New Phytologist* **211**(3): 771-789.

Park SY, Yin XY, Duan KX, Gelvin SB, Zhang ZYJ (2014) Heat Shock Protein 90.1 Plays a Role in *Agrobacterium*-Mediated Plant Transformation. *Molecular Plant* **7**(12): 1793-1796.

Perata P, Alpi A, Loschiavo F (1986) Influence of Ethanol on Plant-Cells and Tissues. *Journal of Plant Physiology* **126**(2-3): 181-188.

Petho M (2002) Physiological role of the cyclic hydroxamic acids. *Acta Biologica Szegediensis* **46**: 175-176.

Peyret H, Lomonossoff GP (2015) When plant virology met *Agrobacterium*: the rise of the deconstructed clones. *Plant Biotechnology Journal* **13**(8): 1121-1135.

Pfalz M, Mikkelsen MD, Bednarek P, Olsen CE, Halkier BA, Kroymann J (2011) Metabolic Engineering in *Nicotiana benthamiana* Reveals Key Enzyme Functions in *Arabidopsis* Indole Glucosinolate Modification. *Plant Cell* **23**(2): 716-729.

Radwanski ER, Last RL (1995) Tryptophan Biosynthesis and Metabolism - Biochemical and Molecular-Genetics. *Plant Cell* **7**(7): 921-934.

Schullehner K, Dick R, Vitzthum F, Schwab W, Brandt W, Frey M, Gierl A (2008) Benzoxazinoid biosynthesis in dicot plants. *Phytochemistry* **69**(15): 2668-2677.

Sheludko YV, Sindarovska YR, Gerasymenko IM, Bannikova MA, Kuchuk NV (2007) Comparison of several *Nicotiana* species as hosts for high-scale *Agrobacterium*-mediated transient expression. *Biotechnology and Bioengineering* **96**(3): 608-614.

Sicker D, Frey M, Schulz M, Gierl A (2000) Role of natural benzoxazinones in the survival strategy of plants. *International Review of Cytology - a Survey of Cell Biology*, Vol 198 **198**: 319-346.

Simmons CW, VanderGheynst JS, Upadhyaya SK (2009) A Model of *Agrobacterium tumefaciens* Vacuum Infiltration Into Harvested Leaf Tissue and Subsequent In Planta Transgene Transient Expression. *Biotechnology and Bioengineering* **102**(3): 965-970.

Sivanandhan G, Dev GK, Theboral J, Selvaraj N, Ganapathi A, Manickavasagam M (2015) Sonication, Vacuum Infiltration and Thiol Compounds Enhance the *Agrobacterium*-Mediated Transformation Frequency of *Withania somnifera* (L.) Dunal. *Plos One* **10**(4).

Song HS, Brotherton JE, Gonzales RA, Widholm JM (1998) Tissue culture-specific expression of a naturally occurring tobacco feedback-insensitive anthranilate synthase. *Plant Physiology* **117**(2): 533-543.

Stitt M, Wirtz W, Gerhardt R, Heldt HW, Spencer C, Walker D, Foyer C (1985) A Comparative-Study of Metabolite Levels in Plant Leaf Material in the Dark. *Planta* **166**(3): 354-364.

Teasdale JR, Rice CP, Cai GM, Mangum RW (2012) Expression of allelopathy in the soil environment: soil concentration and activity of benzoxazinoid compounds released by rye cover crop residue. *Plant Ecology* **213**(12): 1893-1905.

Ting HM, Wang B, Ryden AM, Woittiez L, van Herpen T, Verstappen FWA, Ruyter-Spira C, Beekwilder J, Bouwmeester HJ, van der Krol A (2013) The metabolite chemotype of *Nicotiana benthamiana* transiently expressing artemisinin biosynthetic pathway genes is a function of CYP71AV1 type and relative gene dosage. *New Phytologist* **199**(2): 352-366.

VanEtten HD, Mansfield JW, Bailey JA, Farmer EE (1994) Two Classes of Plant Antibiotics: Phytoalexins versus "Phytoanticipins". *The Plant Cell* **6**(9): 1191-1192.

Voinnet O, Rivas S, Mestre P, Baulcombe D (2003) An enhanced transient expression system in plants based on suppression of gene silencing by the p19 protein of tomato bushy stunt virus (Retracted article. See vol. 84, pg. 846, 2015). *Plant Journal* **33**(5): 949-956.

von Rad U, Huttli R, Lottspeich F, Gierl A, Frey M (2001) Two glucosyltransferases are involved in detoxification of benzoxazinoids in maize. *Plant Journal* **28**(6): 633-642.

Wang B, Kashkooli AB, Sallets A, Ting HM, de Ruijter NCA, Olofsson L, Brodelius P, Pottier M, Boutry M, Bouwmeester H, van der Krol AR (2016) Transient production of artemisinin in *Nicotiana benthamiana* is boosted by a specific lipid transfer protein from *A. annua*. *Metabolic Engineering* **38**: 159-169.

Wiktorek-Smagur A, Hnatuszko-Konka K, Kononowicz AK (2009) Flower bud dipping or vacuum infiltration-two methods of *Arabidopsis thaliana* transformation. *Russian Journal of Plant Physiology* **56**(4): 560-568.

Willard JI, Penner D (1976) Benzoxazinones: cyclic hydroxamic acids found in plants. *Residue Rev* **64**: 67-76.

Wisecaver JH, Borowsky AT, Tzin V, Jander G, Kliebenstein DJ, Rokas A (2017) A Global Coexpression Network Approach for Connecting Genes to Specialized Metabolic Pathways in Plants. *Plant Cell* **29**(5): 944-959.

Wouters FC, Gershenzon J, Vassao DG (2016) Benzoxazinoids: Reactivity and Modes of Action of a Versatile Class of Plant Chemical Defenses. *Journal of the Brazilian Chemical Society* **27**(8): 1379-1397.

Zhang XR, Henriques R, Lin SS, Niu QW, Chua NH (2006) Agrobacterium-mediated transformation of *Arabidopsis thaliana* using the floral dip method. *Nature Protocols* **1**(2): 641-646.

Zhao HM, Tan ZL, Wen XJ, Wang YC (2017) An Improved Syringe Agroinfiltration Protocol to Enhance Transformation Efficiency by Combinative Use of 5-Azacytidine, Ascorbate Acid and Tween-20. *Plants-Basel* **6**(1).

Zhou SQ, Richter A, Jander G (2018) Beyond Defense: Multiple Functions of Benzoxazinoids in Maize Metabolism. *Plant and Cell Physiology* **59**(8): 1528-1537.

Zupan J, Muth TR, Draper O, Zambryski P (2000) The transfer of DNA from *Agrobacterium tumefaciens* into plants: a feast of fundamental insights. *Plant Journal* **23**(1): 11-28.

B. Supplementary

Table I: List of used chemicals and their vendors.

Chemical	Vendor
Acetic Acid	VWR International GmbH, Darmstadt, Germany
Acetonitrile	VWR International GmbH, Darmstadt, Germany
Acetosyringone	Sigma-Aldrich Chemie GmbH, Taufkirchen, Germany
Agarose	Carl Roth GmbH & Co. KG, Karlsruhe, Germany
Anthranilate	Sigma-Aldrich Chemie GmbH, Taufkirchen, Germany
Calcium chloride	Carl Roth GmbH & Co. KG, Karlsruhe, Germany
DMSO	Fisher Scientific GmbH, Schwerte, Germany
DTT	Fisher Scientific GmbH, Schwerte, Germany
EDTA	Fisher Scientific GmbH, Schwerte, Germany
Ethanol	VWR International GmbH, Darmstadt, Germany
Formic acid	VWR International GmbH, Darmstadt, Germany
Gentamycin	Duchefa Biochemie B.V, Harleem, Netherlands
Glycerol	Carl Roth GmbH & Co. KG, Karlsruhe, Germany
Kanamycin	Sigma-Aldrich Chemie GmbH, Taufkirchen, Germany
Magnesium chloride	Carl Roth GmbH & Co. KG, Karlsruhe, Germany
MES	Carl Roth GmbH & Co. KG, Karlsruhe, Germany
Methanol	Sigma-Aldrich Chemie GmbH, Taufkirchen, Germany
Natrium chloride	Carl Roth GmbH & Co. KG, Karlsruhe, Germany
Rifampicin	Duchefa Biochemie B.V, Harleem, Netherlands
TRIS	Carl Roth GmbH & Co. KG, Karlsruhe, Germany
Tryptone	Carl Roth GmbH & Co. KG, Karlsruhe, Germany
Yeast extract	Carl Roth GmbH & Co. KG, Karlsruhe, Germany

All oligonucleotides listed in tables II-V below were ordered from Sigma-Aldrich Chemie GmbH (Taufkirchen, Germany).

Table II: List of primers for amplification of *Bx* genes from *Zea mays* cDNA. T_m = Melting temperature, Fwd = Forward primer, Rev. = Reverse primer.

Gene	Sequence	T_m (°C)
<i>Bx1</i>	Fwd.: CACCATGGCTTTTCGCGCCCAAACGTCCTCCTCCTCCTC	88.8
	Rev.: TCATGGCAGCGCGTTCTTCATGCCCTGGCATACTC	87.3
<i>Bx2</i>	Fwd.: ATGTACGGCGCCACCGAC	60.5
	Rev.: TCACGCAGCCTGTGGGACTAG	63.7
<i>Bx3</i>	Fwd.: ATGGCCCTTGAGCTGCGTAC	63.7
	Rev.: TCAGGAAGCAATCCTTGGAAACAAGG	63.0
<i>Bx4</i>	Fwd.: ATGGCTCTCGAAGCAGCG	58.2
	Rev.: TCATTTGGGAATTCTAGGAACAAGG	59.7
<i>Bx5</i>	Fwd.: ATGGCACTCCAGGCAGCCTAC	63.7
	Rev.: CTAGACGGCCCTAGGAACAAGG	64.0
<i>Bx6</i>	Fwd.: ATGGCTCCAACGACCGCC	58.2
	Rev.: CTAGAGCCTGAAGTGGTCGAGC	59.7
<i>Bx7</i>	Fwd.: ATGGGGCACCAGGCG	73.0
	Rev.: TCACGGGAAGACCTCGATGAT	58.1
<i>Bx8</i>	Fwd.: ATGCACACGGACGACGTC	60.5
	Rev.: TCAGTAGGAGTTTATGAGATGAACC	63.7
<i>Bx9</i>	Fwd.: ATGGCGTCGTCGCGCACCGGAGCC	63.7
	Rev.: TCAGAAGGATTTTATGAGATCAACC	63.0

Table III: List of USER-PCR primers for amplification of *Bx* genes. T_m = Melting temperature, Fwd = Forward primer, Rev. = Reverse primer.

Gene	Sequence	T_m (°C)
<i>Bx1</i>	Fwd.: GGCTTAAUATGGCTTTCGCGCCCAAACG	78.5
	Rev.: GGTTTAAUTCATGGCAGCGCGTTCTTCATGC	78.9
<i>Bx2</i>	Fwd.: GGCTTAAUATGTACGGCGCCACCGAC	75.0
	Rev.: GGTTTAAUTCACGCAGCCTGTGGGACTAG	74.1
<i>Bx3</i>	Fwd.: GGCTTAAUATGGCCCTTGGAGCTGCGTAC	75.8
	Rev.: GGTTTAAUTCAGGAAGCAATCCTTGAACAAGG	74.9
<i>Bx4</i>	Fwd.: GGCTTAAUATGGCTCTCGAAGCAGCG	73.2
	Rev.: GGTTTAAUTCATTTGGGAATTCTAGGAACAAGG	71.2
<i>Bx5</i>	Fwd.: GGCTTAAUATGGCACTCCAGGCAGCCTAC	74.7
	Rev.: GGTTTAAUCTAGACGGCCCTAGGAACAAGG	72.1
<i>Bx6</i>	Fwd.: GGCTTAAUATGGCTCCAACGACCGCC	75.9
	Rev.: GGTTTAAUCTAGAGCCTGAAGTGGTCGAGC	72.1
<i>Bx7</i>	Fwd.: GGCTTAAUATGGGGCACCAGGCG	74.1
	Rev.: GGTTTAAUTCACGGGAAGACCTCGATGAT	72.8
<i>Bx8</i>	Fwd.: GGCTTAAUATGCACACGGACGACGTC	73.2
	Rev.: GGTTTAAUTCAGTAGGAGTTTATGAGATGAACC	67.5
<i>Bx9</i>	Fwd.: GGCTTAAUATGGCGTCGTCGCGCACC	79.1
	Rev.: GGTTTAAUTCAGAAGGATTTTATGAGATCAACC	68.7

Table IV: List of primers for outward sequencing of *Bx* genes in reverse direction. T_m = Melting temperature.

Gene	Sequence	T_m (°C)
<i>Bx1</i>	ACCTGTCACTCCGTTACGC	60.0
<i>Bx2</i>	GTGTTGGCCGGGATGGTGTAGC	63.6
<i>Bx3</i>	CCACCTCTGGTTGAGCCGCC	70.0
<i>Bx4</i>	TCCCACCGCTTGCTGACGCC	70.0
<i>Bx5</i>	ACAGCTTCCTCATCTCCACGTGC	56.5
<i>Bx9</i>	TACAGCACGGAGCCCGGC	72.2

Table V: List of qPCR primers for *Bx* genes and *GAPDH* gene. T_m = Melting temperature, Fwd = Forward primer, Rev. = Reverse primer, bp = base pair. The length of the amplified fragment is indicated for each gene. Primers for *GAPDH*, *Bx2*-*Bx5* and *Bx7* were taken from literature (Ahmad et al., 2011).

Gene	Sequence	T_m (°C)	Fragment length (bp)
<i>GAPDH</i>	Fwd.: AGCTCAAGGGAATTCTCGATG	64.8	125
	Rev.: AACCTTAACCATGTCATCTCCC	63.2	
<i>Bx1</i>	Fwd.: CCAGAGCACGTGAAGCAGAT	66.7	137
	Rev.: CTTCATGCCCTGGCATACT	66.5	
<i>Bx2</i>	Fwd.: GACGAGGACGACGATAAGGACTT	66.8	60
	Rev.: GGCCATACTCCTTCTGAAGAGACAG	67.4	
<i>Bx3</i>	Fwd.: ATGGCCGAGCTCATCAACAA	68.2	60
	Rev.: TCGTCCTCACCTCCGTCTGT	67.7	
<i>Bx4</i>	Fwd.: TGTTCCCTCCGGATCATCTGC	67.8	60
	Rev.: AAGAGGCTGTCCCACCGCT	68.8	
<i>Bx5</i>	Fwd.: CCATTTGACTGGGAGGTCC	68.2	60
	Rev.: GTCCATGCTCACCTTCCC GC	71.6	
<i>Bx6</i>	Fwd.: CAGCGACCACCTGTACGAGA	66.9	123
	Rev.: AAGAAGCCAGGGTCCGTGTG	68.9	
<i>Bx7</i>	Fwd.: GGCTGGGTTCCGTGACTACA	67.7	60
	Rev.: GACCTCGATGATGGACGGG	68.3	

Table VI: Average Cq values for *Bx* genes and *GAPDH* gene from qPCR. Cq = Cycle of quantification.

qPCR-Analysis	
Gene	Average Cq
<i>Bx1</i>	21.774
<i>Bx2</i>	24.164
<i>Bx3</i>	20.84
<i>Bx4</i>	24.67
<i>Bx5</i>	19.336
<i>Bx6</i>	20.476
<i>Bx7</i>	19.916

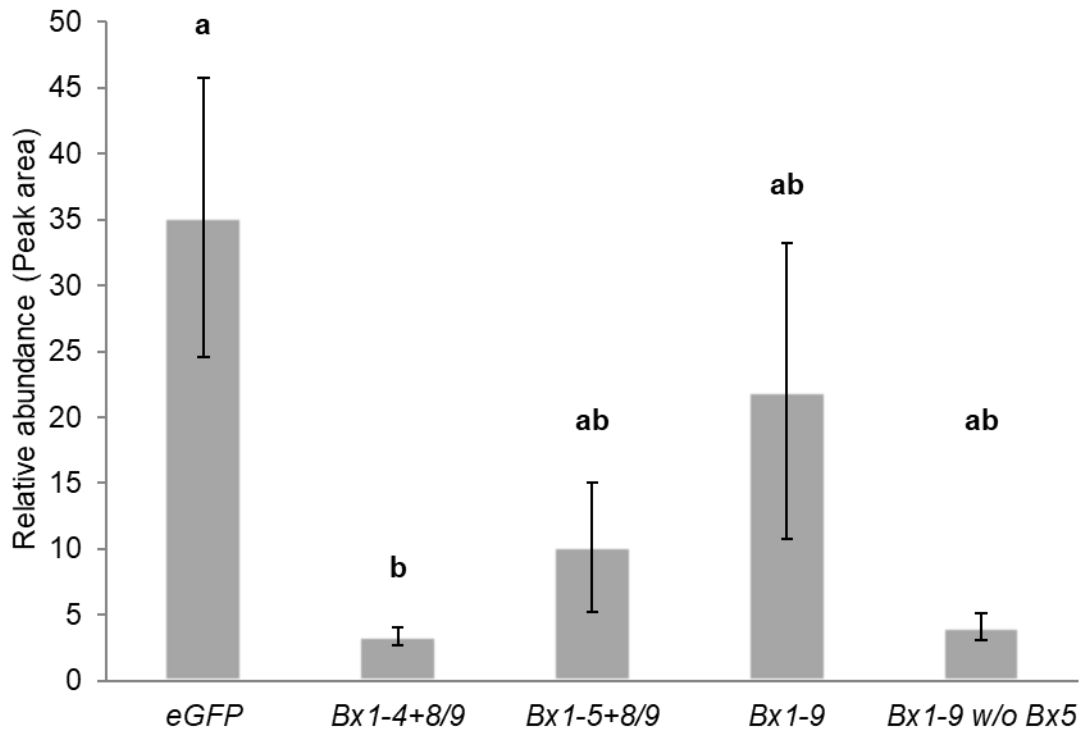


Figure I: Tryptophan content of transgenic *Nicotiana benthamiana* plants. The plants were co-transformed with genes described on the vertical axis via agroinfiltration. Five days after agroinfiltration, leaves were harvested from these plants and analysed via LC-MS/MS for tryptophan content. The letters indicate separation into statistically different groups. The bars show means +/- standard error (n=5, Kruskal-Wallis One-Way-ANOVA on ranks, followed by multiple comparison via Tukey, p-value < 0.05).

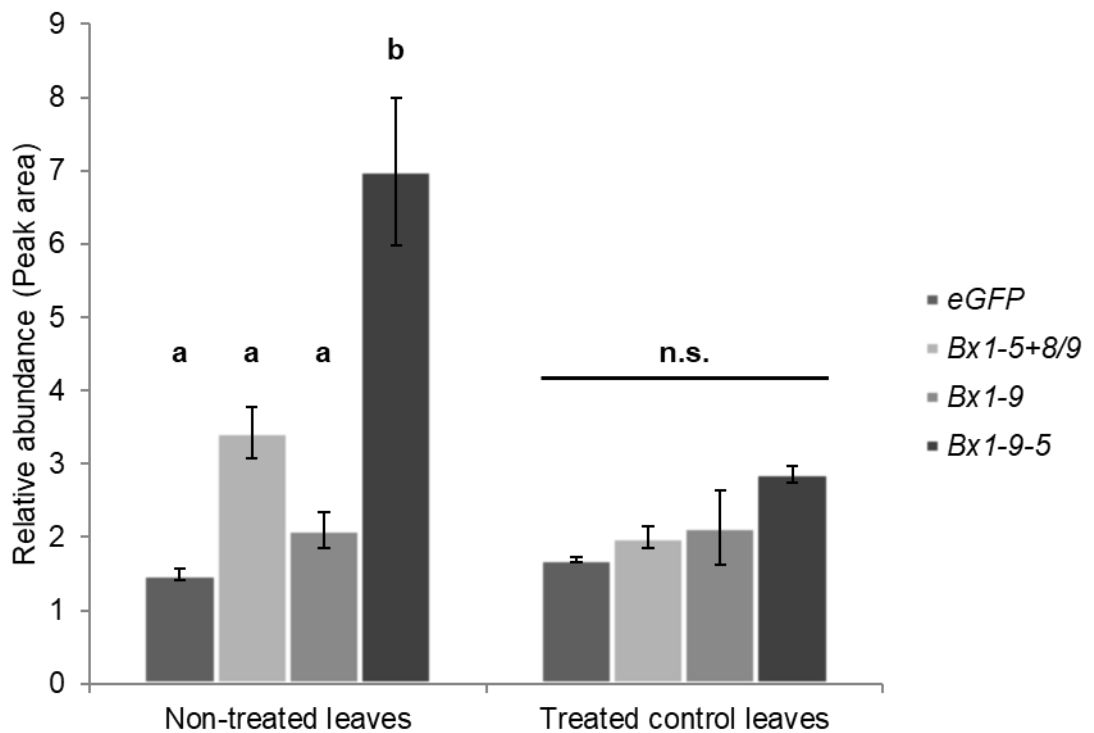


Figure II: HBOA-Glc content of transgenic *Nicotiana benthamiana* leaves in different treatments. The leaves were harvested from transgenic plants five days after transformation via agroinfiltration. Treated leaves were cut off from plants three days after infiltration and placed in

water for two days. After the harvest, leaves were analysed via LC-MS/MS on their HBOA-Glc content. The letters indicate separation into statistically different groups. The bars show means +/- standard error (n=5, Two-Way-ANOVA, followed by multiple comparison via Holm-Sidak, p-value < 0.05). n.s. = not significant.

Table VII: DIBOA mono- and di-glucoside content of transgenic *Nicotiana benthamiana* plants in different treatments. The plants were transformed via agroinfiltration with either eGFP or Bx1-5+8/9 and harvested after five days. Some leaves were cut off three days post-infiltration and placed in water or 1 mM anthranilate (AA) solution. The numbers indicate the mean of relative abundance in peak area of DIBOA mono- and di-glucoside +/- standard error (N=5). n.d. = not detected.

Gene	Post-infiltrational Treatment	DIBOA-Glc	DIBOA-Glc ₂
eGFP	Not treated	n.d.	n.d.
eGFP	Cut off and placed in Water	n.d.	n.d.
eGFP	Cut off and placed in 1 mM AA	n.d.	n.d.
Bx1-5+8/9	Not treated	8168 +/- 949	5090 +/- 499
Bx1-5+8/9	Cut off and placed in Water	382 +/- 147	383 +/- 128
Bx1-5+8/9	Cut off and placed in 1 mM AA	3909 +/- 1112	3760 +/- 1294

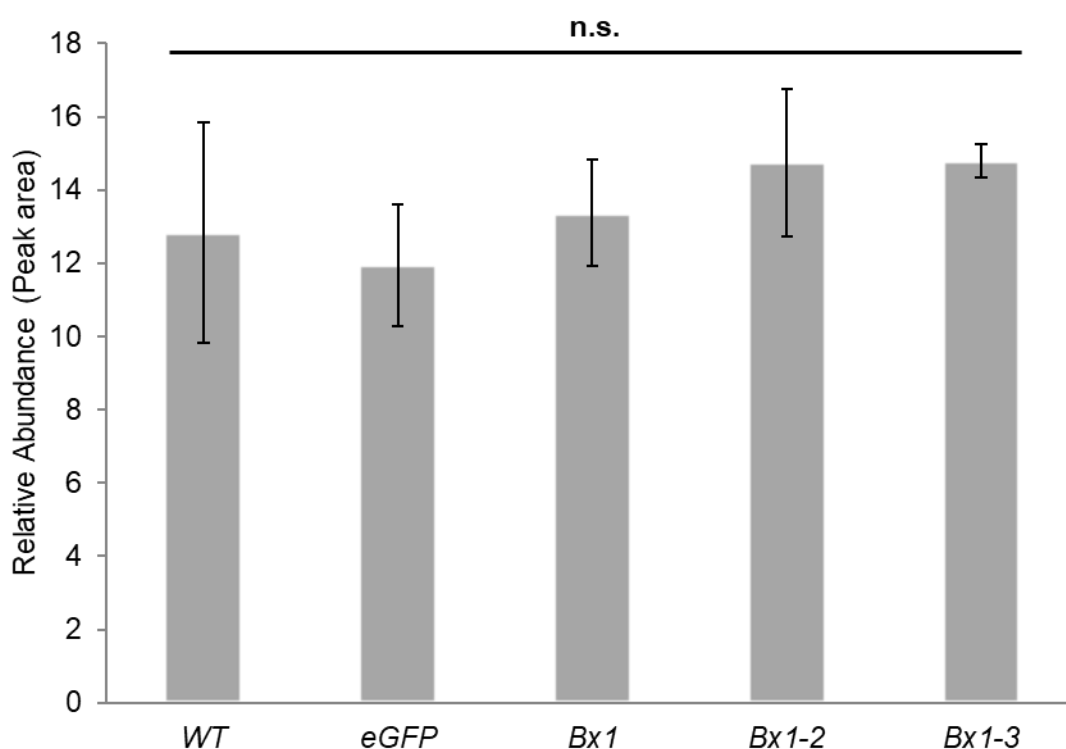


Figure III: HBOA-Glc content of *Nicotiana benthamiana* plants transformed with Bx genes up to Bx3. *N. benthamiana* specimen were transformed via agroinfiltration with the genes indicated on the vertical axis and compared to wild-type (WT) plants in their HBOA-Glc content. The bars show means +/- standard error (n=4, One-Way ANOVA, followed by multiple comparison via Tukey, p-value > 0.05). n.s. = not significant

C. Danksagung

Ich möchte mich bei Christiane Förster und Tobias Köllner für die Betreuung meines Projektes bedanken und dafür, dass sie mir bei meiner Arbeit im Labor geholfen und für Rückfragen zur Verfügung gestanden haben. Ich danke Katrin Luck und Jan Günther für ihre Einweisung in die Methodik der Agroinfiltration. Ich möchte mich auch bei den restlichen Mitgliedern der Arbeitsgruppe bedanken, bei denen ich mich sehr gut aufgehoben gefühlt habe.

Weiterhin danke ich der gesamten Abteilung der Biochemie des Max-Planck-Institutes für chemische Ökologie, wo schlichtweg eine wahnsinnig angenehme Arbeitsatmosphäre herrscht, die ich sehr genossen habe. Ich möchte Bettina Raguschke für ihre Sequenzierungsarbeit und den Gärtnern für das Aufziehen der Tabakpflanzen danken.

Besonderen Dank möchte ich an Tom Kache und Dennis Krettler aussprechen. Sie haben mich in meiner Studienzeit viel begleitet. Tom danke ich für die gemeinsame Durchsicht des Manuskriptes.

Allen voran will ich aber meiner atemberaubenden See danken, dass sie mir immer einen Platz zur Rast bot und ich an ihrer Seite Ruhe finden konnte.

D. Selbständigkeitserklärung

Hiermit versichere ich, dass ich die vorliegende Arbeit selbständig verfasst und keine anderen als die angegebenen Quellen und Hilfsmittel benutzt habe. Alle Ausführungen, die anderen Schriften wörtlich oder sinngemäß entnommen wurden, sind kenntlich gemacht und die Arbeit war in gleicher oder ähnlicher Fassung noch nicht Bestandteil einer Studien- oder Prüfungsleistung.

Jena, 17.12.2019

Paul Anton Himmighofen